

# ULRR

## Parameter uniform numerical solution of elliptic singular perturbation problems with discontinuous data

Item Type	Thesis
Authors	Branley, Deirdre
Download date	2026-06-08 18:03:05
Item License	<a href="https://creativecommons.org/licenses/by-nc-sa/4.0/">https://creativecommons.org/licenses/by-nc-sa/4.0/</a>
Link to Item	<a href="https://doi.org/10.34961/researchrepository-ul.28182578">https://doi.org/10.34961/researchrepository-ul.28182578</a>

---

**Parameter uniform numerical  
solution of elliptic singular  
perturbation problems with  
discontinuous data**

---

Deirdre Branley

University of Limerick

A thesis submitted for the degree of

*Doctor of Philosophy*

Supervisor: Dr. Alan Hegarty

Submitted to the University of Limerick, November 2024

# Author's Declaration

This thesis is presented in fulfilment of the requirements for the degree of Doctor of Philosophy. It is entirely my own work and has not been submitted to any other university or higher education institution, or for any other academic award in this university. Where use has been made of the work of other people it has been fully acknowledged and fully referenced.

Signed:

---

Date:

---

# Abstract

In the first chapter of this thesis a singularly perturbed convection-diffusion equation with a source term which is continuous but whose first derivative contains a point of discontinuity is considered. The solution features a boundary layer and a weak interior layer. A numerical method is constructed which involves a Shishkin mesh fitted at the boundary layer, but not at the interior layer. The method is shown, both theoretically and by numerical experiments, to be uniformly convergent with respect to the singular perturbation parameter.

In the second chapter we consider the following boundary value problem in a domain  $\Omega$ , the unit square.

$$\begin{aligned}Lu_\varepsilon &\equiv \varepsilon\Delta u_\varepsilon + p_1\frac{\partial u_\varepsilon}{\partial x} + p_2\frac{\partial u_\varepsilon}{\partial y} - qu_\varepsilon = f \text{ in } \Omega, \\u_\varepsilon(x, 0) &= g_s(x), \quad u_\varepsilon(x, 1) = g_n(x), \quad x \in (0, 1) \\u_\varepsilon(0, y) &= g_w(y), \quad u_\varepsilon(1, y) = g_e(y) \quad y \in (0, 1) \\g_s(0) &\neq g_w(0),\end{aligned}$$

where  $p_1$ ,  $p_2$  and  $q$  are positive constants and  $0 < \varepsilon \leq 1$ , and the boundary data are smooth except at the point  $(0, 0)$ . Analogously to the methods introduced in [45] we derive a pointwise bound on the solution which highlights the influence of the boundary conditions at the corners of the domain, as well as that of the singular perturbation parameter  $\varepsilon$ .

In the final chapter we examine experimentally the performance of numerical methods comprising domain decomposition and Schwarz iterative techniques ([67], [72], [73] and [91]) extended to the class of singularly perturbed convection-diffusion problems with more general boundary conditions as described above.

# Acknowledgements

I am grateful to the Irish Research Council for Science Engineering and Technology for funding this PhD.

I want to thank my supervisor, Prof. Alan Hegarty for his unfailing patience and positivity and for his encouragement to continue this work after my life became more complicated.

Through Alan, I benefitted from invaluable advice from several experts in the field including the late Prof. Bruce Kellogg, the late Prof. Pieter Hemker, Prof. Grigorii Shishkin, Prof. Martin Stynes, Prof. Eugene O’Riordan and Prof. Natalia Kopteva.

I also want to thank my former colleagues Ana, Marguerite, Maria Gonzalez, and Maria Pickett for their friendship during our years researching and teaching together.

My late parents, Padraig and Eileen, had enormous respect for education and I dearly wish they were still here to enjoy this moment with me.

Finally, thank you to my husband, Seamus, and my sisters, Dorothy and Mary, for their practical and moral support; to my dear friend and one-time childminder, Madeleine, who made finishing this thesis possible; to my children, Julia, Eleanor, and Harry, for bearing with me through my viva preparation and amendments; and last but not least, to my canine companions, especially Billy, whose emotional support was pure gold.

# Contents

<b>1</b>	<b>Introduction</b>	<b>2</b>
<b>2</b>	<b>Singularly perturbed convection-diffusion problems with boundary and weak interior layers: partially-fitted mesh method</b>	<b>10</b>
2.1	Statement of the Problem . . . . .	10
2.2	Discrete Problem . . . . .	23
2.3	Error Analysis . . . . .	25
2.4	Numerical Results . . . . .	48
2.5	Summary . . . . .	50
<b>3</b>	<b>A singularly perturbed convection-diffusion problem with discontinuous boundary data</b>	<b>53</b>
3.1	Introduction . . . . .	53
3.2	Decomposition . . . . .	55
3.2.1	Summary of alternative decomposition . . . . .	63
3.3	Bounds on components . . . . .	65
3.3.1	Smooth components $S_1$ and $S_2$ . . . . .	65
3.3.2	Exponential layer components $E_1$ and $E_2$ . . . . .	75
3.3.3	Outflow corner component $z_{00}$ . . . . .	79
3.3.4	Inflow corner component $z_{11}$ . . . . .	89
3.3.5	Corner components $z_{10}$ and $z_{01}$ . . . . .	92

3.3.6	Remainder term $\tilde{u}_\varepsilon$ . . . . .	94
3.3.7	Solution of the original problem $u_\varepsilon$ . . . . .	95
3.4	Summary . . . . .	95
<b>4</b>	<b>On A Schwarz method for a singularly perturbed convection- diffusion problem with discontinuous boundary conditions</b>	<b>97</b>
4.1	Introduction . . . . .	97
4.2	Direct Method: non-iterative discrete method on piecewise uni- form fitted meshes . . . . .	101
4.3	Schwarz Method 1: domain decomposition with restricted over- lap region . . . . .	103
4.4	Schwarz Method 2: domain decomposition with maximal over- lap region . . . . .	114
4.4.1	Alternative translation in polar region . . . . .	118
4.4.2	Use of upwinding in the polar region . . . . .	119
4.5	Schwarz Method 3: alternative domain decomposition with square sub-region . . . . .	122
4.6	Conclusion . . . . .	126

# List of Figures

2.1	Approximate global error for problem (2.37) with $\varepsilon = 0.0001$ and $N = 64$ . . . . .	50
2.2	Approximate global error for problem (2.38) with $\varepsilon = 0.0001$ and $N = 64$ . . . . .	51
3.1	Boundary data on $\Omega, S_1 + S_2 + E_1 + E_2$ . . . . .	57
3.2	Domain and boundary conditions, $z_{00}$ . . . . .	58
3.3	Boundary data on $\Omega, S_1 + S_2 + E_1 + E_2 + z_{00}$ . . . . .	58
3.4	Domain and boundary conditions, $z_{11}$ . . . . .	59
3.5	Domain and boundary conditions, $z_{10}$ . . . . .	61
3.6	Domain and boundary conditions, $z_{01}$ . . . . .	62
4.1	Picture of our domain, $\Omega$ , with the location of the boundary layers and the discontinuity at the outflow corner . . . . .	100
4.2	Approximate global error for problem (2.38) with $\varepsilon = 0.0001$ and $N = 64$ . . . . .	102
4.3	Domain decomposition with restricted overlap region, $\Omega_S$ is pictured with the overlapping subdomain, $\Omega_P$ , depicted in grey . . . . .	104

4.4	The advantage of the shape of subregion $\Omega_P$ is that translating to polar coordinates here enables us to smooth out the discontinuity when solving on this subdomain. The point of discontinuity becomes our left hand boundary in polar coordinates and we use linear interpolation to give us smooth boundary conditions in polar coordinates. . . . .	106
4.5	The iterative process . . . . .	109
4.6	$N = 64$ . When $R$ is small we get satisfactory results for the pointwise errors using Schwarz Method 1. However, the method requires many iterations to converge when $R$ is small. . . . .	112
4.7	$N = 64$ . With large $R$ we see the pointwise errors for Schwarz Method 1 blow up. . . . .	113
4.8	Domain decomposition with maximal overlap. . . . .	114
4.9	Numerical solutions of problem (4.1) for $\varepsilon = 2^{-1}$ , $N = 32$ . . .	117
4.10	Numerical solutions of problem (4.1) for $\varepsilon = 2^{-6}$ , $N = 32$ . . .	117
4.11	Domain decomposition with square overlap region of side $\sigma/8$ , i.e., the overlap region is comparable magnitude to that of the quarter disk subdomain for the domain decomposition with maximal overlap.	122

# List of Tables

2.1	Global errors $\bar{E}_\varepsilon^N$ and the uniform order of convergence $p_N$ for the discrete solution, partially fitted mesh method $(P_\varepsilon^N)$ applied to problem (2.37). . . . .	50
2.2	Maximum pointwise errors $E_\varepsilon^N$ , and the uniform order of convergence $p_N$ in the scaled discrete derivatives for the partially fitted mesh method $(P_\varepsilon^N)$ applied to problem (2.37). . . . .	51
2.3	Global errors $\bar{E}_\varepsilon^N$ and the uniform order of convergence $p_N$ for the discrete solution, partially fitted mesh method $(P_\varepsilon^N)$ applied to problem (2.38). . . . .	52
2.4	Maximum pointwise errors $E_\varepsilon^N$ , and the uniform order of convergence $p_N$ in the scaled discrete derivatives for the partially fitted mesh method $(P_\varepsilon^N)$ applied to problem (2.38). . . . .	52
4.1	Maximum pointwise errors $E_\varepsilon^N$ and $E^N$ for the Direct Method applied to problem (4.1). . . . .	102
4.2	Computed orders of convergence $p^N$ for the Direct Method applied to problem (4.1). . . . .	103
4.3	Iteration counts for Schwarz Method 1 (restricted overlap) applied to problem (4.1) for tolerance $10^{-4}$ , variable R . . . . .	111
4.4	Computed orders of convergence for Schwarz Method 1 (restricted overlap) applied to problem (4.1) with $R = 0.4\sigma$ . . . . .	111
4.5	Iteration counts for Schwarz Method 2 applied to problem (4.1) with domain decomposition allowing maximal overlap. . . . .	116
4.6	Maximum pointwise errors $E_\varepsilon^N$ and $E^N$ for Schwarz Method 2 applied to problem (4.1) with domain decomposition allowing maximal overlap. . . . .	117
4.7	Computed orders of convergence $p_\varepsilon^N$ for Schwarz Method 2 applied to problem (4.1) with domain decomposition allowing maximal overlap. . . . .	118

4.8	Iteration counts for modified Schwarz Method 2 applied to problem (4.1) with domain decomposition allowing maximal overlap and upwinding in the polar region. . . . .	119
4.9	Computed orders of convergence $p_\epsilon^N$ for modified Schwarz Method 2 applied to problem (4.1) with domain decomposition allowing maximal overlap and upwinding in the polar region. . . . .	120
4.10	Maximum pointwise errors $E_\epsilon^N$ and $E^N$ for modified Schwarz Method 2 applied to problem (4.1) with upwinding in the polar region . . . . .	121
4.11	Iteration counts for Schwarz Method 3 applied to problem (4.1). . . . .	124
4.12	Maximum pointwise errors $E_\epsilon^N$ and $E^N$ for Schwarz Method 3 applied to problem (4.1).	125
4.13	Computed orders of convergence $p_\epsilon^N$ for Schwarz Method 3 applied to problem (4.1). .	125

# Chapter 1

## Introduction

We are concerned with singularly perturbed convection-diffusion equations in one and two dimensions. Examples of such equations are widespread, e.g., in the modelling of the dispersal of a pollutant in a river, semi-conductor equations, financial modelling, flows in chemical reactors, etc. [74, 89, 72, 64, 10, 9, 40, 49, 68, 103, 16]. Singularly perturbed differential equations depend on a perturbation parameter,  $\varepsilon \in (0, 1]$ , which, in the case of convection-diffusion equations, multiplies the weaker diffusion term [96, 17, 106, 77]. As  $\varepsilon$  approaches zero, the solution of such an equation (or its derivatives) may become unbounded, in narrow  $\varepsilon$ -dependent subdomains known as boundary (or interior) layers and it does not converge to the solution of the reduced problem where  $\varepsilon$  is set to zero [74, 89, 34, 72, 96, 24, 97]. The numerical solution of such equations is of interest where asymptotic expansions may not be helpful or possible [89].

Standard numerical methods fail when applied to singularly perturbed problems due to the very small domains in which boundary or interior layers appear [21, 96, 63]. Fitted operator methods such as Allen-Southwell are restricted in their applicability [96], while complication of construction as well

as theoretical techniques needed to bound error estimates have limited the extension of complex fitted meshes such as Bakhvalov meshes to two dimensions [21]. Fitted mesh methods comprising standard monotone finite difference operators on simple piecewise-uniform meshes (with fine meshes in layer regions and coarse meshes elsewhere, separated by carefully chosen transition points), known as Shishkin meshes, have been shown to be robust, layer-resolving or parameter-uniform methods applicable to a wide class of linear problems [91, 21, 51, 95]. That is, they generate numerical approximations of the exact solution and its derivatives at each point of the solution domain for all values of  $\varepsilon$ , which satisfy pointwise error bounds independent of  $\varepsilon$ ; the amount of work required to compute such approximations must also be  $\varepsilon$ -independent [21]. Robustness refers to the stability of the finite difference operator, e.g., the upwind finite difference operator, which preserves the monotonicity of the original problem [21, 72]. Much work has been done on the application and analysis of this and related methods, see [21, 72, 89, 34, 62, 50, 60, 37, 93, 94, 19, 36, 83, 20, 58, 65, 4] and survey articles [59, 88]. For adaptations of this method to problems featuring nonsmooth data, corner singularities, interior layers, see [92, 71, 81, 32, 33, 30, 31, 107, 107].

In Chapter 2 we are concerned with the use of this method in solving a two-point boundary value problem for a singularly perturbed convection-diffusion problem with singular perturbation parameter  $\varepsilon$ . We examine the case where the source term in the differential equation is continuous but has a point of discontinuity in its first derivative, in addition to which there is a possible discontinuity in the first derivative of the convection coefficient, at some point in the interior of the domain. This causes an interior layer in the exact solution of the problem, besides which there is a boundary layer at the outflow boundary point.

When the convection coefficient, the source term and their first derivatives are continuous over the domain a boundary layer appears at the outflow boundary point. We shall refer to the convection coefficient, the source term and the domain as  $a$ ,  $f$  and  $\Omega$  respectively. It was shown by Miller et al. [72] (with the assumption  $a, f \in C^3(\Omega)$ ) and by Farrell et al. [21] (assuming  $a, f \in C^2(\Omega)$ ) that a similar problem can be solved with uniform convergence with respect to  $\varepsilon$  using a standard upwind finite difference method on a Shishkin mesh. In terms of finite element methods, Sun and Stynes [102] constructed a parameter-uniform convergent Galerkin finite element method comprising piece-wise polynomial test functions on a Shishkin mesh for singularly perturbed convection-diffusion problems with  $a$  and  $f$  assumed to be sufficiently smooth, i.e., no interior layers were present. Additionally, Guo and Stynes [35] examined an  $\varepsilon$ -uniform convergent streamline diffusion method on a Shishkin mesh for a singularly perturbed time-dependent convection diffusion equation with constant convection coefficient and  $f \in L^2(\Omega)$ .

The case where the convection coefficient has a sign change at one or more points in the domain was considered by Farrell et al. in [22] and by O’Riordan in [78]. The solution of such a problem contains a strong interior layer. It was shown that an upwind finite difference method on a Shishkin mesh fitted to the interior layer generates  $\varepsilon$ -uniformly convergent numerical approximations to the solution. Problems with a discontinuous source term were examined by the same authors in [23]. The numerical method introduced here featured a Shishkin mesh fitted to both the boundary and weak interior layer. We show both theoretically and by means of computational experiments that when the source term is barely continuous, a numerical method which consists of a Shishkin mesh fitted only to the boundary layer and not to the interior layer, and a standard upwind finite difference operator generates  $\varepsilon$ -uniformly conver-

gent numerical approximations to the solution and its derivatives in the global maximum norm. This is the most appropriate norm for the measurement of error in the case of singularly perturbed problems, due to the narrowness of layer regions [72, 21, 96, 12]. The construction of piecewise-uniform meshes requires a priori knowledge of the location and width of the layer region. Such knowledge is obtained by means of studying the behaviour of, and deriving bounds on, solutions and their derivatives; these bounds are required for the error analysis of numerical methods. For examples see [39, 61, 41, 42, 43, 18, 13].

In [46], Kellogg and Stynes consider a singularly perturbed convection-diffusion problem on a half-plane with a discontinuity in the boundary data which gives rise to an interior layer. In [45] and [47], the same authors examine a singularly perturbed convection-diffusion problem on the unit square with parabolic and exponential boundary layers and derive pointwise bounds on the solution and its derivatives - the dependence of the bounds on the regularity and compatibility of the data, as well as on the singular perturbation parameter, is made explicit. Analogous results were obtained in [75, 76] for related problems with a Neumann boundary conditions. Survey articles [44] and [48] review recent results and open problems related to elliptic boundary value problems whose solutions have both boundary layers and corner singularities.

In [2] Andreev considers a five-point upwind scheme on a Shishkin mesh for a singularly perturbed convection-diffusion problem on a rectangle with Dirichlet boundary conditions, with the compatibility conditions dropped at three of the four vertices and finds that the error of the discrete solution is of  $O(N^{-1} \ln^2 N)$  in the discrete maximum norm. He obtains a similar result in [3], where he examines a Dirichlet problem for a singularly perturbed steady state convection-diffusion equation with constant coefficients on the unit square, without compatibility conditions at the corners.

In Chapter three we are concerned with obtaining a bound on the solution of a two-dimensional singularly perturbed convection-diffusion problem, which features exponential boundary layers and incompatible outflow boundary data. We were interested in studying the nature of the solution in order to help design a numerical method to solve this type of problem; see Chapter 4. The problem is decomposed into a number of simpler elliptic half and quarter plane problems, which have continuous boundary conditions, with one exception. The functions which comprise the source term and boundary conditions are smoothly extended as required as per [26]. In considering integrability conditions, the solution to the problem on each quarter plane is obtained by means of the Green's function written in terms of modified Bessel functions. The integrability conditions which result show that, once the source term and boundary conditions are themselves such that the integrals are convergent, then the solution to each half or quarter plane problem does not grow to infinity in the open domain. Pointwise bounds are obtained for the solutions of these problems plus a remainder function by means of standard comparison principle arguments. The bounds on all components are then combined to produce the final result.

In Chapter 4 we are concerned with obtaining a numerical solution to a sample problem of the type dealt with in Chapter 3. Where the boundary conditions are sufficiently smooth and compatible, such a problem can be solved with uniform accuracy with respect to the singular perturbation parameter using a standard finite difference operator on special piece-wise uniform meshes such as Shishkin meshes [21]. We design a method which is almost parameter-uniform, using domain decomposition to isolate neighbourhoods of discontinuities together with Schwarz iterative technique and Shishkin meshes.

It was shown by MacMullen et al. [67] that a numerical method based

on Schwarz iterative technique and Shishkin domain decomposition produces parameter-uniformly accurate solutions in the case of singularly perturbed linear convection-diffusion problems in two dimensions with sufficiently smooth and compatible boundary data. Similarly, in another paper by MacMullen et al. [66], it was shown that a two-point boundary-value problem for a singularly perturbed reaction-diffusion equation can be solved with parameter-uniform accuracy using a discrete Schwarz method with a Shishkin subdomain parameter. Miller et al. examined discrete Schwarz methods for singularly-perturbed reaction-diffusion problems with boundary and interior layers [73]. Their numerical method differed from those used by MacMullen et al. in [67] and [66] in that Shishkin, and not uniform, meshes were used on the subdomains. Madden and Stephens devised and analysed a discrete Schwarz method on three overlapping subdomains for a coupled system of one-dimensional reaction-diffusion equations in [101] and achieved rapid convergence due to subdomain overlaps which are just outside the boundary layers. More recently, Kopteva et al applied overlapping Schwarz domain decomposition to semilinear reaction-diffusion equations in one and two dimensions [52, 53]. For further examples, see [69, 14, 14, 56, 57, 105, 104, 54, 55, 25].

In terms of designing a numerical method comprising domain decomposition and Schwarz iterative technique to deal with discontinuous boundary data there are a number of considerations. Broadly, they are the overlap requirement and appropriate tolerance for the discrete Schwarz method, the shape of our subdomains, the nature of the corner singularity at the outflow corner and need for suitable iterative solvers with preconditioning, see [5, 100, 15, 70, 90]. In order to examine the performance of the Schwarz method in general, we first applied the method to a problem with continuous boundary conditions. This highlighted many issues: the need to translate the differential equation

using a type of integrating factor prior to converting to polar coordinates for the quarter-disk region; the need for scaling in this polar region (see p.62 of [74]) the permissible size of the radius of the quarter-disk region; the minimum overlap width needed between subdomains in order for the method to converge to the correct solution; the need for preconditioning of the iterative solver in MATLAB; and the question of a suitable tolerance for the Schwarz method (a tolerance of order  $10^{-4}$  is appropriate given the order of pointwise errors for the method).

Having optimised the performance of the Schwarz method applied to problems with continuous boundary conditions, we then turned our attention to the discontinuous case. Given the bound obtained in Chapter 3 on the singular component of the solution to a problem similar in nature to the one under consideration here, and through numerical experiments, it was clear that the influence of the corner singularity was such that an alteration was required to our initial domain decomposition in order to cluster more nodes at the outflow corner while maintaining the minimum overlap region needed for the Schwarz method. In the discontinuous case the influence of the corner singularity is such that the radius of the quarter-disk region at the outflow corner must not be set too large, since the influence of the discontinuity is greatest in the region where  $r \leq \varepsilon$ . In order to meet the overlap requirement imposed by the Schwarz method and at the same time restrict the size of the quarter-disk region, we found a domain decomposition consisting of our main domain, the unit square, overlapping with a quarter-disk subregion, of radius proportional to  $\varepsilon$  at the outflow corner gave optimal results for the discontinuous case. We include numerical results for this method which show a significant improvement on existing methods. Some alternative Schwarz methods were also considered for comparison purposes, including a method

with an alternative translation applied to the differential equation in the polar region and a method using a square subregion at the outflow corner rather than a quarter-disk region.

# Chapter 2

## Singularly perturbed convection-diffusion problems with boundary and weak interior layers: partially-fitted mesh method

### 2.1 Statement of the Problem

A singularly perturbed convection-diffusion equation in one dimension with a source term whose first derivative is discontinuous is considered on the unit interval  $\Omega = (0, 1)$ . A single discontinuity in the derivative of the source term  $f$  is assumed to occur at a point  $d \in \Omega$ . Additionally, there is a possible discontinuity in the first derivative of the convection coefficient at some point in  $\Omega$ . One dimensional convection-diffusion boundary value problems with a sign change in the convection coefficient were examined by Farrell et al.

in [23]. Their theoretical and numerical results showed that the strong interior layer which appears in the solution of such problems can be discretely solved using a Shishkin mesh fitted to the interior layer. They examined one dimensional convection-diffusion boundary value problems with a discontinuous source term in [23]. Whereas, their numerical method featured a Shishkin mesh fitted to *both* the boundary and weak interior layer, we show both theoretically and through computational experiments that, with a barely continuous source term, a numerical method where a Shishkin mesh is fitted *only* to the boundary layer and not to the interior layer is robust. We do not consider problems including a zero-order term; the analysis in the presence of a reaction term would differ substantially from the analysis undertaken in this chapter.

We introduce the notation  $\Omega^- = (0, d)$  and  $\Omega^+ = (d, 1)$  and denote the jump at  $d$  in any function by  $[\omega](d) = \omega(d^+) - \omega(d^-)$ . The corresponding two-point boundary value problem is

$$(P_\varepsilon) \left\{ \begin{array}{l} \text{Find } u_\varepsilon \in C^2(\Omega) \text{ such that,} \\ \varepsilon u_\varepsilon'' + a(x)u_\varepsilon' = f \text{ for all } x \in \Omega, \\ u_\varepsilon(0) = u_0, \quad u_\varepsilon(1) = u_1, \\ a(x) > \alpha > 0, \text{ for all } x \in \Omega, \end{array} \right.$$

where  $a, f \in C^0(\Omega) \cap C^2(\Omega^- \cup \Omega^+)$ . In [21], singularly perturbed problems of this type with  $a, f \in C^2(\Omega)$  were examined. In such a situation the solution  $u_\varepsilon$  is in  $C^4(\Omega)$ . The case in which the source term has a discontinuity at one or more points in the interior of the domain was examined in [23], where the solution  $u_\varepsilon$  is in  $C^1(\Omega) \cap C^2(\Omega^- \cup \Omega^+)$ . In this chapter we construct and analyse a parameter-uniform numerical method for problems of the form  $(P_\varepsilon)$ .

Let  $L_\varepsilon$  denote the differential operator occurring in  $(P_\varepsilon)$ , which is defined as

$$L_\varepsilon \omega = \varepsilon \omega'' + a(x) \omega'.$$

Then  $L_\varepsilon$  satisfies the following minimum principle on  $\bar{\Omega}$ .

**Lemma 2.1.** *Suppose a function  $\omega \in C^0(\bar{\Omega}) \cap C^2(\Omega^- \cup \Omega^+)$  satisfies*

$$\omega(0) \geq 0, \quad \omega(1) \geq 0,$$

$$L_\varepsilon \omega(x) \leq 0, \quad x \in \Omega^- \cup \Omega^+ \quad \text{and} \quad [\omega'](d) \leq 0,$$

then

$$\omega(x) \geq 0 \quad \text{for all } x \in \bar{\Omega}.$$

**Proof.** The proof here is analogous to that in [23]. Let

$$\omega(x) = \begin{cases} e^{-(\alpha_1(x-d))/2\varepsilon} v(x), & x < d, \\ e^{-(\alpha_2(x-d))/2\varepsilon} v(x), & x \geq d. \end{cases}$$

For  $x \in \Omega^-$

$$L_\varepsilon \omega = e^{-\alpha_1(x-d)/2\varepsilon} (\varepsilon v'' + (a - \alpha_1)v' - \frac{\alpha_1}{2\varepsilon} (a - \frac{\alpha_1}{2})v)$$

and  $x \in \Omega^+$

$$L_\varepsilon \omega = e^{-\alpha_2(x-d)/2\varepsilon} (\varepsilon v'' + (a - \alpha_2)v' - \frac{\alpha_2}{2\varepsilon} (a - \frac{\alpha_2}{2})v)$$

Assume  $\alpha > \alpha_2 > \alpha_1$ . Let  $q$  be a point at which  $v$  attains its minimum value in  $\bar{\Omega}$ . If  $v(q) \geq 0$ , there is nothing to prove. Therefore suppose that  $v(q) < 0$ , the proof is completed by showing that this leads to a contradiction.

With the above assumption on the boundary values, either  $q \in \Omega^- \cup \Omega^+$  or  $q = d$ . If  $q \in \Omega^-$  then

$$L_\varepsilon \omega(q) = e^{-\alpha_1(q-d)/2\varepsilon} [\varepsilon v''(q) + (a(q) - \alpha_1)v'(q) - \frac{\alpha_1}{2\varepsilon}(a(q) - \frac{\alpha_1}{2})v(q)] > 0$$

which is a contradiction, since  $v''(q) = 0$ ,  $v'(q) > 0$  and  $v(q) < 0$  by assumption. Similarly, if  $q \in \Omega^+$  then

$$L_\varepsilon \omega(q) = e^{-\alpha_2(q-d)/2\varepsilon} [\varepsilon v''(q) + (a(q) - \alpha_2)v'(q) - \frac{\alpha_2}{2\varepsilon}(a(q) - \frac{\alpha_2}{2})v(q)] > 0$$

which is also a contradiction.

The only possibility remaining is that  $q = d$ . Note that

$$[\omega'](d) = [v'](d) + \frac{\alpha_1 - \alpha_2}{2\varepsilon} v(d)$$

Since  $q = d$  is where  $v(x)$  is assumed to attain a negative minimum,  $[v'](d) \geq 0$  and  $v(d) < 0$ . Therefore for  $\alpha_1 < \alpha_2$ ,  $[\omega'](d) > 0$ , which is the required contradiction.  $\square$

Throughout this chapter we measure all functions in the  $L^\infty$  norm,

$$\|w\|_D = \sup_{x \in D} |w(x)|.$$

The above minimum principle is used to establish the following a priori

bound on the exact solution.

**Lemma 2.2.** *Let  $u_\varepsilon$  be a solution of  $(P_\varepsilon)$ , then*

$$\|u_\varepsilon\| \leq \max\{|u_0|, |u_1|\} + \frac{1}{\alpha} \|f\|_{\bar{\Omega}}.$$

**Proof.** The result is proved using the arguments from [23]. Let  $\psi_\pm(x) = \max\{|u_0|, |u_1|\} + (1-x)\frac{\|f\|}{\alpha} \pm u_\varepsilon(x)$ . Clearly  $\psi_\pm(x) \in C^2(\bar{\Omega})$ , therefore  $[\psi'_\pm](d) = 0$ . It is also clear that  $\psi_\pm(0) \geq 0$ ,  $\psi_\pm(1) \geq 0$  and for each  $x \in \Omega^- \cup \Omega^+$ ,  $L_\varepsilon \psi_\pm(x) \leq 0$ . It follows from the minimum principle that  $\psi_\pm(x) \geq 0$  for all  $x \in \bar{\Omega}$ , from which the required result immediately follows.  $\square$

**Lemma 2.3.** *The derivatives  $u_\varepsilon^{(k)}$  of the solution  $u_\varepsilon$  of  $(P_\varepsilon)$  satisfy the bounds*

$$\begin{aligned} \|u_\varepsilon^{(k)}\|_{\bar{\Omega}} &\leq C\varepsilon^{-k} \max\{\|f\|, \|u_\varepsilon\|\}, \quad k = 1, 2 \\ \|u_\varepsilon^{(3)}\|_{\bar{\Omega} \setminus d} &\leq C\varepsilon^{-3} \max\{\|f\|, \|f'\|_{\bar{\Omega} \setminus d}, \|u_\varepsilon\|\} \end{aligned}$$

where  $C$  depends only on  $\|a\|$  and  $\|a'\|_{\Omega \setminus d}$ .

**Proof.** The proof is analogous to that in [21], Lemma 3.2, p. 44. Integrating by parts, we get

$$\int_0^x a u'_\varepsilon(t) dt = a u_\varepsilon|_0^x - \int_0^x (a' u_\varepsilon)(t) dt$$

and so

$$\left| \int_0^x (f - au'_\varepsilon)(t) dt \right| \leq \|f\| + C\|u_\varepsilon\|,$$

where  $C$  depends on  $\|a\|$  and  $\|a'\|_{\Omega \setminus d}$ . By the Mean Value Theorem there exists a point  $z \in (0, \varepsilon)$  such that

$$u'_\varepsilon(z) = \frac{u_\varepsilon(\varepsilon) - u_\varepsilon(0)}{\varepsilon}$$

therefore

$$|\varepsilon u'_\varepsilon(z)| \leq 2\|u_\varepsilon\|. \quad (2.1)$$

Integrating the differential equation in  $(P_\varepsilon)$  we get

$$\int_0^z (\varepsilon u''_\varepsilon + a(x)u'_\varepsilon)(t) dt = \int_0^z f(t) dt$$

and so

$$\varepsilon u'_\varepsilon(z) - \varepsilon u'_\varepsilon(0) = \int_0^z (f - au'_\varepsilon)(t) dt.$$

By combining this result with (2.1) we get

$$|\varepsilon u'_\varepsilon(0)| \leq \|f\| + C\|u_\varepsilon\|.$$

Using the integrated differential equation again, with  $z = x$  we obtain the

required bound when  $k = 1$ . Finally, from the differential equation we have

$$\varepsilon u_\varepsilon'' = f - au_\varepsilon' \text{ for all } x \in \bar{\Omega}$$

and

$$\varepsilon u_\varepsilon''' = (f - au_\varepsilon')' \text{ for all } x \in \bar{\Omega} \setminus \{d\}$$

from which the required bounds for  $k = 2, 3$  respectively follow.  $\square$

Consider the following decomposition of the solution into boundary and interior layer components

$$u_\varepsilon = v_\varepsilon + w_\varepsilon$$

where  $v_\varepsilon$  can be written as  $v_\varepsilon = v_0 + \varepsilon v_1 + \varepsilon^2 v_2$  and we define the functions  $v_0 \in C^1(\Omega)$ ,  $v_1 \in C^0(\Omega)$  and  $v_2 \in C^0(\Omega)$  as follows

$$\begin{aligned} av_0' &= f, \quad x \in \Omega, \\ v_0(1) &= u_\varepsilon(1) \\ av_1' &= -v_0'', \quad x \in \Omega \setminus \{d\}, \\ v_1(1) &= 0 \\ L_\varepsilon v_2 &= -v_1'', \quad x \in \Omega \setminus \{d\} \\ v_2(0) &= v_2(1) = v_2(d) = 0. \end{aligned}$$

Therefore  $v_\varepsilon$  is defined as

Find  $v_\varepsilon \in C^0(\Omega)$  such that

$$L_\varepsilon v_\varepsilon = f, \quad x \in \Omega^- \cup \Omega^+$$

$$v_\varepsilon(0) = v_0(0) + \varepsilon v_1(0)$$

$$v_\varepsilon(d) = v_0(d) + \varepsilon v_1(d)$$

$$v_\varepsilon(1) = u_\varepsilon(1).$$

The layer component  $w_\varepsilon \in C^0(\Omega)$  is then the solution of the homogeneous problem

$$L_\varepsilon w_\varepsilon = 0,$$

$$w_\varepsilon(0) = u_\varepsilon(0) - v_\varepsilon(0), \quad w_\varepsilon(1) = 0,$$

$$[w'_\varepsilon](d) = -[v'_\varepsilon](d).$$

We further decompose  $w_\varepsilon$  as follows

$$w_\varepsilon = w_1 + w_2$$

where the boundary layer component  $w_1$  satisfies

$$w_1 \in C^2(\Omega),$$

$$L_\varepsilon w_1 = 0, \quad x \in \Omega,$$

$$w_1(0) = u_\varepsilon(0) - v_\varepsilon(0),$$

$$w_1(1) = 0$$

and the interior layer component  $w_2$  satisfies

$$\begin{aligned} w_2 &\in C^0(\Omega), \\ L_\varepsilon w_2 &= 0, \quad x \in \Omega^- \cup \Omega^+, \\ w_2(0) &= 0, w_2(1) = 0, \\ [w_2'](d) &= -[v_\varepsilon'](d). \end{aligned}$$

**Lemma 2.4.** *The component  $v_\varepsilon$  of the solution  $u_\varepsilon$  of  $(P_\varepsilon)$  and its derivatives satisfy the bounds*

$$\begin{aligned} \|v_\varepsilon^{(k)}\|_{\Omega^- \cup \Omega^+} &\leq C(1 + \varepsilon^{2-k}), \quad k = 0, 1, 2, 3. \\ |[v_\varepsilon'](d)| &\leq C\varepsilon \end{aligned}$$

where  $C$  is a constant independent of  $\varepsilon$ .

**Proof.** The first part of the proof is analogous to that in [21]. By the triangle inequality we have

$$|v_\varepsilon| \leq |v_0| + \varepsilon|v_1| + \varepsilon^2|v_2|.$$

Since  $v_0$  is independent of  $\varepsilon$ , the first two terms on the right-hand side are bounded. Note that  $v_2$  is the solution of a problem similar to that defining  $u_\varepsilon$ , therefore by Lemma (2.3) the required bounds for  $k = 0, 1, 2$  follow. For  $k = 3$  we have  $\varepsilon v_\varepsilon''' = (f - av_\varepsilon)'$ , which leads to the required bound.

In order to bound  $|[v_\varepsilon'](d)|$ , we obtain bounds on the jump at  $d$  in the first derivative of each of the components of  $v_\varepsilon$ . Since  $v_0 \in C^1(\Omega)$ ,  $[v_0'](d) = 0$ . As noted above,  $v_1$  is independent of  $\varepsilon$  and  $v_2$  is the solution of a problem similar to that defining  $u_\varepsilon$ , therefore we have  $|[v_1'](d)| \leq C$  and  $|[v_2'](d)| \leq C\varepsilon^{-1}$ . Collecting the inequalities yields the required bound.  $\square$

**Lemma 2.5.** *The boundary layer component  $w_1$  of the solution  $u_\varepsilon$  of  $(P_\varepsilon)$  and its derivatives satisfy the bounds*

$$|w_1^{(k)}| \leq C\varepsilon^{-k}e^{-\alpha x/\varepsilon} \text{ for all } x \in \bar{\Omega}, k = 0, 1, 2, 3.$$

where  $C$  is a constant independent of  $\varepsilon$ .

**Proof.** Analogously to the proof in [21], p. 46, we introduce the two mesh functions

$$\psi^\pm(x) = |w_1(0)|e^{-\alpha x/\varepsilon} \pm w_1(x)$$

Clearly  $\psi^\pm(0) \geq 0, \psi^\pm(1) \geq 0, [\psi'^\pm](d) = 0$  and  $L_\varepsilon\psi^\pm = -|w_1(0)|\frac{\alpha}{\varepsilon}(a - \alpha)e^{-\alpha x/\varepsilon} \leq 0$ . Therefore, by Lemma 2.1,  $\psi^\pm \geq 0$ , for all  $x \in \bar{\Omega}$ , from which required bound on  $w_1$  follows.

In order to bound  $w_1'$  we integrate by parts and use the pointwise bound for  $|w_1|$  established above, as follows

$$\left| \int_x^1 aw_1'(t)dt \right| = \left| aw_1|_x^1 - \int_x^1 (a'w_1)(t)dt \right| \leq Ce^{-\alpha x/\varepsilon}. \quad (2.2)$$

By the Mean Value Theorem, there exists a point  $z \in (1 - \varepsilon, 1)$  such that

$$|w_1'(z)| = \left| \frac{w_1(1) - w_1(1 - \varepsilon)}{\varepsilon} \right| = \left| \frac{w_1(1 - \varepsilon)}{\varepsilon} \right| \leq C\varepsilon^{-1}e^{-\alpha(1-\varepsilon)/\varepsilon} \leq C\varepsilon^{-1}e^{-\alpha/\varepsilon}. \quad (2.3)$$

We now integrate the differential equation defining  $w_1$  to give

$$\varepsilon w_1'(x) = \varepsilon w_1'(1) + \int_x^1 (aw_1')(t)dt. \quad (2.4)$$

Therefore, using (2.2) and (2.3) we have

$$|\varepsilon w_1'(1)| = | -w_1'(z) + \int_z^1 (aw_1')(t)dt | \leq Ce^{-\alpha x/\varepsilon}.$$

Using (2.4) and (2.2) we get

$$|\varepsilon w_1'(x)| \leq Ce^{-\alpha x/\varepsilon}$$

from which the required bound for  $k = 1$  follows. Using the differential equation again we have

$$\varepsilon w_1'' = -aw_1' \text{ and } \varepsilon w_1''' = (-w_1')'$$

from which the bounds for  $k = 2, 3$  respectively are obtained.  $\square$

**Lemma 2.6.** *The interior layer component  $w_2$  of the solution  $u_\varepsilon$  of  $(P_\varepsilon)$  and its derivatives satisfy the following bounds, for  $k=0, 1, 2, 3$ .*

$$|w_2(x)| \leq C\varepsilon^2$$

$$|w_2^{(k)}| \leq \begin{cases} C\varepsilon^{2-k}e^{-\alpha x/\varepsilon}, & x \in \Omega^- \\ C\varepsilon^{2-k}e^{-\alpha(x-d)/\varepsilon}, & x \in \Omega^+ \end{cases}$$

where  $C$  is a constant independent of  $\varepsilon$ .

**Proof.** The proof is analogous to that in [23]. We bound  $w_2$  using Lemma 2.1 and the barrier function  $\psi^\pm(x) = \phi(x) \pm w_2(x)$  where  $\phi(x)$  is defined as follows

$$\phi(x) = \frac{\varepsilon^2 A}{\alpha} \begin{cases} 1, & x \in \Omega^- \\ e^{-\alpha(x-d)/\varepsilon}, & x \in \Omega^+. \end{cases}$$

Clearly  $\psi^\pm(0) \geq 0, \psi^\pm(1) \geq 0, L_\varepsilon \psi^\pm \leq 0$  and  $[\psi'^\pm](d) \leq 0$ . Therefore, by Lemma 2.1,  $\psi^\pm \geq 0$ , for all  $x \in \bar{\Omega}$ , from which required bound on  $w_2$  follows.

In order to bound  $w'_2$  we introduce the function  $\tilde{w}_2(x) = w_2(x) - w_2(d)$ , from which it follows that  $L_\varepsilon \tilde{w} = 0, x \in \Omega^-, \tilde{w}(0) = -w_2(d), \tilde{w}(d) = 0$ . Consider the mesh functions

$$\psi^\pm = C\varepsilon^2 e^{-\alpha x/\varepsilon} \pm \tilde{w}(x)$$

It is clear that  $\psi^\pm(0) \geq 0, \psi^\pm(d) > 0$  and  $L_\varepsilon \psi^\pm \leq 0$ , therefore  $\psi^\pm \geq 0, x \in \Omega^-,$  from which we obtain  $|\tilde{w}(x)| \leq C\varepsilon^2 e^{-\alpha x/\varepsilon}$ . Then, as in Lemmas 2.5 and 2.6

$$\begin{aligned} \left| \int_x^d (a\tilde{w}') (t) dt \right| &= \left| a\tilde{w}|_x^d - \int_x^d (a'\tilde{w})(t) dt \right| \\ &\leq C\varepsilon^2 e^{-\alpha x/\varepsilon}. \end{aligned} \quad (2.5)$$

By the Mean Value Theorem there exists a point  $z \in (d - \varepsilon, d)$  such that

$$\begin{aligned} |\tilde{w}'(z)| &= \left| \frac{\tilde{w}(d) - \tilde{w}(d - \varepsilon)}{\varepsilon} \right| = \left| \frac{\tilde{w}(d - \varepsilon)}{\varepsilon} \right| \\ &\leq C'\varepsilon e^{-\alpha d/\varepsilon} \\ &\leq C'\varepsilon e^{-\alpha x/\varepsilon}, \quad x \in \Omega^-. \end{aligned} \quad (2.6)$$

Now integrating the differential equation defining  $\tilde{w}$  we get

$$\varepsilon \tilde{w}'(x) = \varepsilon \tilde{w}(d) + \int_x^d (a\tilde{w}') (t) dt \quad (2.7)$$

Using (2.5) and (2.6) we then obtain

$$\begin{aligned} |\varepsilon \tilde{w}'(d)| &\leq |\varepsilon \tilde{w}(z)| + \left| \int_z^d (a\tilde{w}')(t) dt \right| \\ &\leq C\varepsilon^2 e^{-\alpha x/\varepsilon} \end{aligned} \quad (2.8)$$

From (2.7) and (2.5) it then follows that  $|\tilde{w}'(x)| \leq C\varepsilon e^{-\alpha x/\varepsilon}$ ,  $x \in \Omega^-$ , the required bound for  $k = 1$ . From the differential equation we have

$$\begin{aligned} \varepsilon \tilde{w}''(x) &= -a\tilde{w}'(x) \text{ and} \\ \varepsilon \tilde{w}'''(x) &= -(a\tilde{w}')'(x) \end{aligned}$$

from which the bounds for  $k = 2, 3$  can be obtained for all  $x \in \Omega^-$ .

It only remains to obtain similar bounds for  $x \in \Omega^+$ . Consider the following barrier function

$$\psi^\pm(x) = C\varepsilon^2 e^{-\alpha(x-d)/\varepsilon} \pm \tilde{w}(x)$$

Then, by Lemma 1  $|\tilde{w}(x)| \leq C\varepsilon^2 e^{-\alpha(x-d)/\varepsilon}$ . Repeating the arguments above and choosing  $z \in (1 - \varepsilon, 1)$  we have

$$\begin{aligned} \left| \int_d^x (a\tilde{w}')'(t) dt \right| &\leq C\varepsilon^2 e^{-\alpha(x-d)/\varepsilon} \\ |\tilde{w}(z)| &\leq C'\varepsilon e^{-\alpha(x-d)/\varepsilon} \\ |\varepsilon \tilde{w}'(d)| &\leq C\varepsilon e^{-\alpha(x-d)/\varepsilon} \end{aligned}$$

Then, repeating the earlier arguments we obtain the required bounds for  $k = 1, 2, 3$ ,  $x \in \Omega^+$ .  $\square$

## 2.2 Discrete Problem

We now introduce a fitted mesh for  $(P_\varepsilon)$ . On  $\Omega$  a Shishkin mesh of  $N$  mesh intervals is constructed as follows. The domain,  $\bar{\Omega}$  is subdivided into the 3 subintervals

$$[0, \sigma] \cup [\sigma, d] \cup [d, 1]$$

for some  $\sigma$  such that  $0 < \sigma \leq \frac{d}{2}$ . On the first two subintervals, uniform meshes with  $\frac{N}{4}$  mesh-intervals are placed. A uniform mesh with  $\frac{N}{2}$  mesh-intervals is placed on the third subinterval. We use this subdivision as it is necessary to locate a mesh point at  $x = d$  in order to obtain bounds on the error in the scaled discrete derivatives; however, for the purposes of numerical computations, this is not required.

The points of the mesh contained in the domain  $\Omega^- \cup \Omega^+$  are denoted by

$$\Omega_\varepsilon^N = \{x_i : 1 \leq i \leq \frac{N}{2} - 1\} \cup \{x_i : \frac{N}{2} + 1 \leq i \leq N - 1\}$$

Clearly,  $x_{N/4} = \sigma$ ,  $x_{N/2} = d$  and  $\bar{\Omega}_\varepsilon^N = \{x_i\}_0^N$ . The mesh is fitted to  $(P_\varepsilon)$  by choosing  $\sigma$  as follows

$$\sigma = \min\left\{\frac{d}{2}, \frac{\varepsilon}{\alpha} \ln N\right\}$$

The three mesh widths are denoted in the following way

$$h = \frac{4\sigma}{N}, \quad H_1 = \frac{4(d - \sigma)}{N}, \quad H_2 = \frac{2(1 - d)}{N}$$

We use a standard upwind finite difference operator on the Shishkin mesh  $\bar{\Omega}_\varepsilon^N$ . Therefore the fitted mesh method for  $(P_\varepsilon)$  is

$$(P_\varepsilon) \left\{ \begin{array}{l} \text{Find a mesh function } U_\varepsilon \text{ such that,} \\ L_\varepsilon^N U_\varepsilon = \varepsilon \delta^2 U_\varepsilon + a(x_i) D^+ U_\varepsilon = f(x_i) \text{ for all } x \in \Omega_\varepsilon^N \cup \{d\}, \\ U_\varepsilon(0) = u_0, U_\varepsilon(1) = u_1, [DU(d)] = 0 \end{array} \right.$$

where

$$\delta^2 Z_i = \left( \frac{Z_{i+1} - Z_i}{x_{i+1} - x_i} - \frac{Z_i - Z_{i-1}}{x_i - x_{i-1}} \right) \frac{2}{x_{i+1} - x_{i-1}} \text{ and } D^+ Z_i = \frac{Z_{i+1} - Z_i}{x_{i+1} - x_i}$$

The following lemma establishes a discrete minimum principle, analogous to the continuous minimum principle in Lemma 1.

**Lemma 2.7.** *Suppose a mesh function  $Z$  satisfies*

$$Z(0) \geq 0, Z(1) \geq 0, L_\varepsilon^N Z(x_i) \leq 0, \text{ for all } x_i \in \Omega_\varepsilon^N,$$

and

$$D^+ Z(x_{N/2}) - D^- Z(x_{N/2}) \leq 0$$

then

$$Z(x_i) \geq 0 \text{ for all } x_i \in \bar{\Omega}_\varepsilon^N.$$

**Proof.** The proof is analogous to that in [23]. Let  $x_p$  be any point at which  $Z$  attains its minimum value on  $\bar{\Omega}_\varepsilon^N$ . If  $Z(x_p) \geq 0$  then there is nothing to prove. Therefore suppose that  $Z(x_p) < 0$ . From the hypothesis it is clear that  $p \neq 0, N$ , that is,  $x_p \in \Omega$ . First consider the case  $x_p \neq d$ , without loss of generality assume  $x_p > d$ . Since  $Z(x_p)$  is the minimum value

$$D^+ Z(x_p) \geq 0 \geq D^- Z(x_p)$$

which implies that

$$L_\varepsilon^N Z(x_p) \geq 0$$

In order to avoid a contradiction we must have  $L_\varepsilon^N Z(x_p) = 0$ , which implies that

$$Z(x_p) = Z(x_{p-1}) = Z(x_{p+1})$$

Repeating this argument at  $x_{p+1}$  we eventually conclude that  $Z(x_N) < 0$ , which is a contradiction.

We now consider  $x_p = d$ , therefore

$$D^+ Z(x_{N/2}) \geq 0 \geq D^- Z(x_{N/2}) \geq D^+ Z(x_{N/2})$$

implying that

$$Z(x_{N/2-1}) = Z(x_{N/2}) = Z(x_{N/2+1})$$

Repeating the earlier argument yields the desired conclusion.  $\square$

## 2.3 Error Analysis

The discrete solution  $U_\varepsilon$  can be decomposed, analogously to the continuous case, as follows.

$$U_\varepsilon = V_\varepsilon + W_\varepsilon$$

where  $V_\varepsilon$  and  $W_\varepsilon$  are respectively the solutions of the problems

$$\begin{aligned} L_\varepsilon^N V_\varepsilon &= f(x_i), \quad x_i \in \Omega_\varepsilon^N \setminus \{d\}, \\ V_\varepsilon(0) &= v_\varepsilon(0), \quad V_\varepsilon(1) = v_\varepsilon(1), \quad V_\varepsilon(d) = v_\varepsilon(d). \end{aligned}$$

$$\begin{aligned} L_\varepsilon^N W_\varepsilon &= 0, \quad x_i \in \Omega_\varepsilon^N \setminus \{d\}, \\ W_\varepsilon(0) &= w_\varepsilon(0), \quad W_\varepsilon(1) = 0, \\ [DW_\varepsilon(d)] &= -[DV_\varepsilon(d)] \end{aligned}$$

We denote the jump in the discrete derivative of a mesh function  $Z$  at the point  $x_i = d$  by  $[DZ(d)] = D^+Z(d) - D^-Z(d)$ . As in the continuous case we further decompose  $W_\varepsilon$  as  $W_\varepsilon = W_1 + W_2$  where  $W_1$  is defined as the solution of

$$\begin{aligned} L_\varepsilon^N W_1 &= 0, \quad x_i \in \Omega_\varepsilon^N \cup \{d\}, \\ W_1(0) &= w_\varepsilon(0), \quad W_1(1) = 0. \end{aligned}$$

and  $W_2$  is defined as the solution of

$$\begin{aligned} L_\varepsilon^N W_2 &= 0, \quad x_i \in \Omega_\varepsilon^N \setminus \{d\}, \\ W_2(0) &= W_2(1) = 0, \\ [DW_2(d)] &= -[DV_\varepsilon(d)] - [DW_1(d)] \end{aligned} \tag{2.9}$$

Combining the discrete and continuous decompositions we arrive at an analogous decomposition of the error,  $U_\varepsilon - u_\varepsilon = V_\varepsilon - v_\varepsilon + W_\varepsilon - w_\varepsilon$ . Therefore we can estimate the error  $U_\varepsilon - u_\varepsilon$  by estimating the errors  $V_\varepsilon - v_\varepsilon$  and  $W_\varepsilon - w_\varepsilon$  separately.

**Lemma 2.8.** *At each mesh point  $x_i \in \bar{\Omega}_\varepsilon^N$  the non-layer component of the error satisfies the estimates*

$$|(V_\varepsilon - v_\varepsilon)(x_i)| \leq \begin{cases} CN^{-1}(d - x_i), & x_i \leq d, \\ CN^{-1}(1 - x_i), & x_i \geq d. \end{cases}$$

where  $C$  is a constant independent of  $\varepsilon$  and  $N$ .

**Proof.** The proof here is analogous to that in [23]. Consider the local truncation error

$$L_\varepsilon^N(V_\varepsilon - v_\varepsilon) = (L_\varepsilon - L_\varepsilon^N)v_\varepsilon = \varepsilon\left(\frac{d^2}{dx^2} - \delta^2\right)v_\varepsilon + a\left(\frac{d}{dx} - D^+\right)v_\varepsilon.$$

Therefore by standard local truncation error estimates and Lemma 2.4 we have

$$|L_\varepsilon^N(V_\varepsilon - v_\varepsilon)(x_i)| \leq \frac{\varepsilon}{3}(x_{i+1} - x_{i-1})\|v_\varepsilon^{(3)}\| + \frac{a(x_i)}{2}(x_{i+1} - x_i)\|v_\varepsilon^{(2)}\| \leq CN^{-1}$$

for all  $x_i \in \bar{\Omega}_\varepsilon^N \setminus d$ . With the barrier functions

$$\psi^\pm(x_i) = \begin{cases} CN^{-1}(d - x_i) \pm (V_\varepsilon - v_\varepsilon)(x_i), & x_i \leq d \\ CN^{-1}(1 - x_i) \pm (V_\varepsilon - v_\varepsilon)(x_i), & x_i \geq d \end{cases}$$

and Lemma 2.7 the proof is completed in the usual manner.  $\square$

**Lemma 2.9.** *For all  $N \geq 4$  and at each mesh point  $x_i \in \Omega_\varepsilon^N \cup \{d\}$  the singular component of the error satisfies the estimate*

$$|(W_1 - w_1)(x_i)| \leq CN^{-1} \ln N$$

where  $C$  is a constant independent of  $\varepsilon$  and  $N$ .

**Proof.** Using the arguments from [21], we will first examine the case  $\sigma = d/2$ , which implies that  $\varepsilon^{-1} \leq C \ln N$  and  $h = H_1$ . Consider the local truncation error

$$L_\varepsilon^N(W_1 - w_1) \leq \frac{\varepsilon}{3}(x_{i+1} - x_{i-1})\|w_1^{(3)}\| + \frac{a(x_i)}{2}(x_{i+1} - x_{i-1})\|w_1^{(2)}\| \leq C\varepsilon^{-2}N^{-1}e^{-\alpha x_{i-1}/\varepsilon} \quad (2.10)$$

We introduce the two mesh functions

$$\psi_i^\pm = \begin{cases} \frac{1}{1-Y_{N/2}} \frac{Ce^{2\gamma h/\varepsilon}}{\gamma(\alpha-\gamma)} \varepsilon^{-1} N^{-1} Y_i \pm (W_1 - w_1)(x_i), & i < N/2 \\ \frac{1}{Y_{N/2}} \frac{Ce^{\gamma(h+H_2)/\varepsilon}}{\gamma(\alpha-\gamma)} \varepsilon^{-1} N^{-1} Y_i \pm (W_1 - w_1)(x_i), & i = N/2 \\ \frac{1}{Y_{N/2}} \frac{Ce^{2\gamma H_2/\varepsilon}}{\gamma(\alpha-\gamma)} \varepsilon^{-1} N^{-1} Y_i \pm (W_1 - w_1)(x_i), & i > N/2, \end{cases}$$

where  $\gamma$  is any constant satisfying  $0 < \gamma < \alpha$  and  $Y_i$  is the solution of the constant coefficient finite difference problem

$$\begin{aligned} (\varepsilon\delta^2 + \gamma D^+)Y_i &= 0, \quad 1 \leq i \leq N-1, \\ Y_0 &= 1, \quad Y_N = 0. \end{aligned} \quad (2.11)$$

Then

$$Y_i = \begin{cases} 1 + (Y_{N/2} - 1)l_i, & i \leq N/2 \\ Y_{N/2}r_i, & i \geq N/2 \end{cases} \quad (2.12)$$

where

$$\begin{aligned} l_i &= \frac{\lambda^{-i} - 1}{\lambda^{-N/2} - 1}, \quad \lambda = 1 + \frac{\gamma h}{\varepsilon} \\ r_i &= \frac{\Lambda^{-i} - \Lambda^{-N}}{\Lambda^{-N/2} - \Lambda^{-N}}, \quad \Lambda = 1 + \frac{\gamma H_2}{\varepsilon} \end{aligned} \quad (2.13)$$

and  $Y_{N/2}$  satisfies

$$(\varepsilon\delta^2 + \gamma D^+)Y_{N/2} = 0$$

therefore

$$Y_{N/2} = \left(1 - \frac{D^+ r_{N/2} \lambda + \Lambda}{D^- l_{N/2} 2}\right)^{-1}$$

where

$$D^+ r_{N/2} = -\frac{\gamma}{\varepsilon} \frac{1}{\Lambda - \Lambda^{-N/2+1}}$$

$$D^- l_{N/2} = \frac{\gamma}{\varepsilon} \frac{1}{\lambda^{N/2} - 1}.$$

It is easy to see that

$$0 \leq Y_{N/2} \leq 1. \quad (2.14)$$

We have, from (2.12), (2.13) and (2.14)

$$D^+ Y_i \leq \begin{cases} -\frac{\gamma}{\varepsilon} [1 - Y_{N/2}] e^{-\gamma x_{i+1}/\varepsilon}, & i < N/2 \\ -\frac{\gamma}{\varepsilon} Y_{N/2} e^{-\gamma(x_{i+1}-d)/\varepsilon}, & i \geq N/2 \end{cases} \quad (2.15)$$

It is clear that  $\psi_0^\pm > 0$ ,  $\psi_N^\pm = 0$  and using (2.10) and (2.15) we obtain the following for  $i < N/2$

$$\begin{aligned} L_\varepsilon^N \psi_i^\pm &= \frac{1}{1 - Y_{N/2}} \frac{C e^{2\gamma h/\varepsilon}}{\gamma(\alpha - \gamma)} \varepsilon^{-1} N^{-1} (a(x_i) - \gamma) D^+ Y_i \pm L_\varepsilon^N (W_1 - w_1) \\ &\leq C \varepsilon^{-2} N^{-1} \left( e^{-\alpha x_{i-1}/\varepsilon} - \frac{a(x_i) - \gamma}{\alpha - \gamma} e^{-\gamma x_{i-1}/\varepsilon} \right) \\ &< 0. \end{aligned}$$

When  $i = N/2$

$$\begin{aligned}
L_\varepsilon^N \psi_{N/2}^\pm &= \frac{1}{Y_{N/2}} \frac{C e^{\gamma(h+H_2)/\varepsilon}}{\gamma(\alpha - \gamma)} \varepsilon^{-1} N^{-1} (a(x_i) - \gamma) D^+ Y_{N/2} \pm L_\varepsilon^N (W_1 - w_1) \\
&\leq C \varepsilon^{-2} N^{-1} (e^{-\alpha x_{N/2-1}/\varepsilon} - \frac{a(x_i) - \gamma}{\alpha - \gamma} e^{\gamma h/\varepsilon}) \\
&< 0.
\end{aligned}$$

Finally, when  $i > N/2$

$$\begin{aligned}
L_\varepsilon^N \psi_i^\pm &= \frac{1}{Y_{N/2}} \frac{C e^{2\gamma H_2/\varepsilon}}{\gamma(\alpha - \gamma)} \varepsilon^{-1} N^{-1} (a(x_i) - \gamma) D^+ Y_i \pm L_\varepsilon^N (W_1 - w_1) \\
&\leq C \varepsilon^{-2} N^{-1} (e^{-\alpha x_{i-1}/\varepsilon} - \frac{a(x_i) - \gamma}{\alpha - \gamma} e^{-\gamma(x_{i-1}-d)/\varepsilon}) \\
&< 0.
\end{aligned}$$

Therefore using the discrete minimum principle in Section 2.3 of [21] we conclude that  $\psi_i^\pm \geq 0$ . And so for all  $x_i \in \bar{\Omega}_\varepsilon^N \cup d$ ,  $i < N/2$  we have

$$\begin{aligned}
|(W_1 - w_1)| &\leq \frac{Y_i}{1 - Y_{N/2}} \frac{C e^{2\gamma h/\varepsilon}}{\gamma(\alpha - \gamma)} \varepsilon^{-1} N^{-1} \\
&\leq C N^{-1} \ln N
\end{aligned}$$

since

$$\begin{aligned}
\frac{Y_i}{1 - Y_{N/2}} &\leq \frac{1}{1 - Y_{N/2}} \\
&= 1 + \frac{2}{\lambda + \Lambda} \frac{\Lambda(1 - \Lambda^{-N/2})}{\lambda^{N/2} - 1} \\
&\leq 1 + \frac{2}{\lambda + \Lambda} \frac{\varepsilon}{\gamma d} \leq C.
\end{aligned}$$

When  $i = N/2$  we have

$$\begin{aligned} |(W_1 - w_1)| &\leq \frac{Ce^{\gamma(h+H_2)/\varepsilon}}{\gamma(\alpha - \gamma)} \varepsilon^{-1} N^{-1} \\ &\leq CN^{-1} \ln N. \end{aligned}$$

And when  $i > N/2$  we have

$$\begin{aligned} |(W_1 - w_1)| &\leq \frac{Y_i}{Y_{N/2}} \frac{Ce^{2\gamma H_2/\varepsilon}}{\gamma(\alpha - \gamma)} \varepsilon^{-1} N^{-1} \\ &\leq r_i \frac{Ce^{2\gamma H_2/\varepsilon}}{\gamma(\alpha - \gamma)} \varepsilon^{-1} N^{-1} \\ &\leq CN^{-1} \ln N \end{aligned}$$

We now consider the case where  $\sigma = \frac{\varepsilon}{\alpha} \ln N$  and give separate proofs in the coarse and fine mesh subintervals. First take  $x_i \in [\sigma, 1]$ . By the triangle inequality

$$|(W_1 - w_1)(x_i)| \leq |W_1(x_i)| + |w_1(x_i)|$$

By Lemma 2.5 we have

$$|w_1(x_i)| \leq Ce^{-\alpha x_i/\varepsilon} \varepsilon \leq Ce^{-\alpha \sigma/\varepsilon} = CN^{-1}.$$

To bound  $|W_1(x_i)|$  we introduce a mesh function  $Y_i$  which is the solution of the constant coefficient finite difference problem

$$\begin{aligned} (\varepsilon \delta^2 + \alpha D^+) Y_i &= 0, \quad 1 \leq i \leq N-1, \\ Y_0 &= 1, \quad Y_N = 0. \end{aligned}$$

Then

$$Y_i = \begin{cases} 1 + (Y_{N/4} - 1)l_i, & i \leq N/4 \\ Y_{N/4} + (Y_{N/2} - Y_{N/4})m_i, & N/4 \leq i \leq N/2 \\ Y_{N/2} n_i, & i \geq N/2 \end{cases} \quad (2.16)$$

where

$$\begin{aligned} l_i &= \frac{1 - \lambda^{-i}}{1 - \lambda^{-N/4}}, \quad \lambda = 1 + \frac{\alpha h}{\varepsilon}, \\ m_i &= \frac{\Lambda_1^{-i} - \Lambda_1^{-N/4}}{\Lambda_1^{-N/2} - \Lambda_1^{-N/4}}, \quad \Lambda_1 = 1 + \frac{\alpha H_1}{\varepsilon}, \\ n_i &= \frac{\Lambda_2^{-i} - \Lambda_2^{-N}}{\Lambda_2^{-N/2} - \Lambda_2^{-N}}, \quad \Lambda_2 = 1 + \frac{\alpha H_2}{\varepsilon} \end{aligned} \quad (2.17)$$

and  $Y_{N/4}$ ,  $Y_{N/2}$  satisfy

$$\begin{aligned} (\varepsilon\delta^2 + \alpha D^+)Y_{N/4} &= 0, \\ (\varepsilon\delta^2 + \alpha D^+)Y_{N/2} &= 0 \end{aligned} \quad (2.18)$$

respectively. Also, from (2.16) we have

$$D^+Y_i = \begin{cases} -\frac{\alpha}{\varepsilon}(1 - Y_{N/4})\frac{\lambda^{-i-1}}{1 - \lambda^{-N/4}}, & i < N/4 \\ -\frac{\alpha}{\varepsilon}(Y_{N/4} - Y_{N/2})\frac{\Lambda_1^{-i-1}}{\Lambda_1^{-N/4} - \Lambda_1^{-N/2}}, & N/4 \leq i < N/2 \\ -\frac{\alpha}{\varepsilon}Y_{N/2}\frac{\Lambda_2^{-i-1}}{\Lambda_2^{-N/2} - \Lambda_2^{-N}}, & i \geq N/2 \end{cases} \quad (2.19)$$

It is easy to see that

$$\begin{aligned}
D^- l_{N/4} &= \frac{\alpha}{\varepsilon} \frac{\lambda^{-N/4}}{1 - \lambda^{-N/4}} > 0 \\
D^+ m_{N/4} &= \frac{\alpha}{\varepsilon} \frac{\Lambda_1^{-1}}{1 - \Lambda_1^{-N/4}} > 0 \\
D^- m_{N/2} &= \frac{\alpha}{\varepsilon} \frac{1}{\Lambda_1^{N/4} - 1} > 0 \\
D^+ n_{N/2} &= -\frac{\alpha}{\varepsilon} \frac{\Lambda_2^{-1}}{1 - \Lambda_2^{-N/2}}
\end{aligned} \tag{2.20}$$

Solving (2.18) and using (2.20) it can be shown that

$$0 \leq Y_{N/2} \leq Y_{N/4} \leq 1. \tag{2.21}$$

Combining (2.21) and (2.19) it is clear that

$$D^+ Y_i \leq 0, \quad 1 \leq i \leq N - 1 \tag{2.22}$$

We now observe the inequality, analogous to that in [21], for all  $N \geq 1$

$$\left(1 + \frac{4 \ln N}{N}\right)^{-N/4} \leq 4N^{-1} \tag{2.23}$$

Also note that

$$\lambda = 1 + \frac{\alpha h}{\varepsilon} = 1 + 4N^{-1} \ln N. \tag{2.24}$$

Combining the above inequalities we obtain

$$\lambda^{-N/4} \leq 4N^{-1}. \tag{2.25}$$

Then, from (2.20) and (2.25) we obtain

$$\begin{aligned}0 &\leq \frac{\varepsilon}{\alpha} D^- l_{N/4} \leq \frac{4N^{-1}}{1-4N^{-1}} \leq 8N^{-1} \\ \frac{\varepsilon}{\alpha} D^+ m_{N/4} &\geq \frac{1}{\Lambda_1} \\ 0 &\leq \frac{\varepsilon}{\alpha} D^- m_{N/2} \leq \frac{4N^{-1}}{1-4N^{-1}} \leq 8N^{-1} \\ -\frac{\varepsilon}{\alpha} D^+ n_{N/2} &\geq \frac{1}{\Lambda_2}\end{aligned}$$

which we use to establish the following inequality

$$\begin{aligned}
0 \leq Y_{N/4} &= \frac{D^- l_{N/4} \left(1 - \frac{\Lambda_1 + \Lambda_2}{2} \frac{D^+ n_{N/2}}{D^- m_{N/2}}\right)}{\left(D^- l_{N/4} + \frac{\lambda + \Lambda_1}{2} D^+ m_{N/4}\right) \left(1 - \frac{\Lambda_1 + \Lambda_2}{2} \frac{D^+ n_{N/2}}{D^- m_{N/2}}\right) - \frac{\lambda + \Lambda_1}{2} D^+ m_{N/4}} \\
&\leq \frac{D^- l_{N/4} \left(1 - \frac{\Lambda_1 + \Lambda_2}{2} \frac{D^+ n_{N/2}}{D^- m_{N/2}}\right)}{\frac{\lambda + \Lambda_1}{2} D^+ m_{N/4} \left(-\frac{\Lambda_1 + \Lambda_2}{2} \frac{D^+ n_{N/2}}{D^- m_{N/2}}\right)} \\
&= \frac{2}{\lambda + \Lambda_1} \frac{D^- l_{N/4}}{D^+ m_{N/4}} \left(1 - \frac{2}{\Lambda_1 + \Lambda_2} \frac{D^- m_{N/2}}{D^+ n_{N/2}}\right) \\
&\leq 16N^{-1} \left(1 - \frac{2}{\Lambda_1 + \Lambda_2} \frac{D^- m_{N/2}}{D^+ n_{N/2}}\right) \\
&\leq 16N^{-1} \left(1 + \frac{2\Lambda_2}{\Lambda_1 + \Lambda_2} 8N^{-1}\right) \\
&\leq 48N^{-1}
\end{aligned}$$

We introduce the 2 mesh functions

$$\psi_i^\pm = |W_1(0)| Y_i \pm W_1(x_i)$$

Clearly  $\psi_0^\pm \geq 0$ ,  $\psi_N^\pm = 0$ , and  $L_\varepsilon^N \psi_i^\pm = |W_1(0)| (a(x_i) - \alpha) D^+ Y_i \leq 0$ . Therefore by the discrete minimum principle in Section 2.3 of [21] it follows that  $\psi_i^\pm \geq 0$ ,  $1 \leq i \leq N - 1$ . Using Lemma 2.5 we have, for all  $x_i \in [\sigma, 1]$

$$|W_1(x_i)| \leq |W_1(0)| Y_i \leq |W_1(0)| Y_{N/4} \leq CN^{-1}$$

as required

To complete the proof we use the arguments from [21]. We must show that the result holds for  $x_i \in (0, \sigma)$ , since for  $i = 0$  there is nothing to prove. From (2.10) and  $\sigma = \frac{\varepsilon}{\alpha} \ln N$  we have

$$L_\varepsilon^N (W_1 - w_1) \leq C\sigma\varepsilon^{-2} N^{-1} e^{-\alpha x_{i-1}/\varepsilon} \quad (2.26)$$

For  $i \in [0, N/4]$  we introduce the two mesh functions

$$\psi_i^\pm = \frac{Ce^{2\gamma h/\varepsilon}}{\gamma(\alpha - \gamma)} \sigma \varepsilon^{-1} N^{-1} Y_i + C' N^{-1} \pm (W_1 - w_1)(x_i)$$

where  $\gamma$  is as defined above and, for all  $i \in [0, N/4]$ ,

$$Y_i = \frac{\lambda^{N/4-i} - 1}{\lambda^{N/4} - 1}, \quad \lambda = 1 + \frac{\gamma h}{\varepsilon}$$

$$D^+ Y_i \leq -\frac{\gamma}{\varepsilon} e^{-\gamma x_{i+1}/\varepsilon} < 0, \quad 0 \leq Y_i \leq 1.$$

Then  $\psi_0^\pm > 0$ ,  $\psi_{N/4}^\pm \geq 0$  and  $L_\varepsilon^N \psi_i^\pm \leq 0$ , therefore by the discrete minimum principle in Section 2.3 of [21],  $\psi_i^\pm \geq 0$  for all  $i \in [0, N/4]$ , from which the required result follows.  $\square$

**Lemma 2.10.** *The following parameter-uniform bound holds for  $N \geq 8$*

$$|(W_2 - w_2)(x_i)| \leq CN^{-1} \ln N$$

where  $C$  is a constant independent of  $N$  and  $\varepsilon$ .

**Proof.** The proof is analogous to that in [23]. We start by obtaining a bound on  $|[D(W_2 - w_2)(d)]|$ , firstly re-writing the expression as follows:

$$\begin{aligned} [D(W_2 - w_2)(d)] &= [DW_2(d)] - [Dw_2(d)] \\ &= [v'_\varepsilon(d)] - [DV_\varepsilon(d)] + [w'_2(d)] - [Dw_2(d)] - [DW_1(d)]. \end{aligned}$$

Furthermore note that

$$[v'_\varepsilon(d)] - [DV_\varepsilon(d)] = v'_\varepsilon(d^+) - D^+ v_\varepsilon(d) - \left( v'_\varepsilon(d^-) - D^- v_\varepsilon(d) \right) + [D(v_\varepsilon - V_\varepsilon)(d)].$$

By the triangle inequality

$$|[D(v_\varepsilon - V_\varepsilon)]| \leq |D^+(v_\varepsilon - V_\varepsilon)| + |D^-(v_\varepsilon - V_\varepsilon)|$$

As in [21] on  $[d, 1]$ ,  $|\varepsilon D^+(v_\varepsilon - V_\varepsilon)(x_i)| \leq CN^{-1}$  and by Lemma (2.8)

$$|D^-(v_\varepsilon - V_\varepsilon)(d)| = |(v_\varepsilon - V_\varepsilon)(d - H_1)/H_1| \leq CN^{-1}.$$

Therefore,

$$|[D(v_\varepsilon - V_\varepsilon)(d)]| \leq C(\varepsilon N)^{-1}.$$

Additionally note that

$$|[v'_\varepsilon(d)] - [Dv_\varepsilon(d)]| \leq CN^{-1}\|v_\varepsilon^{(2)}\|_{\Omega \cup \Omega^+} \leq CN^{-1}.$$

Therefore

$$|[v'_\varepsilon(d)] - [DV_\varepsilon(d)]| \leq C(\varepsilon N)^{-1}.$$

Similarly

$$[w'_2(d)] - [Dw_2(d)] = w'_2(d^+) - D^+w_2(d) - \left( w'_2(d^-) - D^-w_2(d) \right).$$

And so

$$\begin{aligned} |[w'_2(d)] - [Dw_2(d)]| &\leq CH_2\|w_2^{(2)}\|_{[d, d+H_2]} + CH_1\|w_2^{(2)}\|_{[d-H_1, d]} \\ &\leq CH_2 + CH_1e^{-\alpha(d-H_1)/\varepsilon} \leq CN^{-1} \end{aligned}$$

Finally, we have

$$|[Dw_1(d)]| \leq (H_2 + H_1)|w_1''(d - H_1)| \leq C\varepsilon^{-2}e^{-\alpha(d-H_1)/\varepsilon} \leq CN^{-1},$$

since  $e^{-\alpha(d-H_1)/\varepsilon} \leq e^{-\alpha(d-4/N)/\varepsilon} \leq e^{-\alpha d/2\varepsilon}$ . Note that by the arguments in [21] and by Lemma 2.9,  $|[D(w_1 - W_1)(d)]| \leq C(\varepsilon N)^{-1} \ln N$ . Therefore by the triangle inequality we have

$$|[D(w_2 - W_2)(d)]| \leq C(\varepsilon N)^{-1} \ln N.$$

We now consider the local truncation error on  $\Omega_\varepsilon^N$ . Using the bounds on the derivatives of  $w_2$  and standard local truncation error bounds we obtain the following for  $x_i \in (d, 1)$

$$\begin{aligned} |L_\varepsilon^N(W_2 - w_2)(x_i)| &\leq \frac{\varepsilon}{3}(x_{i+1} - x_{i-1})\|w_2^{(3)}\|_{[x_{i-1}, x_{i+1}]} + \frac{a(x_i)}{2}(x_{i+1} - x_i)\|w_2^{(2)}\|_{[x_i, x_{i+1}]} \\ &\leq CH_2e^{-\alpha(x_{i-1}-d)/\varepsilon} \\ &\leq CN^{-1}. \end{aligned}$$

For  $x \in [\sigma, d)$  we have

$$\begin{aligned} |L_\varepsilon^N(W_2 - w_2)(x_i)| &\leq C(h + H_1)e^{-\alpha(\sigma-h)/\varepsilon} \\ &\leq CN^{-1}. \end{aligned}$$

Finally, for  $x_i \in (0, \sigma)$  we get

$$|L_\varepsilon^N(W_2 - w_2)(x_i)| \leq Ch \leq CN^{-1}.$$

In summary we have

$$|L_\varepsilon^N(W_2 - w_2)| \leq CN^{-1} \text{ and } |[D(w_2 - W_2)(d)]| \leq C(\varepsilon N)^{-1} \ln N.$$

The remainder of the proof is analogous to that in [23]. Consider the following mesh functions

$$\phi_i^\pm = CN^{-1} \ln N \begin{cases} 1, & x_i \leq d \\ \psi_i, & x_i \geq d, \end{cases} + CN^{-1} \ln N(1 - x_i) \pm (W_2 - w_2)(x_i)$$

where  $\psi_i$  is defined as follows

$$(\varepsilon\delta^2 + \alpha D^+)\psi_i = 0, \quad \psi_{N/2} = 1, \quad \psi_N = 0.$$

Then  $\phi_0^\pm > 0$ ,  $\phi_N^\pm = 0$ ,  $L_\varepsilon^N \phi^\pm \leq 0$  and  $[D\phi^\pm(d)] \leq 0$ , from which the required bound follows.

**Theorem 2.11.** *Let  $U_\varepsilon$ ,  $u_\varepsilon$  be, respectively, the solutions of  $(P_\varepsilon^N)$  and  $(P_\varepsilon)$ . Then for all  $N \geq 4$*

$$\sup_{0 < \varepsilon \leq 1} \|(U_\varepsilon - u_\varepsilon)(x_i)\|_{\Omega_\varepsilon^N} \leq CN^{-1} \ln N$$

where  $C$  is a constant independent of  $N$  and  $\varepsilon$ .

**Proof.** This result is obtained by combining Lemmas 2.8, 2.9 and 2.10.  $\square$

**Lemma 2.12.** *For all  $N \geq 8$*

$$\sup_{0 < \varepsilon \leq 1} \|(\bar{U}_\varepsilon - u_\varepsilon)(x_i)\|_{\Omega_\varepsilon^N} \leq CN^{-1} \ln N$$

where  $\bar{U}_\varepsilon$  is the piecewise linear interpolant of  $U_\varepsilon$  on  $\bar{\Omega}$  and  $C$  is a constant independent of  $N$  and  $\varepsilon$  and  $C$  is a constant independent of  $\varepsilon$  and  $N$ .

**Proof.** The proof is analogous to that in [21]. Let  $\bar{u}_\varepsilon$  be the piecewise linear interpolant of the values of  $u_\varepsilon$  at the mesh points  $\bar{\Omega}_\varepsilon^N$ , i.e.

$$\bar{u}_\varepsilon = \sum_{i=0}^N u_\varepsilon(x_i) \phi_i(x)$$

where  $\phi_i(x)$  is the piecewise linear function defined by  $\phi_i(x_j) = \delta_{i,j}$ , for all  $i, j \in [0, N]$ . By the triangle inequality we have

$$\|\bar{U}_\varepsilon - u_\varepsilon\| \leq \|\bar{U}_\varepsilon - \bar{u}_\varepsilon\| + \|\bar{u}_\varepsilon - u_\varepsilon\|. \quad (2.27)$$

To bound the first term on the right-hand side, note that

$$\bar{U}_\varepsilon - \bar{u}_\varepsilon = \sum_{i=0}^{N-1} (U_\varepsilon - u_\varepsilon)(x_i) \phi_i(x)$$

By Theorem 2.11 we have

$$|(U_\varepsilon - u_\varepsilon)(x_i)| \leq CN^{-1} \ln N$$

and since  $\phi_i(x) \geq 0$  and  $\|\sum_{i=1}^{N-1} \phi_i\| \leq 1$ , it is easy to see that

$$\|\bar{U}_\varepsilon - \bar{u}_\varepsilon\| \leq CN^{-1} \ln N.$$

It remains to bound the second term on the right-hand side. Note the classical estimate for linear interpolation,  $i \in [0, N-1]$  and  $f \in C^2(\Omega_i)$ , where  $\Omega_i = (x_i, x_{i+1})$  and  $x_i \in \bar{\Omega}_i$

$$|(\bar{f} - f)(x)| \leq \frac{1}{2} (x_{i+1} - x_i)^2 \|f''\|_{\Omega_i}. \quad (2.28)$$

We now decompose the interpolation error analogously to the decomposition

of the exact solution  $u_\varepsilon$

$$\bar{u}_\varepsilon - u_\varepsilon = \bar{v}_\varepsilon - v_\varepsilon + \bar{w}_\varepsilon - w_\varepsilon$$

where  $\bar{v}_\varepsilon$  and  $\bar{w}_\varepsilon$  are the piecewise linear interpolants of the values of  $v_\varepsilon$  and  $w_\varepsilon$  respectively at the mesh points  $\bar{\Omega}_\varepsilon^N$ . We bound each of the two components on the right-hand side separately. From (2.28) and Lemma 2.4 we have

$$\|\bar{v}_\varepsilon - v_\varepsilon\| \leq CN^{-2}. \quad (2.29)$$

and, for all  $x_i \in \bar{\Omega}_i$ ,

$$|(\bar{w}_\varepsilon - w_\varepsilon)(x)| \leq C(x_{i+1} - x_i)^2 \varepsilon^{-2}. \quad (2.30)$$

When  $\sigma = \frac{d}{2}$  we have  $\varepsilon^{-1} \leq C \ln N$ . Therefore from (2.30) we get

$$\|(\bar{w}_\varepsilon - w_\varepsilon)(x)\| \leq C(N^{-1} \ln N)^2.$$

In the case where  $\sigma = \frac{\varepsilon}{\alpha} \ln N$  we have, from (2.30)

$$\|(\bar{w}_\varepsilon - w_\varepsilon)(x)\|_{[0, \sigma]} \leq C\left(\frac{\sigma}{\varepsilon}\right)^2 N^{-2} \leq C(N^{-1} \ln N)^2.$$

and from Lemma 2.5 we have

$$\|(\bar{w}_1 - w_1)(x)\|_{[\sigma, 1]} \leq 2\|w_1\|_{[\sigma, 1]} \leq Ce^{-\alpha\sigma/\varepsilon} = CN^{-1}.$$

From Lemma 2.6 we have, for  $x_i \in [\sigma, 1]$

$$\|(\bar{w}_2 - w_2)(x_i)\| \leq CN^{-2}.$$

Therefore,

$$\|(\bar{w}_\varepsilon - w_\varepsilon)(x)\| \leq CN^{-1} \ln N. \quad (2.31)$$

The proof is completed by combining (2.29) and (2.31) and using the triangle inequality.  $\square$

**Lemma 2.13.** *For each  $x_i \in \Omega_\varepsilon^N \cup \{0\}$  and all  $x \in \bar{\Omega}_i$  we have*

$$|\varepsilon(D^+u_\varepsilon(x_i) - u'_\varepsilon(x))| \leq CN^{-1} \ln N$$

where  $C$  is a constant independent of  $N$  and  $\varepsilon$ .

**Proof.** The proof is analogous to that in [21]. It is clear that

$$|\varepsilon(D^+u_\varepsilon(x_i) - u'_\varepsilon(x))| \leq |\varepsilon(D^+v_\varepsilon(x_i) - v'_\varepsilon(x))| + |\varepsilon(D^+w_\varepsilon(x_i) - w'_\varepsilon(x))|.$$

We will therefore complete the proof by bounding each term on the right-hand side separately. Note the following identity for any function  $\phi \in C^2(\Omega_i)$

$$D^+\phi(x_i) - \phi'(x) = \frac{1}{x_{i+1} - x_i} \int_{s=x_i}^{x_{i+1}} \int_{t=x_i}^s \phi''(t) dt ds - \int_{t=x_i}^x \phi''(t) dt \quad (2.32)$$

from which we get

$$|D^+\phi(x_i) - \phi'(x)| \leq \frac{3}{2}(x_{i+1} - x_i) \|\phi''\|_{\bar{\Omega}_i} \quad (2.33)$$

We can then use this inequality, along with Lemma 2.4, to bound the first term on the right-hand side as follows

$$\varepsilon|D^+v_\varepsilon(x_i) - v'_\varepsilon(x)| \leq C \frac{3}{2}(x_{i+1} - x_i) \|\varepsilon v''_\varepsilon\|_{\bar{\Omega}_i} \leq CN^{-1} \quad (2.34)$$

For the second term we have

$$\varepsilon|D^+w_\varepsilon(x_i) - w'_\varepsilon(x)| \leq \varepsilon|D^+w_1(x_i) - w'_1(x)| + \varepsilon|D^+w_2(x_i) - w'_2(x)|.$$

By Lemma 2.6 the second term on the right-hand side is bounded as follows

$$\varepsilon|D^+w_2(x_i) - w'_2(x)| \leq C\frac{3}{2}(x_{i+1} - x_i)\|\varepsilon w''_2\|_{\bar{\Omega}_i} \leq CN^{-1}.$$

For the first term on the righthand side we have

$$\varepsilon|D^+w_1(x_i) - w'_1(x)| \leq C\frac{3}{2}(x_{i+1} - x_i)\|\varepsilon w''_1\|_{\bar{\Omega}_i} \leq C\varepsilon^{-1}(x_{i+1} - x_i). \quad (2.35)$$

We first consider the case where  $\sigma = d/2$ , therefore  $x_{i+1} - x_i = CN^{-1}$  and  $\varepsilon^{-1} \leq C' \ln N$ , yielding the required bound. In the case where  $\sigma = \frac{\varepsilon}{\alpha} \ln N$  note that for  $x \in [0, \sigma)$  we have  $x_{i+1} - x_i = 4\sigma N^{-1}$ , from which the required result follows from (2.35).

It only remains to consider the case where  $\sigma = \frac{\varepsilon}{\alpha} \ln N$  and  $x_i \in [\sigma, 1)$ . Using the differential equation for  $w_1$  and integrating by parts and applying Lemma 2.5 we get

$$\left| \int_{t=x_i}^s \varepsilon w''_1(t) dt \right| = \left| \int_{t=x_i}^s (a'w_1)(t) dt - (aw_1)(t)|_{t=x_i}^s \right| \leq Ce^{-\alpha\sigma/\varepsilon} = CN^{-1}.$$

The required bound is then obtained by using the above result and (2.32) for  $\varepsilon w_\varepsilon$ .  $\square$

**Lemma 2.14.** *For each  $x_i \in \Omega_\varepsilon^N \cup \{0\}$  we have*

$$|\varepsilon[D^+(V_\varepsilon(x_i) - v_\varepsilon(x))]| \leq CN^{-1}$$

where  $C$  is a constant independent of  $N$  and  $\varepsilon$ .

**Proof.** The proof is analogous to that in [21]. Let  $e_i = (V_\varepsilon - v_\varepsilon)(x_i)$  and  $\tau_i = L_\varepsilon^N e_i$ , therefore  $e_N = 0$  and, by Lemma 2.8 we have

$$|\varepsilon D^+ e_{N-1}| = \frac{|\varepsilon e_{N-1}|}{1 - x_{N-1}} \leq C\varepsilon N^{-1}$$

We now prove the claim for  $i \in [0, N-2]$ . Rewriting the relation  $\tau_i = L_\varepsilon^N e_i$  we get

$$\varepsilon D^+ e_j - \varepsilon D^+ e_{j-1} + (1/2)(x_{j+1} - x_{j-1})a(x_j)D^+ e_j = (1/2)(x_{j+1} - x_{j-1})\tau_j.$$

Summing and rearranging we obtain

$$|\varepsilon D^+ e_i| \leq |\varepsilon D^+ e_{N-1}| + (1/2) \sum_{j=i+1}^{N-1} (x_{j+1} - x_{j-1})|\tau_j| + (1/2) \left| \sum_{j=i+1}^{N-1} (x_{j+1} - x_{j-1})a(x_j)D^+ e_j \right|.$$

The first term on the right-hand side has already been bounded. It was established in the proof of Lemma 2.8 that  $|\tau_j| \leq CN^{-1}$ , therefore the second term is also bounded by  $CN^{-1}$ . It only remains to bound the final term on the right-hand side. Note that

$$\begin{aligned} (x_{j+1} - x_{j-1})a(x_j)D^+ e_j &= \frac{x_{j+1} - x_{j-1}}{x_{j+1} - x_j} a(x_j)e_{j+1} - \frac{x_j - x_{j-2}}{x_j - x_{j-1}} a(x_{j-1})e_j \\ &\quad - \frac{x_{j+1} - x_{j-1}}{x_{j+1} - x_j} (a(x_j) - a(x_{j-1}))e_j \\ &\quad - \left( \frac{x_{j+1} - x_{j-1}}{x_{j+1} - x_j} - \frac{x_j - x_{j-2}}{x_j - x_{j-1}} \right) a(x_{j-1})e_j. \end{aligned}$$

Summing both sides we have, for  $i < N/4$

$$\begin{aligned}
\sum_{j=i+1}^{N-1} (x_{j+1} - x_{j-1})a(x_j)D^+e_j &= -\frac{x_{i+1} - x_{i-1}}{x_{i+1} - x_i}a(x_i)e_{i+1} \\
&\quad - \sum_{j=i+1}^{N-1} \frac{x_{j+1} - x_{j-1}}{x_{j+1} - x_j}(a(x_j) - a(x_{j-1}))e_j \\
&\quad + (1 - \frac{h}{H_1})(a(x_{N/4-1})e_{N/4} - a(x_{N/4})e_{N/4+1}) \\
&\quad + (1 - \frac{H_1}{H_2})(a(x_{N/2-1})e_{N/2} - a(x_{N/2})e_{N/2+1})
\end{aligned}$$

For  $N/4 \leq i < N/2$  some or all of the second last term on the right-hand side will be zero. For  $i \geq N/2$  the second last term on the right-hand side will be zero and some or all of the last term will be zero. From Lemma 2.8 we know  $|e_i| \leq CN^{-1}$ . For  $i \neq N/2$  we have  $\frac{x_{i+1}-x_{i-1}}{x_{i+1}-x_i} \leq 2$  and for  $i = N/2$  we have

$$\frac{x_{N/2+1} - x_{N/2-1}}{x_{N/2+1} - x_{N/2}} = \frac{H_1 + H_2}{H_2} = \frac{(1-d) + 2(d-\sigma)}{1-d} \leq \frac{2}{1-d}.$$

Additionally,

$$\left|1 - \frac{H_1}{H_2}\right| = \left|\frac{1-3d-2\sigma}{1-d}\right| \leq \left|\frac{1-2d}{1-d}\right| \leq 1$$

Therefore we have the following for all  $i \in [0, N-2]$

$$\left|\sum_{j=i+1}^{N-1} (x_{j+1} - x_{j-1})a(x_j)D^+e_j\right| \leq CN^{-1}$$

from which the required result is obtained.  $\square$

**Lemma 2.15.** *For all  $x_i \in \Omega_\varepsilon^N \cup \{0\}$  we have*

$$|\varepsilon D^+(W_\varepsilon - w_\varepsilon)(x_i)| \leq CN^{-1} \ln N$$

where  $C$  is a constant independent of  $N$  and  $\varepsilon$ .

**Proof.** By the triangle inequality we have

$$|\varepsilon D^+(W_\varepsilon - w_\varepsilon)(x_i)| \leq |\varepsilon D^+(W_1 - w_1)(x_i)| + |\varepsilon D^+(W_2 - w_2)(x_i)|$$

The first term on the righthand side may be bounded using the arguments in Section 3.5 of [21]. In the case of the second term, the proof is analogous to that in [23]. We first obtain the required bound on  $[d, 1]$ . Let  $e_i = (W_2 - w_2)(x_i)$  and  $\tau_i = L_\varepsilon^N e_i$ . Note that we can show that for  $x_i \geq d$

$$|(W_2 - w_2)(x_i)| \leq CN^{-1} \ln N(1 - x_i) \quad (2.36)$$

using the following barrier function

$$\phi_i = CN^{-1} \ln N \frac{1 - x_i}{1 - d}.$$

Since  $e_N = 0$ , we have, from (2.36),  $|\varepsilon D^+ e_{N-1}| \leq C\varepsilon N^{-1} \ln N$ . Rewriting the relation  $\tau_i = L_\varepsilon^N e_i$  as follows we have

$$\varepsilon D^+ e_j - \varepsilon D^+ e_{j-1} + \frac{1}{2}(x_{j+1} - x_{j-1})a(x_j)D^+ e_j = \frac{1}{2}(x_{j+1} - x_{j-1})\tau_j.$$

Summing and rearranging we get

$$|\varepsilon D^+ e_i| \leq |\varepsilon D^+ e_{N-1}| + \frac{1}{2} \sum_{j=i+1}^{N-1} (x_{j+1} - x_{j-1})|\tau_j| + \frac{1}{2} \left| \sum_{j=i+1}^{N-1} (x_{j+1} - x_{j-1})a(x_j)D^+ e_j \right|.$$

We have already bounded the first term on the righthand side. The second term is also bounded since  $\tau_j \leq CN^{-1}$ . In the case of the third term we apply the arguments from the proof of Lemma 2.14 to obtain the required bound.

In order to obtain a similar bound on the subdomain  $[0, d]$ , we define

$\tilde{W}_2(x) = W_2(x) - W_2(d)$  which satisfies

$$L_\varepsilon^N \tilde{W}_2 = 0 \text{ for all } x_i \in \Omega_\varepsilon^N,$$

$$\tilde{W}_2(0) = -W_2(d), \quad \tilde{W}_2(d) = 0, \quad \tilde{W}_2(1) = -W_2(d).$$

Then for  $x_i < d$  we have

$$D^+(W_2 - w_2)(x_i) = D^+(W_2 - w_2)(d) + D^+(\tilde{W}_2 - \tilde{w}_2)(x_i).$$

The first term on the righthand side is already bounded and in the case of the second term we repeat the arguments above over  $[0, d]$  to obtain the required bound.  $\square$

**Theorem 2.16.** *For all  $N \geq 8$  and each  $i \in [0, N - 1]$  we have*

$$\sup_{0 < \varepsilon \leq 1} \|\varepsilon(D^+U_\varepsilon(x_i) - u'_\varepsilon)\|_{\bar{\Omega}_i} \leq CN^{-1} \ln N$$

**Proof.** See [21] for the proof.  $\square$

## 2.4 Numerical Results

We will now look at some computational results for specific problems of the type described in Section 2.1. Consider the following:

$$\begin{aligned}
 \varepsilon u_\varepsilon'' + a(x)u_\varepsilon' &= f, \quad x \in (0, 1) \\
 u_\varepsilon(0) &= 0, \quad u_\varepsilon(1) = 0, \\
 \text{where } a(x) &= \begin{cases} 2x + 1, & x \leq \frac{1}{2}, \\ 3x + 1, & x \geq \frac{1}{2}. \end{cases} \\
 \text{and } f(x) &= \begin{cases} 1 - x, & x \leq \frac{1}{2}, \\ x, & x \geq \frac{1}{2}. \end{cases}
 \end{aligned}
 \tag{2.37}$$

We solve this problem numerically using  $(P_\varepsilon^N)$  and the fitted meshes described in Section 2.2 The global error is approximated by

$$\bar{E}_\varepsilon^N = \max_{x_i \in \Omega_\varepsilon^{524288}} |\bar{U}_\varepsilon^N - U_\varepsilon^{524288}|.$$

The approximate global error computed using  $(P_\varepsilon^N)$  is depicted in Fig. 2.1 for  $N = 64$  and  $\varepsilon = 10^{-4}$ . On the same plot we have shown the corresponding approximate global error when a fully fitted mesh is used. The fully fitted mesh is identical to the partially fitted mesh in the boundary layer region, and has a further fine mesh region starting at  $x = d$ , of thickness  $\sigma^* = \min\{(1 - d)/2, \frac{\varepsilon}{\alpha} \ln N\}$ . Therefore we have  $x_{N/4} = \sigma$ ,  $x_{N/2} = d$  as before and additionally now have  $x_{3N/4} = d + \sigma^*$ . The mesh is fitted to The four mesh

widths are denoted in the following way

$$\begin{aligned} h_1 &= \frac{4\sigma}{N}, \quad h_2 = \frac{4(d - \sigma)}{N}, \\ H_1 &= \frac{4\sigma^*}{N}, \quad H_2 = \frac{4(1 - d - \sigma^*)}{N} \end{aligned}$$

The global errors for the numerical solution on the partially fitted mesh for various values of  $N$  and  $\varepsilon$  compared to the reference solution (the numerical solution on the fully fitted mesh with  $N = 524288$ ) are presented in Table 2.1, along with the uniform convergence rates computed using the double grid approach, where

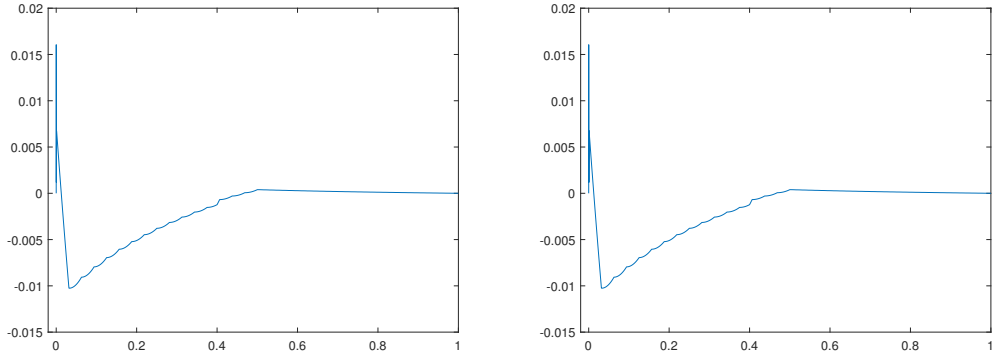
$$\begin{aligned} E_\varepsilon^N &= \max_{x_i \in \Omega_\varepsilon^N} |U_\varepsilon^N - \bar{U}_\varepsilon^{524288}|, \\ D_\varepsilon^N &= \max_{x_i \in \Omega_\varepsilon^N} |U_\varepsilon^N - \bar{U}_\varepsilon^{2N}|, \quad D^N = \max_\varepsilon D_\varepsilon^N, \\ p_N &= \log_2 D^N / D^{2N}. \end{aligned}$$

This table verifies the convergence result. Table 2.2 gives the analogous computed errors and uniform convergence rates for the scaled discrete derivatives. Again, the theoretical error estimate is confirmed.

Consider a second example:

$$\begin{aligned} \varepsilon u_\varepsilon'' + u' &= f, \\ u_\varepsilon(0) &= 0, \quad u_\varepsilon(1) = 0, \\ \text{where } f(x) &= (x - 1/2)^{2/3} \end{aligned} \tag{2.38}$$

Fig. 4.2 shows the approximate global error computed on partially and fully fitted meshes for  $N = 64$  and  $\varepsilon = 10^{-4}$ . Tables 2.3 and 2.4, analogously to Tables 2.1 and 2.2, present the approximate global errors for the numerical



Approximate global error on partially-fitted mesh

Approximate global error on fully-fitted mesh

Figure 2.1: Approximate global error for problem (2.37) with  $\varepsilon = 0.0001$  and  $N = 64$ .

Table 2.1: Global errors  $\bar{E}_\varepsilon^N$  and the uniform order of convergence  $p_N$  for the discrete solution, partially fitted mesh method ( $P_\varepsilon^N$ ) applied to problem (2.37).

Number of intervals $N$							
	$\varepsilon$	64	128	256	512	1024	2048
1		9.04E-04	4.48E-04	2.24E-04	1.12E-04	5.58E-05	2.78E-05
$2^{-2}$		4.02E-03	1.94E-03	9.86E-04	5.11E-04	2.51E-04	1.20E-04
$2^{-4}$		1.64E-02	8.21E-03	4.16E-03	2.12E-03	1.05E-03	5.18E-04
$2^{-6}$		1.46E-02	8.71E-03	5.10E-03	2.91E-03	1.68E-03	9.39E-04
$2^{-8}$		1.52E-02	8.50E-03	4.88E-03	2.68E-03	1.56E-03	8.39E-04
$2^{-10}$		1.58E-02	8.92E-03	4.93E-03	2.75E-03	1.52E-03	8.31E-04
$2^{-12}$		1.60E-02	9.12E-03	5.09E-03	2.88E-03	1.62E-03	8.68E-04
$2^{-14}$		1.61E-02	9.18E-03	5.14E-03	2.93E-03	1.66E-03	9.03E-04
$2^{-16}$		1.61E-02	9.19E-03	5.15E-03	2.94E-03	1.67E-03	9.15E-04
$2^{-18}$		1.61E-02	9.20E-03	5.15E-03	2.95E-03	1.68E-03	9.18E-04
$2^{-20}$		1.61E-02	9.20E-03	5.15E-03	2.95E-03	1.68E-03	9.19E-04
$2^{-22}$		1.61E-02	9.20E-03	5.15E-03	2.95E-03	1.68E-03	9.19E-04
$2^{-24}$		1.61E-02	9.20E-03	5.15E-03	2.95E-03	1.68E-03	9.19E-04
$2^{-26}$		1.61E-02	9.20E-03	5.15E-03	2.95E-03	1.68E-03	9.19E-04
$2^{-28}$		1.61E-02	9.20E-03	5.16E-03	2.95E-03	1.68E-03	9.19E-04
$2^{-30}$		1.61E-02	9.20E-03	5.15E-03	2.95E-03	1.68E-03	9.19E-04
$p_N$		9.33E-01	7.47E-01	7.91E-01	6.97E-01	7.67E-01	8.43E-01

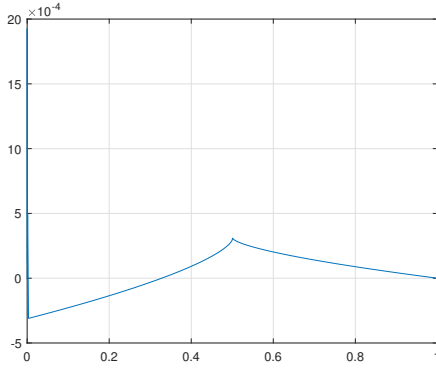
solution and the pointwise errors for the discrete derivative respectively, again confirming the theoretical error estimates.

## 2.5 Summary

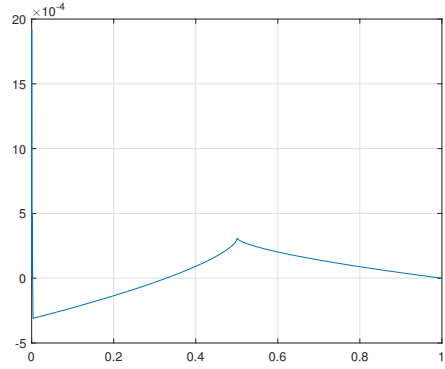
We considered a two-point boundary value problem for a singularly perturbed convection diffusion equation with a singular perturbation parameter  $\varepsilon$  and a source term whose first derivative and convection coefficients are discontin-

Table 2.2: Maximum pointwise errors  $E_\varepsilon^N$ , and the uniform order of convergence  $p_N$  in the scaled discrete derivatives for the partially fitted mesh method ( $P_\varepsilon^N$ ) applied to problem (2.37).

Number of intervals $N$ $\varepsilon$	Number of intervals $N$					
	64	128	256	512	1024	2048
1	1.59E-02	8.01E-03	4.02E-03	2.01E-03	1.01E-03	5.03E-04
$2^{-2}$	3.36E-02	1.72E-02	8.75E-03	4.45E-03	2.22E-03	1.10E-03
$2^{-4}$	8.67E-02	4.80E-02	2.55E-02	1.32E-02	6.66E-03	3.34E-03
$2^{-6}$	7.73E-02	4.94E-02	3.01E-02	1.76E-02	1.01E-02	5.60E-03
$2^{-8}$	7.58E-02	4.77E-02	2.88E-02	1.67E-02	9.54E-03	5.27E-03
$2^{-10}$	7.61E-02	4.80E-02	2.87E-02	1.66E-02	9.41E-03	5.21E-03
$2^{-12}$	7.62E-02	4.81E-02	2.89E-02	1.68E-02	9.55E-03	5.27E-03
$2^{-14}$	7.63E-02	4.82E-02	2.89E-02	1.69E-02	9.61E-03	5.32E-03
$2^{-16}$	7.63E-02	4.82E-02	2.89E-02	1.69E-02	9.63E-03	5.34E-03
$2^{-18}$	7.63E-02	4.82E-02	2.90E-02	1.69E-02	9.64E-03	5.34E-03
$2^{-20}$	7.63E-02	4.82E-02	2.90E-02	1.69E-02	9.64E-03	5.35E-03
$2^{-22}$	7.63E-02	4.82E-02	2.90E-02	1.69E-02	9.64E-03	5.35E-03
$2^{-24}$	7.63E-02	4.82E-02	2.90E-02	1.69E-02	9.64E-03	5.35E-03
$2^{-26}$	7.63E-02	4.82E-02	2.90E-02	1.69E-02	9.64E-03	5.35E-03
$2^{-28}$	7.63E-02	4.82E-02	2.90E-02	1.69E-02	9.64E-03	5.35E-03
$2^{-30}$	7.63E-02	4.82E-02	2.90E-02	1.69E-02	9.64E-03	5.35E-03
$p_N$	5.43E-01	6.79E-01	7.26E-01	7.61E-01	8.19E-01	8.61E-01



Approximate global error on partially-fitted mesh



Approximate global error on fully-fitted mesh

Figure 2.2: Approximate global error for problem (2.38) with  $\varepsilon = 0.0001$  and  $N = 64$ .

uous. We constructed a numerical method for solving this problem, which generates  $\varepsilon$ -uniformly convergent numerical approximations to the the solution and its derivatives. The method consists of the standard upwind finite difference operator on a Shishkin mesh fitted only to the boundary layer and not to the interior layer. It is worth noting that, in view of the bounds obtained on the scaled discrete derivative for this problem, then it is possible to extend the results of this chapter to the case where there are multiple such

Table 2.3: Global errors  $\bar{E}_\varepsilon^N$  and the uniform order of convergence  $p_N$  for the discrete solution, partially fitted mesh method ( $P_\varepsilon^N$ ) applied to problem (2.38).

Number of intervals $N$						
$\varepsilon$	128	256	512	1024	2048	
1	7.96E-04	3.47E-04	1.59E-04	7.51E-05	3.62E-05	1.77E-05
$2^{-2}$	6.90E-03	3.39E-03	1.67E-03	8.27E-04	4.11E-04	2.05E-04
$2^{-4}$	2.84E-02	1.65E-02	8.39E-03	4.23E-03	2.12E-03	1.06E-03
$2^{-6}$	3.16E-02	1.78E-02	1.01E-02	5.73E-03	3.23E-03	1.80E-03
$2^{-8}$	3.42E-02	1.92E-02	1.06E-02	5.85E-03	3.21E-03	1.76E-03
$2^{-10}$	3.52E-02	2.00E-02	1.11E-02	6.13E-03	3.35E-03	1.81E-03
$2^{-12}$	3.54E-02	2.02E-02	1.13E-02	6.29E-03	3.46E-03	1.88E-03
$2^{-14}$	3.55E-02	2.03E-02	1.14E-02	6.33E-03	3.50E-03	1.92E-03
$2^{-16}$	3.55E-02	2.03E-02	1.14E-02	6.35E-03	3.51E-03	1.93E-03
$2^{-18}$	3.55E-02	2.03E-02	1.14E-02	6.35E-03	3.52E-03	1.93E-03
$2^{-20}$	3.55E-02	2.03E-02	1.14E-02	6.35E-03	3.51E-03	1.93E-03
$2^{-22}$	3.55E-02	2.03E-02	1.14E-02	6.35E-03	3.51E-03	1.93E-03
$2^{-24}$	3.55E-02	2.03E-02	1.14E-02	6.35E-03	3.51E-03	1.93E-03
$2^{-26}$	3.55E-02	2.03E-02	1.14E-02	6.35E-03	3.51E-03	1.93E-03
$2^{-28}$	3.55E-02	2.03E-02	1.14E-02	6.35E-03	3.52E-03	1.93E-03
$2^{-30}$	3.55E-02	2.03E-02	1.14E-02	6.35E-03	3.51E-03	1.93E-03
$p_N$	8.00E-01	7.48E-01	8.18E-01	8.22E-01	8.38E-01	8.46E-01

Table 2.4: Maximum pointwise errors  $E_\varepsilon^N$ , and the uniform order of convergence  $p_N$  in the scaled discrete derivatives for the partially fitted mesh method ( $P_\varepsilon^N$ ) applied to problem (2.38).

Number of intervals $N$						
$\varepsilon$	128	256	512	1024	2048	
1	1.70E-02	8.51E-03	4.26E-03	2.13E-03	1.06E-03	5.29E-04
$2^{-2}$	4.32E-02	2.27E-02	1.17E-02	5.91E-03	2.97E-03	1.49E-03
$2^{-4}$	1.15E-01	7.58E-02	4.21E-02	2.22E-02	1.14E-02	5.80E-03
$2^{-6}$	1.18E-01	7.87E-02	4.95E-02	2.98E-02	1.73E-02	9.83E-03
$2^{-8}$	1.21E-01	8.04E-02	5.02E-02	3.00E-02	1.73E-02	9.76E-03
$2^{-10}$	1.22E-01	8.14E-02	5.09E-02	3.04E-02	1.75E-02	9.84E-03
$2^{-12}$	1.23E-01	8.17E-02	5.12E-02	3.06E-02	1.77E-02	9.95E-03
$2^{-14}$	1.23E-01	8.18E-02	5.13E-02	3.07E-02	1.78E-02	1.00E-02
$2^{-16}$	1.23E-01	8.18E-02	5.13E-02	3.07E-02	1.78E-02	1.00E-02
$2^{-18}$	1.23E-01	8.18E-02	5.13E-02	3.07E-02	1.78E-02	1.00E-02
$2^{-20}$	1.23E-01	8.18E-02	5.13E-02	3.07E-02	1.78E-02	1.00E-02
$2^{-22}$	1.23E-01	8.18E-02	5.13E-02	3.07E-02	1.78E-02	1.00E-02
$2^{-24}$	1.23E-01	8.18E-02	5.13E-02	3.07E-02	1.78E-02	1.00E-02
$2^{-26}$	1.23E-01	8.18E-02	5.13E-02	3.07E-02	1.78E-02	1.00E-02
$2^{-28}$	1.23E-01	8.18E-02	5.13E-02	3.07E-02	1.78E-02	1.00E-02
$2^{-30}$	1.23E-01	8.18E-02	5.13E-02	3.07E-02	1.78E-02	1.00E-02
$p_N$	4.28E-01	5.67E-01	6.69E-01	7.41E-01	7.91E-01	8.26E-01

discontinuities in the domain. We introduced a minimum principle for the discrete problem and a decomposition of the discrete solution, by means of which we proved the  $\varepsilon$ -uniform convergence in the global maximum norm of the approximations generated by the numerical method. Numerical results presented were consistent with the theoretical results.

# Chapter 3

## A singularly perturbed convection-diffusion problem with discontinuous boundary data

### 3.1 Introduction

We consider the following boundary value problem in a domain  $\Omega$ , the unit square.

$$\begin{aligned}Lu_\varepsilon &\equiv \varepsilon \Delta u_\varepsilon + p_1 \frac{\partial u_\varepsilon}{\partial x} + p_2 \frac{\partial u_\varepsilon}{\partial y} - qu_\varepsilon = f \text{ in } \Omega, \\u_\varepsilon(x, 0) &= g_s(x), \quad u_\varepsilon(x, 1) = g_n(x), \quad x \in (0, 1) \\u_\varepsilon(0, y) &= g_w(y), \quad u_\varepsilon(1, y) = g_e(y) \quad y \in (0, 1) \\g_s(0) &\neq g_w(0),\end{aligned}\tag{3.1}$$

where  $p_1, p_2$  and  $q$  are positive constants and  $0 < \varepsilon \leq 1$ . While it is unusual to exclude the case where  $q = 0$ , subsequent analysis (Lemma (3.2)) requires it. For  $f(x, y)$  and the boundary data it is assumed that

$$f \in C^{2l,a}(\bar{\Omega}), g_s, g_n, g_w, g_e \in C^{2l,\alpha}([0, 1]) \quad (3.2)$$

for some non-negative integer  $l$  and  $\alpha \in (0, 1)$  and that  $g_n^m(1) = 0, g_e^n(1) = 0 \forall m, n \leq 2$ . We will use the Hölder space  $C^{m,\alpha}(\Omega)$  where  $0 < \alpha < 1$ . While in this thesis we consider only problems with constant coefficients, it may be possible to extend these bounds to the case of variable coefficients under certain assumptions. However, due to the complexity of the analysis here, even in the case of constant coefficients, to extend this analysis to the case of variable coefficients would be challenging.

Throughout this thesis we are concerned with the numerical solution of singularly perturbed problems with discontinuous data. The problem above exhibits exponential layers along the outflow boundaries, a corner boundary layer at the outflow boundary corner as well as a singularity of the solution discontinuity in a neighbourhood of this corner. Whereas in [45] Kellogg and Stynes examine a singularly perturbed convection-diffusion problem on the unit square with parabolic and exponential boundary layers. In contrast, the problems we consider differ in the direction of the flow, which is diagonal across the domain. This gives rise to a different decomposition of the solutions, therefore different expression of the solution in terms of modified Bessel functions and increased difficulty in bounding derivatives.

In [45] and [47], Kellogg and Stynes considered a singularly perturbed convection-diffusion problem on the unit square with exponential and characteristic boundary layers and potential corner singularities at all four corners

of the domain and obtained bounds for the solution of the problem and its derivatives. In [75] and [76] the authors obtained bounds on the solutions to related problems with Neumann boundary conditions. Discontinuities in the boundary data at inflow corners give rise to corner singularities which are propagated through the domain. Such problems are difficult to solve numerically, a special mesh is required to deal with the consequent solution behaviour across the domain. In this chapter we analyse the behaviour of the solution and derivatives of the problem outlined above with the objective of using this information to design an appropriate domain decomposition numerical method, with a suitably adapted mesh, to solve a similar problem in Chapter 4. While the analysis broadly follows a similar structure to that used in [45], the bounds we obtain differ due to the nature of the flow and layers involved. Additionally, there are significant differences in the decomposition of the solution and increased difficulty in the bounding of the higher derivatives of some of the components.

## 3.2 Decomposition

$S_1$  is defined to be the solution of the incoming half-plane problem

$$\begin{aligned} LS_1 &= f^*, \quad x < 1, \\ S_1(1, y) &= g_e^*(y), \quad \forall y \in \mathbb{R}, \end{aligned} \tag{3.3}$$

on the domain  $\Pi_{x < 1}$ . And  $S_2$  is defined to be the solution of the incoming half-plane problem

$$\begin{aligned} LS_2 &= 0, \quad y < 1, \\ S_2(x, 1) &= g_n^*(x) - S_1^*(x, 1), \quad \forall x \in \mathbb{R}, \end{aligned} \quad (3.4)$$

on the domain  $\Pi_{y < 1}$ . Note that  $f^*$ ,  $g_n^*$ ,  $g_e^*$ ,  $g_s^*$ ,  $g_w^*$  are smooth extensions of  $f$ ,  $g_n$ ,  $g_e$ ,  $g_s$ ,  $g_w$  respectively which die off at infinity, [26], that  $g_n^*$  and  $g_e^*$  smoothly go to zero approaching the corner  $(1, 1)$  and that  $S_1^*$  is a smooth extension of  $S_1$  along the boundary of  $\Pi_y$ . The functions  $S_1$  and  $S_2$  will be a good approximations to  $u_\varepsilon$  away from exponential layer regions and corners. In order to deal with the outflow boundary layers and to correct the boundary conditions along  $x = 0$ ,  $y = 0$ ,  $E_1$  is defined to be the solution of the outgoing half-plane problem:

$$\begin{aligned} LE_1 &= 0, \quad x > 0, \\ E_1(0, y) &= -S_1^*(0, y) - S_2^*(0, y), \quad \forall y \in \mathbb{R}, \end{aligned} \quad (3.5)$$

on the domain  $\Pi_x$  and  $E_2$  is defined to be the solution of the outgoing half-plane problem:

$$\begin{aligned} LE_2 &= 0, \quad y > 0, \\ E_2(x, 0) &= -S_1^*(x, 0) - S_2^*(x, 0) - E_1^*(x, 0), \quad \forall x \in \mathbb{R}, \end{aligned} \quad (3.6)$$

on the domain  $\Pi_y$  where  $S_1^*$  and  $S_2^*$  are smooth extensions of  $S_1$  and  $S_2$  along the boundaries of  $\Pi_x$  and  $\Pi_y$  respectively.

$S_1 + S_2 + E_1 + E_2$  satisfies  $L(S_1 + S_2 + E_1 + E_2) = f$  on  $\Omega$  but does not agree with the boundary data for  $u_\varepsilon$  on any of the four sides of  $\Omega$ .

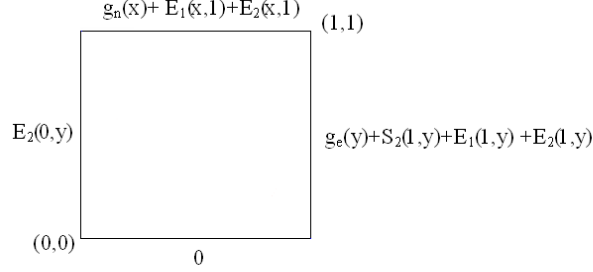


Figure 3.1: Boundary data on  $\Omega$ ,  $S_1 + S_2 + E_1 + E_2$

We introduce  $z_{00}$  to deal with the disagreement between  $S_1 + S_2 + E_1 + E_2$  and the boundary data  $g_w$  and  $g_s$  on the sides  $x = 0$  and  $y = 0$  respectively. The corner function  $z_{00}(x, y)$  is defined as the solution of the outgoing quarter-plane problem

$$\begin{aligned}
 Lz_{00} &= 0, \quad x > 0, \quad y > 0, \\
 z_{00}(x, 0) &= g_s^*(x), \quad x > 0, \\
 z_{00}(0, y) &= g_w^*(y) - E_2^*(0, y), \quad y > 0,
 \end{aligned} \tag{3.7}$$

on the domain  $Q_1$ .

$S_1 + S_2 + E_1 + E_2 + z_{00}$  differs from the boundary data  $g_n$  and  $g_e$  on the sides  $y = 1$  and  $x = 1$  respectively.

Similarly,  $z_{11}$  deals with the disagreement between  $S_1 + S_2 + E_1 + E_2 + z_{00}$  and the boundary data  $g_n$  and  $g_e$  on the sides  $y = 1$  and  $x = 1$  respectively and is defined as the solution of the incoming quarter-plane problem on the

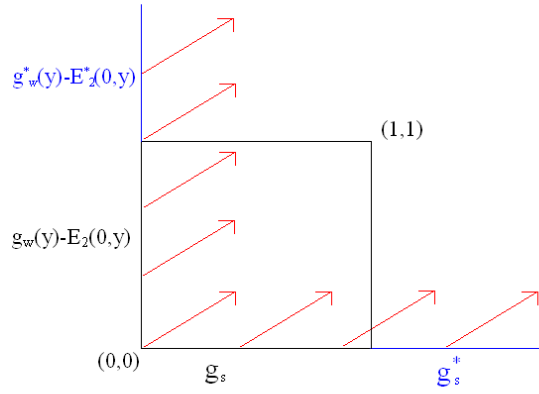


Figure 3.2: Domain and boundary conditions,  $z_{00}$

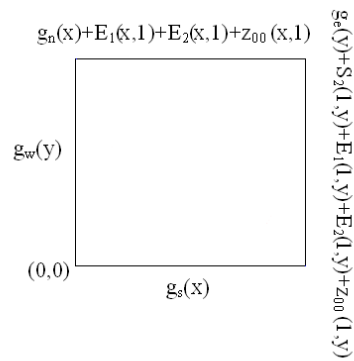


Figure 3.3: Boundary data on  $\Omega$ ,  $S_1 + S_2 + E_1 + E_2 + z_{00}$

domain  $Q_2$

$$\begin{aligned}
Lz_{11} &= 0, \quad x < 1, \quad y < 1, \\
z_{11}(x, 1) &= -E_1^*(x, 1) - E_2^*(x, 1) - z_{00}^*(x, 1), \quad x \leq 1, \\
z_{11}(1, y) &= -E_1^*(1, y) - E_2^*(1, y) - z_{00}^*(1, y) + (\chi(y) - 1)S_2^*(1, y), \quad y \leq 1,
\end{aligned} \tag{3.8}$$

where  $E_1^*$ ,  $E_2^*$ ,  $z_{00}^*$  and  $S_2^*$  are smooth extensions of  $E_1$ ,  $E_2$ ,  $z_{00}$  and  $S_2$  respectively along the boundaries of  $Q_2$  and  $\chi$ , a smooth cut-off function [45], satisfying

$$\chi(t) = \begin{cases} 0, & t \leq 1/2 \\ 1, & t \geq 2/3 \end{cases}$$

ensures that no incompatibilities are introduced at the corners of  $\Omega$ .

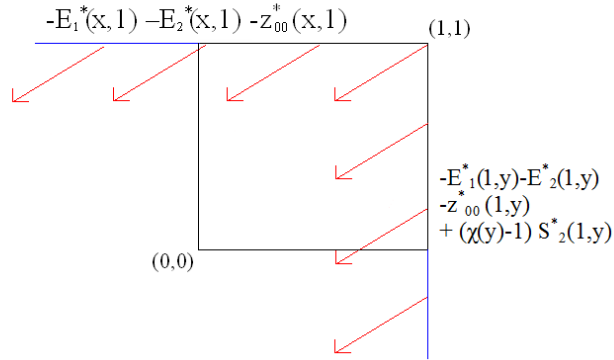


Figure 3.4: Domain and boundary conditions,  $z_{11}$

As in [45] set  $\bar{u}_\varepsilon = u_\varepsilon - (S_1 + S_2 + E_1 + E_2 + z_{00} + z_{11})$ . Then  $\bar{u}_\varepsilon$  is the solution

of the problem

$$\begin{aligned}
L\bar{u}_\varepsilon &= 0 \quad \in \Omega, \\
\bar{u}_\varepsilon(x, 0) &= \bar{g}_s(x), \\
\bar{u}_\varepsilon(x, 1) &= \bar{g}_n(x), \quad 0 < x < 1, \\
\bar{u}_\varepsilon(0, y) &= \bar{g}_w(y), \\
\bar{u}_\varepsilon(1, y) &= \bar{g}_e(y), \quad 0 < y < 1
\end{aligned} \tag{3.9}$$

where

$$\begin{aligned}
\bar{g}_s(x) &= -z_{11}(x, 0), \\
\bar{g}_n(x) &= 0, \\
\bar{g}_w(y) &= -z_{11}(0, y), \\
\bar{g}_e(y) &= -\chi(y)S_2^*(1, y).
\end{aligned} \tag{3.10}$$

The data of the problem (3.9) are compatible to arbitrary order at the corners  $(0, 0)$  and  $(1, 1)$ . However, as compatibility conditions at corners  $(1, 0)$  and  $(0, 1)$  may not be satisfied, we introduce functions  $z_{10}$  and  $z_{01}$  to deal with these incompatibilities. The corner function  $z_{10}$  is defined by the problem

$$\begin{aligned}
Lz_{10} &= 0, \quad x < 1, \quad y > 0, \\
z_{10}(x, 0) &= -\chi(x)z_{11}^*(x, 0), \quad x \leq 1, \\
z_{10}(1, y) &= -\chi(y)S_2^*(1, y), \quad y \geq 0.
\end{aligned} \tag{3.11}$$

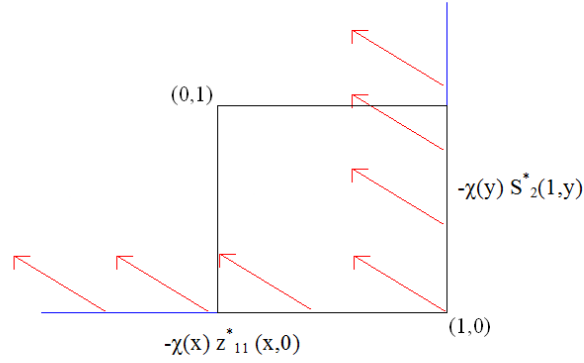


Figure 3.5: Domain and boundary conditions,  $z_{10}$

The corner function  $z_{01}$  is defined to be the solution of the following problem

$$\begin{aligned}
 Lz_{01} &= 0, \quad x > 0, \quad y < 1, \\
 z_{01}(x, 1) &= (1 - \chi(x))z_{11}^*(x, 1), \quad x \geq 0, \\
 z_{01}(0, y) &= 0, \quad y \leq 1.
 \end{aligned} \tag{3.12}$$

As in [45] set  $\tilde{u}_\varepsilon = \bar{u}_\varepsilon - (z_{10} + z_{01})$ . Then  $\tilde{u}_\varepsilon(x, 0)$  satisfies

$$\begin{aligned}
 L\tilde{u}_\varepsilon &= 0 \quad \in \Omega, \\
 \tilde{u}_\varepsilon(x, 0) &= \tilde{g}_s(x), \\
 \tilde{u}_\varepsilon(x, 1) &= \tilde{g}_n(x), \quad 0 \leq x \leq 1, \\
 \tilde{u}_\varepsilon(0, y) &= \tilde{g}_w(y), \\
 \tilde{u}_\varepsilon(1, y) &= \tilde{g}_e(y), \quad 0 \leq y \leq 1
 \end{aligned} \tag{3.13}$$

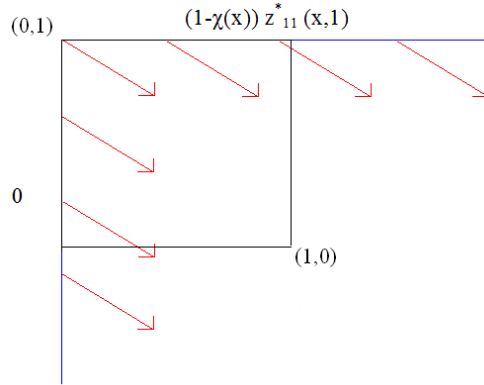


Figure 3.6: Domain and boundary conditions,  $z_{01}$

where

$$\begin{aligned}
\tilde{g}_s(x) &= -(1 - \chi(x))z_{11}(x, 0) - z_{01}(x, 0), \\
\tilde{g}_n(x) &= -(1 - \chi(x))z_{11}(x, 1) - z_{10}(x, 1), \\
\tilde{g}_w(y) &= -z_{11}(0, y) - z_{10}(0, y), \\
\tilde{g}_e(y) &= -z_{01}(1, y).
\end{aligned} \tag{3.14}$$

We examine the boundary data (3.14). Note that, near  $(0, 0)$ ,

$$\begin{aligned}
\tilde{g}_s(x) &= -z_{11}(x, 0) \\
\tilde{g}_w(y) &= -z_{11}(0, y),
\end{aligned}$$

since  $z_{01}(x, 0)$  and  $z_{10}(0, y)$  both equal zero at  $(0, 0)$ . As  $z_{11}$  is smooth at  $(0, 0)$  it follows that the data are compatible at  $(0, 0)$  to arbitrary order. Similar arguments hold near the remaining corners of  $\Omega$ . Therefore it follows that the data are compatible to arbitrary order at all four corners of  $\Omega$ . In this way

we arrive at the following decomposition

$$u_\varepsilon = S_1 + S_2 + E_1 + E_2 + z_{00} + z_{11} + z_{01} + z_{10} + \tilde{u}_\varepsilon. \quad (3.15)$$

### 3.2.1 Summary of alternative decomposition

We include a brief descriptions of an alternative decomposition of the solution composed only of quarter-plane problems. Such a decomposition appears appropriate given the characteristic layers present. However, due to the difficulty in attaining bounds on mixed derivatives in quarter-plane domains, for the purposes of analysis we proceeded with the decomposition detailed in the previous section, which permits the bounding of mixed derivatives on its half-plane components.

$S$  is defined to be the solution of the incoming quarter-plane problem

$$\begin{aligned} LS &= f^*, \quad x < 1, \quad y < 1, \\ S(x, 1) &= g_n^*(x), \quad x < 1, \\ S(1, y) &= g_e^*(y), \quad y < 1. \end{aligned} \quad (3.16)$$

Let  $E$  be the solution to the outgoing quarter-plane problem

$$\begin{aligned} LE &= 0, \quad x > 0, \quad y > 0, \\ E(x, 0) &= -S^*(x, 0), \quad x > 0, \\ E(0, y) &= -S^*(0, y), \quad y > 0, \end{aligned} \quad (3.17)$$

where  $S^*$  is a smooth extension of  $S$  along the boundaries of  $Q_1$ . The corner function  $z_{00}(x, y)$  is defined as the solution of the outgoing quarter-plane

problem

$$\begin{aligned}
Lz_{00} &= 0, \quad x > 0, \quad y > 0, \\
z_{00}(x, 0) &= g_s^*(x), \quad x > 0, \\
z_{00}(0, y) &= g_w^*(y), \quad y > 0.
\end{aligned} \tag{3.18}$$

$z_{11}$  is defined as the solution of the incoming quarter-plane problem

$$\begin{aligned}
Lz_{11} &= 0, \quad x < 1, \quad y < 1, \\
z_{11}(x, 1) &= -E^*(x, 1) - z_{00}^*(x, 1), \quad x < 1, \\
z_{11}(1, y) &= -E^*(1, y) - z_{00}^*(1, y), \quad y < 1,
\end{aligned} \tag{3.19}$$

where  $E^*$  and  $z_{00}^*$  are smooth extensions of  $E$  and  $z_{00}$  along the boundaries of  $Q_2$ . The corner function  $z_{10}$  is defined by the problem

$$\begin{aligned}
Lz_{10} &= 0, \quad x < 1, \quad y > 0, \\
z_{10}(x, 0) &= -\chi(x)z_{11}(x, 0), \quad x < 1, \\
z_{10}(1, y) &= 0, \quad y > 0.
\end{aligned} \tag{3.20}$$

The corner function  $z_{01}$  is defined to be the solution of the following problem

$$\begin{aligned}
Lz_{01} &= 0, \quad x > 0, \quad y < 1, \\
z_{01}(x, 1) &= 0, \quad x > 0, \\
z_{01}(0, y) &= -\chi(y)z_{11}(0, y), \quad y < 1.
\end{aligned} \tag{3.21}$$

As before let  $\tilde{u}_\varepsilon$  be the remainder function on the unit square. In this way we

arrive at the following alternative decomposition

$$u_\varepsilon = S + E + z_{01} + z_{10} + z_{00} + z_{11} + \tilde{u}_\varepsilon. \quad (3.22)$$

### 3.3 Bounds on components

#### 3.3.1 Smooth components $S_1$ and $S_2$

**Growth conditions and Maximum Principle:  $S_1$**

The analysis is analogous to that in [45]. Consider the incoming half plane problem below:

$$\begin{aligned} Lv &\equiv \varepsilon \Delta v + p_1 \frac{\partial v}{\partial x} + p_2 \frac{\partial v}{\partial y} - qv = f, \quad x < 1, y \in (-\infty, \infty), \\ v(1, y) &= h_e(y), \quad y \in (-\infty, \infty) \end{aligned} \quad (3.23)$$

where  $p_1, p_2$  and  $q$  are positive constants. Setting  $v_1(x, y) = e^{(p_1 x + p_2 y)/2\varepsilon} v(x, y)$  we have

$$\begin{aligned} 4\varepsilon^2 \Delta v_1 - \kappa^2 v_1 &= f_1(x, y), \quad x < 1, y \in (-\infty, \infty), \\ v_1(1, y) &= h_{e,1}(y) = e^{p_2 y/2\varepsilon} h_e(y), \quad y \in (-\infty, \infty) \end{aligned} \quad (3.24)$$

where  $f_1(x, y) = 4\varepsilon e^{(p_1x+p_2y)/2\varepsilon} f(x, y)$  and  $\kappa^2 = p_1^2 + p_2^2 + 4\varepsilon q$ . Set

$$\begin{aligned}\xi &= (1-x)/2\varepsilon, \quad \eta = (1-y)/2\varepsilon, \\ v_2(\xi, \eta) &= v_1(x, y), \quad f_2(\xi, \eta) = f_1(x, y), \\ h_{e,2}(\eta) &= h_{e,1}(y)\end{aligned}$$

yielding the Helmholtz equation

$$\begin{aligned}\Delta v_2 - \kappa^2 v_2 &= f_2(\xi, \eta), \quad \xi > 0, \eta \in (-\infty, \infty), \\ v_2(0, \eta) &= h_{e,2}(\eta), \quad \eta \in (-\infty, \infty).\end{aligned}\tag{3.25}$$

The Green's function for this problem is

$$G(\xi, \eta; \sigma, \tau) = \frac{1}{2\pi} [K_0(\kappa\rho_1) - K_0(\kappa\rho_2)]\tag{3.26}$$

where

$$\begin{aligned}\rho_1 &= \sqrt{(\sigma - \xi)^2 + (\eta - \tau)^2}, \\ \rho_2 &= \sqrt{(\xi + \sigma)^2 + (\eta - \tau)^2},\end{aligned}$$

and  $K_0$  is a modified Bessel function of the second kind [87]. With

$$\rho_3 = \sqrt{\xi^2 + (\eta - \tau)^2},$$

we have the solution formula for (3.25) as follows

$$\begin{aligned}
v_2(\xi, \eta) &= -\frac{1}{2\pi} \int_0^\infty \int_{-\infty}^\infty f_2(\sigma, \tau) [K_0(\kappa\rho_1) - K_0(\kappa\rho_2)] d\tau d\sigma \\
&\quad + \frac{\xi\kappa}{\pi} \int_{-\infty}^\infty h_{e,2}(\tau) \left[ \frac{1}{\rho_3} K_1(\kappa\rho_3) \right] d\tau
\end{aligned} \tag{3.27}$$

As in [45], the solution of (3.25) exists and is given by (3.27) provided the functions  $f_2$  and  $h_{2,e}$  are such that the integrals are convergent.

In examining the finiteness of the integrals, note that

$$|K_0(\kappa\rho_1)| + |K_0(\kappa\rho_2)| \leq C|K_0(\kappa\rho_1)|$$

and that in the case of  $\sigma \leq 2\xi$ ,  $\tau \leq 2\eta$  we have  $K_0(t) \leq C|\ln(t)|$  for  $0 < t \leq 1$  and  $\int_0^1 |\ln t| dt$  is finite. For  $\sigma > 2\xi$  and  $\tau > 2\eta$ ,

$$\begin{aligned}
\rho_1 &= \sqrt{(\xi - \sigma)^2 + (\eta - \tau)^2} \\
&= \sqrt{(\sigma - \xi)^2 + (\tau - \eta)^2} \\
&= \sqrt{\left(\frac{\sigma}{2} + \frac{\sigma}{2} - \xi\right)^2 + \left(\frac{\tau}{2} + \frac{\tau}{2} - \eta\right)^2} \\
&> \frac{1}{2}\sqrt{\sigma^2 + \tau^2}
\end{aligned}$$

and, as in [45], using the bound derived from (9.6.23) in [1],  $|K_j(t)| \leq Ct^{-1/2}e^{-t}$  for  $t > 1$ , we obtain the following integrability condition for the  $f_2$  integral

$$\left| \int_{|\sigma| > 2|\xi|} \int_{|\tau| > 2|\eta|} (\sigma^2 + \tau^2)^{-1/4} f_2(\sigma, \tau) e^{-\kappa/2(\sigma^2 + \tau^2)^{1/2}} d\tau d\sigma \right| < \infty.$$

In the case of the  $h_2$  integrals note that  $\rho_3$  cannot be zero, therefore we need only establish that large  $\sigma$  and  $\tau$  do not cause the integral to become infinitely

large. For  $\tau > 2\eta$  we have  $\rho_3 > \tau/2$  and the integrability condition is as follows

$$\int_{|\tau|>2|\eta|} \tau^{-3/2} |h_{e,2}(\tau)| e^{-\kappa\tau/2} d\tau < \infty.$$

Reverting to the original variables and setting  $r = (x^2 + y^2)^{1/2}$  the integrability conditions become

$$\begin{aligned} \left| \int_{|x|>1} \int_{|y|>1} r^{-1/2} |f(x, y)| e^{-(\kappa r + p_1 x + p_2 y)/2\varepsilon} dy dx \right| < \infty, \\ \int_{|y|>1} |y|^{-3/2} |h_e(y)| e^{-(\kappa|y| + p_2 y)/2\varepsilon} dy < \infty. \end{aligned} \quad (3.28)$$

We then obtain the following maximum principle.

**Lemma 3.1.** *Let  $\Phi \in C^2(\bar{\Pi}_{x<1})$  satisfy  $L\Phi \leq 0$ ,  $\Phi(1, y) \geq 0 \forall y \in \mathbb{R}$  on  $\Pi_{x<1}$  and let  $p = \min\{p_1, p_2\}$*

$$\begin{aligned} \left| \int_{-\infty}^1 \int_{-\infty}^{\infty} (1+r)^{-1/2} |L\Phi| e^{-pr/2\varepsilon} dy dx \right| < \infty, \\ \int_{-\infty}^{\infty} (1+|y|)^{-3/2} |\Phi(1, y)| e^{-p|y|/2\varepsilon} dy < \infty, \end{aligned} \quad (3.29)$$

then  $\Phi \geq 0$  in  $\Pi_{x<1}$ .

If  $U \in C^2(\Pi_{x<1})$  satisfies  $|LU(x, y)| \leq |L\Phi(x, y)|$  in  $\Pi_{x<1}$  and  $|U(1, y)| \leq \Phi(1, y)$ ,  $\forall y \in \mathbb{R}$ , then  $|U(x, y)| \leq \Phi(x, y)$  in  $\Pi_{x<1}$ .  $\square$

$S_0$  is defined to be the solution of the incoming half-plane problem

$$\begin{aligned} LS_0 &= f^*, \quad x < 1, \\ S_0(1, y) &= 0, \quad \forall y \in \mathbb{R}. \end{aligned} \quad (3.30)$$

Much of the analysis on  $S_0, S_1$  and  $S_2$  which follows is analogous to that in [45]; however, a number of modifications are used in Lemma 3.4 due to the

differing nature of the operator  $L$  defined in (3.1), compared with that in [45]. We use the Sobolev space  $W^{m,\infty}(S)$  with the norm  $\|\cdot\|_{m,\infty,S}$  and where  $m = 0$  we write  $\|\cdot\|_{\infty,S}$ .

**Lemma 3.2.** *Let  $n$  be a non-negative integer. Let  $f^* \in W^{n,\infty}(\Pi_{x<1})$ . Then*

$$\|D_y^n S_0\|_{\infty,\Pi_{x<1}} \leq \frac{\|f^*\|_{n,\infty,\Pi_{x<1}}}{q}.$$

**Proof.** From the boundary conditions  $D_y^n S_0(1, y) = 0 \forall y$ . Differentiating (3.30) we get  $L(D_y^n S_0) = D_y^n f^*$  on  $\Pi_{x<1}$ . Let  $w(x, y) = \frac{\|D_y^n f^*\|_{\infty,\Pi_{x<1}}}{q}$  on  $\Pi_{x<1}$ . Then  $w(1, y) \geq |D_y^n S_0(1, y)| \forall y$ . Also,  $|L(w(x, y))| = \|D_y^n f^*\|_{\infty,\Pi_{x<1}}$  and  $|L(D_y^n S_0)| = |D_y^n f^*|$  on  $\Pi_{x<1}$ , therefore the result follows by Lemma 3.1.  $\square$

**Lemma 3.3.** *Let  $n$  be a non-negative integer. Let  $f^* \in W^{n+1,\infty}(\Pi_{x<1})$ . Then there exists a constant  $C$  such that*

$$\|D_x D_y^n S_0\|_{\infty,\Pi_{x<1}} \leq C \|f^*\|_{n+1,\infty,\Pi_{x<1}}.$$

**Proof.** Let

$$w(x, y) = \frac{(1-x)\|D_y^n f^*\|_{\infty,\Pi_{x<1}}}{p_1} \forall (x, y) \in \Pi_{x<1}.$$

Then  $w(1, y) = 0 = |D_y^n S_0(1, y)| \forall y$  from the boundary conditions,  $Lw(x, y) \leq 0$  and

$$\begin{aligned} |Lw(x, y)| &= \left[1 + \frac{(1-x)q}{p_1}\right] \|D_y^n f^*\|_{\infty,\Pi_{x<1}} \\ &\geq |L(D_y^n S_0)(x, y)|. \end{aligned}$$

Therefore by Lemma 3.1

$$|D_y^n S_0(x, y)| \leq \frac{1-x}{p_1} \|D_y^n f^*\|_{\infty, \Pi_{x < 1}}$$

on  $\bar{\Pi}_{x < 1}$ . As  $D_y^n S_0(1, y) = 0 \forall y$  the inequality implies that

$$\begin{aligned} |D_x D_y^n S_0(1, y)| &= \left| \lim_{x \rightarrow 1^-} \frac{D_y^n S_0(1, y) - D_y^n S_0(x, y)}{1-x} \right| \\ &\leq \frac{\|D_y^n f^*\|_{\infty, \Pi_{x < 1}}}{p_1}. \end{aligned} \quad (3.31)$$

Also,

$$|L(D_x D_y^n S_0)| = |D_x D_y^n f^*| \leq \|D_x D_y^n f^*\|_{\infty, \Pi_{x < 1}}, \quad \forall (x, y) \in \Pi_{x < 1}. \quad (3.32)$$

Using (3.31) and (3.32) and a constant barrier function,

$$W(x, y) = \frac{\|D_y^n f^*\|_{\infty, \Pi_{x < 1}}}{p_1} + \frac{\|D_x D_y^n f^*\|_{\infty, \Pi_{x < 1}}}{q}$$

the desired result is obtained.  $\square$

Given a differential operator  $D = D_x^m D_y^n$ , set  $|D| = m + n$ .

**Lemma 3.4.** *Let  $m$  and  $n$  be non-negative integers. Set  $D \equiv D_x^m D_y^n$ . Let  $f^* \in W^{|D|+2, \infty}(\Pi_{x < 1})$ . Then there exists a constant  $C$  such that*

$$\begin{aligned} \|D_x^2 D S_0\|_{\infty, \Pi_{x < 1}} &\leq C[\|f^*\|_{|D|+2, \infty, \Pi_{x < 1}} + \|D S_0\|_{\infty, \Pi_{x < 1}} + \|D_y D S_0\|_{\infty, \Pi_{x < 1}} \\ &\quad + \|D_y^2 D S_0\|_{\infty, \Pi_{x < 1}} + \|D_y^3 D S_0\|_{\infty, \Pi_{x < 1}}]. \end{aligned}$$

**Proof.** Let

$$\tilde{S}_0(x, y) = DS_0(1, y) - DS_0(x, y) + \frac{1-x}{p_1} [-Df^*(1, y) + p_2 D_y DS_0(1, y) - q DS_0(1, y)]$$

so  $\tilde{S}_0(1, y) = 0 \forall y$  and

$$\begin{aligned} L\tilde{S}_0(x, y) &= [Df^*(1, y) - Df^*(x, y)] + \varepsilon D_y^2 DS_0(1, y) \\ &\quad + \frac{\varepsilon(1-x)}{p_1} [-D_y^2 Df^*(1, y) + p_2 D_y^3 DS_0(1, y) - q D_y^2 DS_0(1, y)] \\ &\quad + \frac{p_2(1-x)}{p_1} [-D_y Df^*(1, y) + p_2 D_y^2 DS_0(1, y) - q D_y DS_0(1, y)] \\ &\quad - \frac{q(1-x)}{p_1} [-Df^*(1, y) + p_2 D_y DS_0(1, y) - q DS_0(1, y)]. \end{aligned}$$

Therefore

$$\begin{aligned} |L\tilde{S}_0(x, y)| &\leq (1-x) \|f^*\|_{|D|+1, \infty, \Pi_{x<1}} + \varepsilon \|D_y^2 DS_0\|_{\infty, \Pi_{x<1}} \\ &\quad + \frac{\varepsilon(1-x)}{p_1} (1+p_2+q) [\|D_y^2 Df^*\|_{\infty, \Pi_{x<1}} + \|D_y^3 DS_0\|_{\infty, \Pi_{x<1}} + \|D_y^2 DS_0\|_{\infty, \Pi_{x<1}}] \\ &\quad + \frac{p_2(1-x)}{p_1} (1+p_2+q) [\|D_y Df^*\|_{\infty, \Pi_{x<1}} + \|D_y^2 DS_0\|_{\infty, \Pi_{x<1}} + \|D_y DS_0\|_{\infty, \Pi_{x<1}}] \\ &\quad + \frac{q(1-x)}{p_1} (1+p_2+q) [\|Df^*\|_{\infty, \Pi_{x<1}} + \|D_y DS_0\|_{\infty, \Pi_{x<1}} + \|DS_0\|_{\infty, \Pi_{x<1}}]. \end{aligned}$$

The following barrier function can then be used to bound  $\tilde{S}_0$ :

$$\begin{aligned} \psi(x, y) &= C_1 \{ \varepsilon(1-x) \|D_y^2 DS_0\|_{\infty, \Pi_{x<1}} \\ &\quad + \left[ \frac{1-x}{p_1} (2\varepsilon - p_2) + (1-x)^2 \right] [\|f^*\|_{|D|+2, \infty, \Pi_{x<1}} + \|DS_0\|_{\infty, \Pi_{x<1}} \\ &\quad + \|D_y DS_0\|_{\infty, \Pi_{x<1}} + \|D_y^2 DS_0\|_{\infty, \Pi_{x<1}} + \|D_y^3 DS_0\|_{\infty, \Pi_{x<1}}] \}. \quad (3.33) \end{aligned}$$

Since  $\psi(1, y) = 0$ ,  $L\psi(x, y) \leq 0$  and

$$|L\psi(x, y)| \geq |L\tilde{S}_0(x, y)|, \quad (3.34)$$

then for all  $y$

$$\begin{aligned} DS_{0,x}(1, y) &= \lim_{x \rightarrow 1^-} \frac{DS_0(1, y) - DS_0(x, y)}{1 - x} \\ &= \lim_{x \rightarrow 1^-} \frac{\tilde{S}_0(x, y) - \frac{1-x}{p_1} [-Df^*(1, y) + p_2 D_y DS_0(1, y) - q DS_0(1, y)]}{1 - x}. \end{aligned}$$

Since  $|\tilde{S}_0(x, y)| \leq \psi(x, y) \forall (x, y) \in \bar{\Pi}_{x < 1}$ , it is easy to see that

$$\begin{aligned} &|DS_{0,x}(1, y) - \frac{1}{p_1} Df^*(1, y) + \frac{p_2}{p_1} D_y DS_0(1, y) - q DS_0(1, y)| \\ &\leq C_1 \{ \varepsilon [\|D_y^2 DS_0\|_{\infty, \Pi_{x < 1}} \\ &+ \frac{2\varepsilon - p_2}{p_1} [\|f^*\|_{|D|+2, \infty, \Pi_{x < 1}} + \|DS_0\|_{\infty, \Pi_{x < 1}} \\ &+ \|D_y DS_0\|_{\infty, \Pi_{x < 1}} + \|D_y^2 DS_0\|_{\infty, \Pi_{x < 1}} + \|D_y^3 DS_0\|_{\infty, \Pi_{x < 1}}] \}. \quad (3.35) \end{aligned}$$

Now  $L(DS_0) = Df^*$ , therefore

$$\begin{aligned} (\varepsilon D_x^2 DS_0 + \varepsilon D_y^2 DS_0)(1, y) &= Df^*(1, y) - p_1 D_x DS_0(1, y) \\ &\quad - p_2 D_y DS_0(1, y) + q DS_0(1, y) \forall y. \end{aligned}$$

Using the above we see that

$$\begin{aligned} |(D_x^2 DS_0 + D_y^2 DS_0)(1, y)| &\leq C_1 \{ p_1 [\|D_y^2 DS_0\|_{\infty, \Pi_{x < 1}}] \\ &\quad + 2[\|f^*\|_{|D|+2, \infty, \Pi_{x < 1}} + \|DS_0\|_{\infty, \Pi_{x < 1}} \\ &\quad + \|D_y DS_0\|_{\infty, \Pi_{x < 1}} + \|D_y^2 DS_0\|_{\infty, \Pi_{x < 1}} + \|D_y^3 DS_0\|_{\infty, \Pi_{x < 1}}] \}. \end{aligned}$$

Therefore

$$\begin{aligned}
|(D_x^2 D S_0)(1, y)| &\leq C_1 \{p_1 [\|D_y^2 D S_0\|_{\infty, \Pi_{x < 1}}] \\
&\quad + 2[\|f^*\|_{|D|+2, \infty, \Pi_{x < 1}} + \|D S_0\|_{\infty, \Pi_{x < 1}} \\
&\quad + \|D_y D S_0\|_{\infty, \Pi_{x < 1}} + \|D_y^2 D S_0\|_{\infty, \Pi_{x < 1}} + \|D_y^3 D S_0(1, y)\|_{\infty, \Pi_{x < 1}}] \} \\
&\quad + \|D_y^2 D S_0(1, y)\|_{\infty, \Pi_{x < 1}} \quad \forall y. \tag{3.36}
\end{aligned}$$

Finally,

$$L(D_x^2 D S_0)(x, y) = D_x^2 D f^*(x, y) \quad \forall (x, y) \in \Pi_{x < 1}.$$

Using the above and the barrier function:

$$\begin{aligned}
\Phi(x, y) &= C_1 \{p_1 \|D_y^2 D S_0\|_{\infty, \Pi_{x < 1}} \\
&\quad + 2[\|f^*\|_{|D|+2, \infty, \Pi_{x < 1}} + \|D S_0\|_{\infty, \Pi_{x < 1}} \\
&\quad + \|D_y D S_0\|_{\infty, \Pi_{x < 1}} + \|D_y^2 D S_0\|_{\infty, \Pi_{x < 1}}] \} \\
&\quad + \frac{\|D_x^2 D f^*\|_{\infty, \Pi_{x < 1}}}{q}
\end{aligned}$$

and the maximum principle we obtain the desired result.  $\square$

**Theorem 3.5.** *Let  $m$  and  $n$  be non-negative integers. Let  $f^* \in W^{m+n, \infty}$ .*

*Then*

$$\|D_x^m D_y^n S_0\|_{\infty, \Pi_{x < 1}} \leq C \|f^*\|_{m+n, \infty, \Pi_{x < 1}},$$

where  $C$  is a constant independent of  $\varepsilon$ .

**Proof.** We use induction on  $m$  and note that the cases  $m = 0, 1$  are proved in Lemmas 3.2 and 3.3. Let  $k$  be a positive integer and assume that the result

is true for  $m = 0, 1, \dots, k$ . Let  $n$  be a non-negative integer. Applying Lemma 3.4 with  $D = D_x^{k-1} D_y^n$  and using the inductive hypothesis we see that

$$\begin{aligned} \|D_x^{k+1} D_y^n\|_{\infty, \Pi_x} &\leq C(\|f^*\|_{k+n+1} + \|DS_0\|_{\infty, \Pi_{x < 1}} \\ &\quad + \|D_y DS_0\|_{\infty, \Pi_{x < 1}} + \|D_y^2 DS_0\|_{\infty, \Pi_{x < 1}} + \|D_y^3 DS_0\|_{\infty, \Pi_{x < 1}}) \\ &\leq C\|f^*\|_{k+n+1, \infty, \Pi_{x < 1}}. \end{aligned}$$

That is, the result is true for  $m = k + 1$ , completing the proof.  $\square$

We can use the above result to obtain a bound for  $S_1$  by reducing (3.3) to the case of homogeneous boundary conditions by letting

$$U(x, y) = S_1(x, y) - g_e^*(y) \quad \forall x < 1, y \in \mathbb{R}. \quad (3.37)$$

Then

$$LU(x, y) = f^*(x, y) - \varepsilon g_e^{*''}(y) - p_2 g_e^{*'}(y) + q g_e^*(y) \quad \forall x < 1, y \in \mathbb{R}$$

and  $U(1, y) \equiv 0 \quad \forall y$ . Using (3.37) and Theorem 3.5 it is easy to see that

$$\begin{aligned} \|D_x^m D_y^n S_1\|_{\infty, \Pi_{y < 1}} &\leq \|D_x^m D_y^n U\|_{\infty, \Pi_{y < 1}} + \|D_y^n g_e^*\|_{\infty, \mathbb{R}} \\ &\leq C(\|f^*\|_{m+n, \infty, \Pi_{y < 1}} + \|g_e^*\|_{n+2, \infty, \mathbb{R}}). \end{aligned}$$

By the same arguments a similar result hold for  $S_2$  as follows:

$$\|D_x^m D_y^n S_2\|_{\infty, \Pi_{y < 1}} \leq C(\|f^*\|_{m+n, \infty, \Pi_{y < 1}} + \|g_e^*\|_{n+2, \infty, \mathbb{R}} + \|g_n^*\|_{m+2, \infty, \mathbb{R}}).$$

### 3.3.2 Exponential layer components $E_1$ and $E_2$

#### Growth conditions and Maximum Principle: $E_1$

$E_1$  is defined to be the solution of the outgoing half-plane problem given in Section 3.2, (3.5). Growth conditions for a similar problem are shown in [45], Section 3.1. We use the following maximum principle in order to obtain bounds on  $E_1$ .

**Lemma 3.6.** *Let  $\Phi \in C^2(\bar{\Pi}_x)$  satisfy  $L\Phi \leq 0$ ,  $\Phi(0, y) \geq 0 \forall y \in \mathbb{R}$  on  $\Pi_x$  and*

$$\int_{-\infty}^{\infty} (1 + |y|)^{-3/2} |\Phi(1, y)| e^{-p|y|/2\varepsilon} dy < \infty, \quad (3.38)$$

then  $\Phi \geq 0$  in  $\Pi_{x < 1}$ .

If  $U \in C^2(\Pi_x)$  satisfies  $|LU(x, y)| \leq |L\Phi(x, y)|$  in  $\Pi_x$  and  $|U(0, y)| \leq \Phi(0, y)$ ,  $\forall y \in \mathbb{R}$ , then  $|U(x, y)| \leq \Phi(x, y)$  in  $\Pi_x$ .  $\square$

**Lemma 3.7.** *Let  $E_1(0, y) = E_{1,0}(y) \forall y$ . Note that  $\|E_{1,0}\|$  was bounded  $\forall y$  in section 3.3.1. Then*

$$|E_1(x, y)| \leq C_0 \|E_{1,0}\|_{\infty, \mathbb{R}} e^{-p_1 x / \varepsilon} \forall (x, y) \in \bar{\Pi}_x, \quad (3.39)$$

where  $C_0 = 1$ . And since  $\|E_{1,0}\|_{2, \infty, \mathbb{R}}$  was bounded  $\forall y$  in section 3.3.1 then

$$|E_{1,x}(x, y)| \leq C_1 \|E_{1,0}\|_{2, \infty, \mathbb{R}} \varepsilon^{-1} e^{-p_1 x / \varepsilon} \forall (x, y) \in \bar{\Pi}_x, \quad (3.40)$$

where  $C_1 = (\frac{2}{p_1} + p_1)(1 + p_2 + 2q)$ .

**Proof.** Let  $\psi(x, y) = \|E_{1,0}\|_{\infty, \mathbb{R}} e^{-p_1 x / \varepsilon}$ , therefore  $\psi(0, y) = \|E_{1,0}\|_{\infty, \mathbb{R}} \geq |E_1(0, y)|$

$\forall y$  and  $|L\psi(x, y)| = q e^{-p_1 x / \varepsilon} \|E_{1,0}\|_{\infty, \mathbb{R}} \geq |LE_1| = 0 \forall (x, y) \in \Pi_x$ .

Therefore, by Lemma 3.6, (3.39) can be shown to be true. In order to prove that (3.40) is true we must first bound  $|E_{1,x}(0, y)|$ . Let  $\theta(x, y) = E_1(x, y) - E_{1,0}(y)e^{-p_1x/\varepsilon}$  on  $\bar{\Pi}_x$ . Then  $\theta(0, y) = 0 \forall y$  and

$$L\theta(x, y) = -e^{-p_1x/\varepsilon}[\varepsilon E''_{1,0}(y) + p_2 E'_{1,0}(y) - 2qE_{1,0}(y)].$$

Therefore

$$|L\theta(x, y)| \leq e^{-p_1x/\varepsilon}[\varepsilon \|E''_{1,0}\|_{\infty, \mathbb{R}} + p_2 \|E'_{1,0}\|_{\infty, \mathbb{R}} + 2q \|E_{1,0}\|_{\infty, \mathbb{R}}].$$

Let

$$\xi(x, y) = \frac{4\varepsilon}{p_1^2}(e^{-p_1x/2\varepsilon} - e^{-p_1x/\varepsilon})[\varepsilon \|E''_{1,0}\|_{\infty, \mathbb{R}} + p_2 \|E'_{1,0}\|_{\infty, \mathbb{R}} + 2q \|E_{1,0}\|_{\infty, \mathbb{R}}].$$

Then  $\xi(0, y) = 0 = \theta(0, y) \forall y$  and

$$\begin{aligned} |L\xi(x, y)| &= (e^{-p_1x/2\varepsilon} + \frac{4\varepsilon q}{p_1^2}(e^{-p_1x/2\varepsilon} - e^{-p_1x/\varepsilon}))[\varepsilon \|E''_{1,0}\|_{\infty, \mathbb{R}} + p_2 \|E'_{1,0}\|_{\infty, \mathbb{R}} + 2q \|E_{1,0}\|_{\infty, \mathbb{R}}] \\ &\geq e^{-p_1x/2\varepsilon}[\varepsilon \|E''_{1,0}\|_{\infty, \mathbb{R}} + p_2 \|E'_{1,0}\|_{\infty, \mathbb{R}} + 2q \|E_{1,0}\|_{\infty, \mathbb{R}}] \\ &\geq |L\theta(x, y)| \forall (x, y) \in \Pi_x. \end{aligned}$$

Therefore by Lemma 3.6  $|\theta(x, y)| \leq \xi(x, y) \forall (x, y) \in \bar{\Pi}_x$ , that is

$$\begin{aligned} |E_1(x, y) - E_{1,0}(y)e^{-p_1x/\varepsilon}| &\leq \frac{4\varepsilon}{p_1^2}(e^{-p_1x/2\varepsilon} - e^{-p_1x/\varepsilon})[\varepsilon \|E''_{1,0}\|_{\infty, \mathbb{R}} + p_2 \|E'_{1,0}\|_{\infty, \mathbb{R}} \\ &\quad + 2q \|E_{1,0}\|_{\infty, \mathbb{R}}]. \end{aligned}$$

Now

$$\begin{aligned}
|E_{1,x}(0, y)| &= \left| \lim_{x \rightarrow 0^+} \frac{E_1(x, y) - E_1(0, y)}{x} \right| \\
&= \left| \lim_{x \rightarrow 0^+} \frac{\theta(x, y) + E_{1,0}(y)e^{-p_1 x/\varepsilon} - E_{1,0}(y)}{x} \right| \\
&\leq \lim_{x \rightarrow 0^+} \frac{|\xi(x, y)|}{x} + |E_{1,0}(y)| \lim_{x \rightarrow 0^+} \left| \frac{e^{-p_1 x/\varepsilon} - 1}{x} \right| \\
&= \frac{2}{p_1} (\varepsilon \|E_{1,0}''\|_{\infty, \mathbb{R}} + p_2 \|E_{1,0}'\|_{\infty, \mathbb{R}} + 2q \|E_{1,0}\|_{\infty, \mathbb{R}}) + \frac{p_1}{\varepsilon} |E_{1,0}(y)| \\
&\leq C_1 \varepsilon^{-1} \|E_1, 0\|_{2, \infty, \mathbb{R}}.
\end{aligned}$$

Applying (3.39) to  $E_{1,x}$  yields

$$|E_{1,x}(x, y)| \leq C_1 \|E_{1,0}\|_{2, \infty, \mathbb{R}} \varepsilon^{-1} e^{-p_1 x/\varepsilon} \text{ on } \bar{\Pi}_x$$

as desired.  $\square$

**Theorem 3.8.** *Let  $m$  and  $n$  be non-negative integers and let  $\bar{m}$  denote the smallest even integer that satisfies  $\bar{m} \geq m$ . Note that*

*$\|E_{1,0}\|_{\bar{m}+n, \infty, \mathbb{R}} \varepsilon^{-m} e^{-p_1 x/\varepsilon} \forall (x, y) \in \Pi_x$ . Then*

$$|D_x^m D_y^n E_1(x, y)| \leq C_m \|E_{1,0}\|_{\bar{m}+n, \infty, \mathbb{R}} \varepsilon^{-m} e^{-p_1 x/\varepsilon}.$$

**Proof.** We start by assuming that  $n = 0$  and prove the result using strong induction on  $m$ . Note that the cases  $m = 0, 1$  were proven in the previous lemma. With  $n = 0$ , assume that the result is true for  $m = 0, 1, \dots, k$  where  $k$  is some positive integer. It has already been shown that  $\|E_{1,0}\|_{\bar{k}-1, \infty, \mathbb{R}}$  and  $\|E_{1,0}\|_{\bar{k}+1, \infty, \mathbb{R}}$  are finite in Section 3.3.1. The function  $E_{1,yy}$  satisfies  $LE_{1,yy} = 0$  on  $\Pi_x$  and  $E_{1,yy}(0, y) = E_{1,0}''(y) \forall y$ , i.e.,  $E_{1,yy}$  is the solution of a problem

similar to (3.5), but with boundary data  $E''_{1,0}$ . Let

$$C_i = p_1 C_{i-1} + (1 + p_2 + q) C_{i-2}, \quad i = 2, 3, \dots, \quad (3.41)$$

where  $C_0$  and  $C_1$  are as defined in the previous lemma. Applying the inductive hypothesis to  $E_{1,yy}$  with  $m = k - 1$  we see that

$$\begin{aligned} |D_x^{k-1} E_{1,yy}(x, y)| &\leq C_{k-1} \|E_{1,yy}\|_{\overline{k-1}, \infty, \mathbb{R}} \varepsilon^{-k+1} e^{-p_1 x/\varepsilon} \\ &\leq C_{k-1} \|E_{1,0}\|_{\overline{k+1}, \infty, \mathbb{R}} \varepsilon^{-k+1} e^{-p_1 x/\varepsilon} \quad \forall (x, y) \in \bar{\Pi}_x. \end{aligned} \quad (3.42)$$

Now  $LE_1 = 0$  is differentiated  $k - 1$  times with respect to  $x$  and rearranged to obtain

$$\begin{aligned} |\varepsilon D_x^{k+1} E_1(x, y)| &= |(-\varepsilon D_x^{k-1} D_y^2 E_1 - p_1 D_x^k E_1 - p_2 D_x^{k-1} D_y E_1 + q D_x^{k-1} E_1)(x, y)| \\ &\leq (C_{k-1} \|E_{1,0}\|_{\overline{k+1}, \infty, \mathbb{R}} \varepsilon^{-k+2} + p_1 C_k \|E_{1,0}\|_{\bar{k}, \infty, \mathbb{R}} \varepsilon^{-k} \\ &\quad + p_2 C_{k-1} \|E_{1,0}\|_{\bar{k}, \infty, \mathbb{R}} \varepsilon^{-k+1} + q C_{k-1} \|E_{1,0}\|_{\overline{k-1}, \infty, \mathbb{R}} \varepsilon^{-k+1}) e^{-p_1 x/\varepsilon} \\ &\leq C_{k+1} \|E_{1,0}\|_{\overline{k+1}, \infty, \mathbb{R}} \varepsilon^{-k} e^{-p_1 x/\varepsilon} \quad \forall (x, y) \in \bar{\Pi}_x, \end{aligned}$$

using (3.42), (3.41) and the inductive hypothesis. Thus we have proven the result for the case  $m = k + 1$  and, by the principle of induction, the proof is complete for the case  $n = 0$ . For  $n > 0$ , apply the result just proven to the function  $D_y^n E_1$ , which satisfies a problem similar to (3.5) but with boundary data  $E_{1,0}^{(n)}$ .  $\square$

By the same arguments a similar result holds for  $E_2$  as follows:

$$|D_x^m D_y^n E_2(x, y)| \leq K_n \|E_{2,0}\|_{m+\bar{n}, \infty, \mathbb{R}} \varepsilon^{-n} e^{-p_2 y/\varepsilon}, \quad (3.43)$$

where  $K_0 = 1$ ,  $K_1 = (\frac{2}{p_2} + p_2)(1 + p_1 + 2q)$  and  $K_i = p_2 K_{i-1} + (1 + p_1 +$

$q)K_{i-2}, i = 2, 3, \dots, \square$

### 3.3.3 Outflow corner component $z_{00}$

**Growth conditions and Maximum Principles on the right-upper quarter plane,  $Q_1$**

Consider the outgoing quarter plane problem on  $Q_1 = \{(x, y) \in R^2 : x > 0, y > 0\}$

$$\begin{aligned}
 Lv &\equiv \varepsilon \Delta v + p_1 \frac{\partial v}{\partial x} + p_2 \frac{\partial v}{\partial y} - qv = f, \quad x > 0, y > 0, \\
 v(x, 0) &= h_s(x), \quad x > 0, \\
 v(0, y) &= h_w(y), \quad y > 0
 \end{aligned}
 \tag{3.44}$$

where  $p_1, p_2$  and  $q$  are positive constants as before. Applying similar transformations and change of variables as in [45], Section 3.1 we have the Green's function for this problem as follows

$$G(\xi, \eta; \sigma, \tau) = \frac{1}{2\pi} [K_0(\kappa\rho_1) - K_0(\kappa\rho_2) - K_0(\kappa\rho_3) + K_0(\kappa\rho_4)] \tag{3.45}$$

where

$$\begin{aligned}
 \rho_1 &= \sqrt{(\xi - \sigma)^2 + (\eta - \tau)^2}, \\
 \rho_2 &= \sqrt{(\xi - \sigma)^2 + (\eta + \tau)^2}, \\
 \rho_3 &= \sqrt{(\xi + \sigma)^2 + (\eta - \tau)^2}, \\
 \rho_4 &= \sqrt{(\xi + \sigma)^2 + (\eta + \tau)^2}
 \end{aligned}$$

and  $K_0$  is a modified Bessel function of the second kind [87]. With

$$\begin{aligned}\rho_5 &= \sqrt{\xi^2 + (\eta - \tau)^2}, \\ \rho_6 &= \sqrt{\xi^2 + (\eta + \tau)^2}, \\ \rho_7 &= \sqrt{(\xi - \sigma)^2 + \eta^2}, \\ \rho_8 &= \sqrt{(\xi + \sigma)^2 + \eta^2}\end{aligned}$$

we have the solution formula for the Helmholtz equation derived from (3.44) as follows

$$\begin{aligned}v_2(\xi, \eta) &= -\frac{1}{2\pi} \int_0^\infty \int_0^\infty f_2(\sigma, \tau) [K_0(\kappa\rho_1) - K_0(\kappa\rho_2) - K_0(\kappa\rho_3) + K_0(\kappa\rho_4)] d\tau d\sigma \\ &\quad + \frac{\xi\kappa}{\pi} \int_0^\infty h_{2,w}(\tau) \left[ \frac{1}{\rho_5} K_1(\kappa\rho_5) - \frac{1}{\rho_6} K_1(\kappa\rho_6) \right] d\tau \\ &\quad + \frac{\eta\kappa}{\pi} \int_0^\infty h_{2,s}(\sigma) \left[ \frac{1}{\rho_7} K_1(\kappa\rho_7) - \frac{1}{\rho_8} K_1(\kappa\rho_8) \right] d\sigma.\end{aligned}\tag{3.46}$$

The solution of the Helmholtz equation exists and is given by (3.46) provided the functions  $f_2$ ,  $h_{2,s}$  and  $h_{2,w}$  are such that the integrals are convergent. In addition, if  $f_2$  is negative and  $h_{2,s}$  and  $h_{2,w}$  are non-negative, then  $v_2$  is non-negative since it can easily be shown that (3.45) is positive by rewriting it as either

$$\int_{\kappa\rho_1}^{\kappa\rho_2} K_1(t) dt - \int_{\kappa\rho_3}^{\kappa\rho_4} K_1(t) dt$$

or

$$\int_{\kappa\rho_1}^{\kappa\rho_3} K_1(t) dt - \int_{\kappa\rho_2}^{\kappa\rho_4} K_1(t) dt$$

and noting that  $\rho_2 - \rho_1 > \rho_4 - \rho_3$  and  $\rho_3 - \rho_1 > \rho_4 - \rho_2$  respectively (since  $\rho_2 - \rho_1 = \frac{4\eta\tau}{\rho_1 + \rho_2}$ , etc.) and that  $K_1(t)$  is a decreasing function of  $t$ .

In examining the finiteness of the integrals, note that

$$|K_0(\kappa\rho_1)| + |K_0(\kappa\rho_2)| + |K_0(\kappa\rho_3)| + |K_0(\kappa\rho_4)| \leq C|K_0(\kappa\rho_1)|$$

and that in the case of  $\sigma \leq 2\xi$ ,  $\tau \leq 2\eta$  we have  $K_0(t) \leq C|\ln(t)|$  for  $0 < t \leq 1$  and  $\int_0^1 |\ln t| dt$  is finite. For  $\sigma > 2\xi$  and  $\tau > 2\eta$ ,

$$\begin{aligned} \rho_1 &= \sqrt{(\xi - \sigma)^2 + (\eta - \tau)^2} = \sqrt{(\sigma - \xi)^2 + (\tau - \eta)^2} \\ &= \sqrt{\left(\frac{\sigma}{2} + \frac{\sigma}{2} - \xi\right)^2 + \left(\frac{\tau}{2} + \frac{\tau}{2} - \eta\right)^2} \\ &> \frac{1}{2}\sqrt{\sigma^2 + \tau^2} \end{aligned}$$

and, as in [45], using the bound derived from (9.6.23) in [1],  $|K_j(t)| \leq Ct^{-1/2}e^{-t}$  for  $t > 1$ , we obtain the following integrability condition for the  $f_2$  integral

$$\int_{2\xi}^{\infty} \int_{2\eta}^{\infty} (\sigma^2 + \tau^2)^{-1/4} |f_2(\sigma, \tau)| e^{-\kappa/2(\sigma^2 + \tau^2)^{1/2}} d\tau d\sigma < \infty.$$

In the case of the  $h_2$  integrals note that neither  $\rho_5$  nor  $\rho_7$  can be zero, therefore we need only establish that large  $\sigma$  and  $\tau$  do not cause the integrals to become infinitely large. For  $\sigma > 2\xi$  and  $\tau > 2\eta$  we have  $\rho_5 > \tau/2$  and  $\rho_7 > \sigma/2$  and the integrability conditions are as follows

$$\begin{aligned} \int_{2\xi}^{\infty} \sigma^{-3/2} |h_{2,s}(\sigma)| e^{-\kappa\sigma/2} d\sigma &< \infty, \\ \int_{2\eta}^{\infty} \tau^{-3/2} |h_{2,w}(\tau)| e^{-\kappa\tau/2} d\tau &< \infty. \end{aligned}$$

Reverting to the original variables and setting  $r = (x^2 + y^2)^{1/2}$  the integrability

conditions become

$$\begin{aligned}
\int_{x=2s}^{\infty} \int_{y=2t}^{\infty} r^{-1/2} |f(x, y)| e^{-(\kappa r + p_1 x + p_2 y)/2\varepsilon} dy dx &< \infty, \\
\int_{2s}^{\infty} x^{-3/2} |h_s(x)| e^{-(\kappa x + p_1 x)/2\varepsilon} dx &< \infty, \\
\int_{2t}^{\infty} y^{-3/2} |h_w(y)| e^{-(\kappa y + p_2 y)/2\varepsilon} dy &< \infty.
\end{aligned} \tag{3.47}$$

We then obtain the following maximum principles for  $Q_1$  and  $Q_\varepsilon$  respectively.

**Lemma 3.9.** *Let  $\Phi \in C^2(\bar{Q}_1)$  satisfy  $L\Phi \leq 0$  on  $Q_1$ ,  $\Phi(x, 0) \geq 0$  for  $x > 0$ ,  $\Phi(0, y) \geq 0$  for  $y > 0$  and*

$$\begin{aligned}
\left| \int_{x=0}^{\infty} \int_{y=0}^{\infty} (1+r)^{-1/2} L\Phi(x, y) e^{-(pr/2\varepsilon)} dy dx \right| &< \infty, \\
\int_0^{\infty} (1+x)^{-3/2} \Phi(x, 0) e^{-px/2\varepsilon} dx &< \infty, \\
\int_0^{\infty} (1+y)^{-3/2} \Phi(0, y) e^{-py/2\varepsilon} dy &< \infty,
\end{aligned}$$

where  $p = \min\{p_1, p_2\}$ . Then  $\Phi \geq 0$  in  $Q_1$ . If  $U \in C^2(Q_1)$  satisfies  $|LU(x, y)| \leq |L\Phi(x, y)|$  in  $Q_1$  and  $|U(x, 0)| \leq \Phi(x, 0)$  for  $x > 0$ ,  $|U(0, y)| \leq \Phi(0, y)$  for  $y > 0$ , then  $|U(x, y)| \leq \Phi(x, y)$  in  $Q_1$ .  $\square$

**Remark 3.10.** *The above proof applies to problems with continuous boundary data but can be extended as follows to problems with discontinuous boundary data as set out below, from private correspondence with N. Kopteva, 2012:*

*Let  $g(y)$  be the boundary condition function. Consider a sequence of continuous functions  $g_n(y)$  such that it converges to  $g(y)$ . Let the sequence  $g_n$  generate the sequence of solutions  $U_n$ ; one can apply the comparison principle to each  $U_n$ , and using an appropriate barrier function, show  $|U_n(x, y)| \leq \Phi(x, y)$ . Then take the limit to prove  $|U(x, y)| \leq \Phi(x, y)$ .*

Alternatively, for any elliptic problem  $Lu = f$  subject to  $u = g$  on the boundary, one can represent the unique solution via the Green's function,  $G$ , and its normal derivative,  $K$ , as  $u = \int_{\Omega} Gf + \int_{\partial\Omega} Kg$ . Here  $f$  and  $g$  can be continuous or discontinuous. If the problem satisfies the maximum principle (for any continuous and smooth  $f$  and  $g$ ), then one concludes that  $G > 0$  and  $K > 0$ . Now, using the solution representation formula with possibly discontinuous  $f > 0$  and  $g > 0$ , one also concludes that  $u > 0$ .  $\square$

**Lemma 3.11.** Define  $Q_{\varepsilon} = \{(x, y) \in R^2 : x > 0, y > 0, \sqrt{x^2 + y^2} > \varepsilon\}$  and let  $\Phi \in C^2(\bar{Q}_{\varepsilon})$  satisfy  $L\Phi \leq 0$  on  $Q_{\varepsilon}$  and  $\Phi(x, y) \geq 0$  for  $(x, y) \in \Gamma_{\varepsilon}$

$$\begin{aligned} \left| \int_{x=\varepsilon}^{\infty} \int_{y=\varepsilon}^{\infty} (1+r)^{-1/2} L\Phi(x, y) e^{-(pr/2\varepsilon)} dy dx \right| &< \infty, \\ \int_{\varepsilon}^{\infty} (1+x)^{-3/2} \Phi(x, 0) e^{-px/2\varepsilon} dx &< \infty, \\ \int_{\varepsilon}^{\infty} (1+y)^{-3/2} \Phi(0, y) e^{-py/2\varepsilon} dy &< \infty, \end{aligned}$$

where  $p = \min\{p_1, p_2\}$ . Then  $\Phi \geq 0$  in  $Q_{\varepsilon}$ . If  $U \in C^2(Q_{\varepsilon})$  satisfies  $|LU(x, y)| \leq |L\Phi(x, y)|$  in  $Q_{\varepsilon}$  and  $|U(x, y)| \leq \Phi(x, y)$  for  $(x, y) \in \Gamma_{\varepsilon}$ , then  $|U(x, y)| \leq \Phi(x, y)$  in  $Q_{\varepsilon}$ .  $\square$

We give two different sets of analysis showing how  $z_{00}$  can be bounded. The following lemma is analogous to Lemma 4.1 in [45]. In the region of the corner of  $Q_1$  the analysis is by means of Green's functions expressed in terms of modified Bessel functions of the second kind. A maximum principle is used on the remainder of the domain. An alternative method is given subsequently.

**Lemma 3.12.** For all  $x, y \in Q_1$  we have

$$\begin{aligned}
|z_{00}(x, y)| &\leq C, \quad r \leq \varepsilon, \\
|z_{00}(x, y)| &\leq \max\{\|g_s^*\|_{\infty, Q_1}, \|g_w^*\|_{\infty, Q_1}\} e^{-pr/\varepsilon} + \|g_w^*\|_{\infty, Q_1} e^{-px/\varepsilon} \\
&\quad + \|g_s^*\|_{\infty, Q_1} e^{-py/\varepsilon}, \quad r > \varepsilon.
\end{aligned}$$

**Proof.** Since  $z_{00}$  is discontinuous at  $(0, 0)$ , the maximum principle Lemma 3.9 cannot be used directly to obtain the desired bound on the whole domain,  $Q_1$ . Instead, we first establish a bound on  $z_{00}$  where  $r \leq \varepsilon$  using modified Bessel functions to give a solution formula for (3.7). We can then bound  $z_{00}$  on the remaining portion of the domain using an appropriate maximum principle. As in Section 3.3.1, using the Green's function stated in terms of modified Bessel functions for the translated problem, we arrive at the following solution formula for (3.7).

$$\begin{aligned}
z_{00}(x, y) &= \frac{e^{-(p_1x+p_2y)/2\varepsilon} x\kappa}{2\varepsilon\pi} \int_0^\infty e^{-p_2t/2\varepsilon} [g_w^*(t) - E_2(0, t)] \left[ \frac{K_1(\kappa r_5/2\varepsilon)}{r_5} - \frac{K_1(\kappa r_6/2\varepsilon)}{r_6} \right] dt \\
&\quad + \frac{e^{-(p_1x+p_2y)/2\varepsilon} y\kappa}{2\varepsilon\pi} \int_0^\infty e^{-p_1s/2\varepsilon} g_s^*(s) \left[ \frac{K_1(\kappa r_7/2\varepsilon)}{r_7} - \frac{K_1(\kappa r_8/2\varepsilon)}{r_8} \right] ds
\end{aligned} \tag{3.48}$$

where  $r_5 = \sqrt{x^2 + (y-t)^2}$ ,  $r_6 = \sqrt{x^2 + (y+t)^2}$ ,  $r_7 = \sqrt{(x-s)^2 + y^2}$  and  $r_8 = \sqrt{(x+s)^2 + y^2}$ . In the case where  $r \leq \varepsilon$  we have

$$\begin{aligned}
|z_{00}(x, y)| &\leq \frac{Cx}{\varepsilon} \left( \int_{|t-y| \leq \varepsilon} + \int_{|t-y| > \varepsilon} \right) \left[ \frac{K_1(\kappa r_5/2\varepsilon)}{r_5} - \frac{K_1(\kappa r_6/2\varepsilon)}{r_6} \right] dt \\
&\quad + \frac{Cy}{\varepsilon} \left( \int_{|s-x| \leq \varepsilon} + \int_{|s-x| > \varepsilon} \right) \left[ \frac{K_1(\kappa r_7/2\varepsilon)}{r_7} - \frac{K_1(\kappa r_8/2\varepsilon)}{r_8} \right] ds \\
&= I_1 + I_2 + J_1 + J_2,
\end{aligned} \tag{3.49}$$

since  $x \leq \varepsilon$  and  $y \leq \varepsilon$ . In order to bound  $I_1$ , note that  $x \leq \varepsilon$  and  $|t - y| \leq \varepsilon$  imply that  $\kappa r_5/2\varepsilon \leq C$ , therefore  $K_1(\kappa r_5/2\varepsilon) \leq C\varepsilon/r_5$  from [1], (9.6.9).

Therefore,

$$\begin{aligned}
I_1 &\leq \frac{Cx}{\varepsilon} \int_{|t-y| \leq \varepsilon} \left( \frac{\varepsilon}{r_5^2} - \frac{\varepsilon}{r_6^2} \right) dt \\
&= C \int_{|t-y| \leq \varepsilon} \left( \frac{x}{r_5^2} - \frac{x}{r_6^2} \right) dt \\
&\leq C \int_{|t-y| \leq \varepsilon} \frac{x}{x^2 + (y-t)^2} dt + C \int_{|t-y| \leq \varepsilon} \frac{x}{x^2 + (y+t)^2} dt \\
&= C \tan^{-1} \left( \frac{t-y}{x} \right) + C \tan^{-1} \left( \frac{t+y}{x} \right) \leq C
\end{aligned} \tag{3.50}$$

For  $I_2$ ,  $|t - y| > \varepsilon$  implies that  $\kappa r_5/2\varepsilon \geq \kappa/2 \geq p/2 > 0$ , therefore by [1], (9.7.2)

$$K_1(\kappa r_5/2\varepsilon) \leq C \left( \frac{\varepsilon}{r_5} \right)^{1/2} e^{-\kappa r_5/2\varepsilon} \leq C \left( \frac{\varepsilon}{r_5} \right)^{1/2} e^{-\kappa|t-y|/2\varepsilon}.$$

Therefore,

$$I_2 \leq \frac{Cx}{\sqrt{\varepsilon}} \int_{|t-y| > \varepsilon} \frac{1}{(r_5)^{3/2}} e^{-\kappa|t-y|/2\varepsilon} dt + \frac{Cx}{\sqrt{\varepsilon}} \int_{|t-y| > \varepsilon} \frac{1}{(r_6)^{3/2}} e^{-\kappa|t-y|/2\varepsilon} dt.$$

Since  $x \leq r_5$  and  $\varepsilon \leq r_5$ ,  $xr_5^{-3/2} \leq r_5^{-1/2} \leq \varepsilon^{-1/2}$ , therefore

$$I_2 \leq C\varepsilon^{-1} \int_{|t-y| > \varepsilon} e^{-\kappa|t-y|/2\varepsilon} dt \leq C. \tag{3.51}$$

The terms  $J_1$  and  $J_2$  can be bounded in a similar fashion, and so by combining (3.49), (3.50) and (3.51) we attain the desired bound on  $z_{00}$  where  $r \leq \varepsilon$ .

When  $r > \varepsilon$  let  $\theta = \max\{\|g_s^*\|_{\infty, Q_\varepsilon}, \|g_w^*\|_{\infty, Q_\varepsilon}\} e^{-pr/\varepsilon} + \|g_w^*\|_{\infty, Q_\varepsilon} e^{-px/\varepsilon} +$

$\|g_s^*\|_{\infty, Q_\varepsilon} e^{-py/\varepsilon}$ , then

$$\begin{aligned} L\theta &= -\max\{\|g_s^*\|_{\infty, Q_\varepsilon}, \|g_w^*\|_{\infty, Q_\varepsilon}\} e^{-pr/\varepsilon} \left[ \frac{p}{r} \left[ 1 + \frac{1}{\varepsilon} (p_1 x + p_2 y - pr) \right] + q \right] \\ &\quad - \|g_w^*\|_{\infty, Q_\varepsilon} e^{-px/\varepsilon} \left[ \frac{1}{\varepsilon} (pp_1 - p^2) + q \right] - \|g_s^*\|_{\infty, Q_\varepsilon} e^{-py/\varepsilon} \left[ \frac{1}{\varepsilon} (pp_2 - p^2) + q \right] \\ &\leq 0 \end{aligned}$$

and  $|L\theta| \geq |Lz_{00}|$ . For all  $(x, y)$  such that  $\sqrt{x^2 + y^2} = \varepsilon$  we have

$$\theta(x, y) = \max\{\|g_s^*\|_{\infty, Q_\varepsilon}, \|g_w^*\|_{\infty, Q_\varepsilon}\} e^{-p} + \|g_w^*\|_{\infty, Q_\varepsilon} e^{-px/\varepsilon} + \|g_s^*\|_{\infty, Q_\varepsilon} e^{-py/\varepsilon} \geq C$$

since  $x \leq \varepsilon$  and  $y \leq \varepsilon$  in this case.

Then for  $y = 0$ ,  $x \geq \varepsilon$

$$\begin{aligned} \theta(x, 0) &= (\max\{\|g_s^*\|_{\infty, Q_\varepsilon}, \|g_w^*\|_{\infty, Q_\varepsilon}\} + \|g_w^*\|_{\infty, Q_\varepsilon}) e^{-px/\varepsilon} + \|g_s^*\|_{\infty, Q_\varepsilon} \\ &\geq z_{00}(x, 0) = g_s^*(x). \end{aligned}$$

And for  $x = 0$ ,  $y \geq \varepsilon$

$$\begin{aligned} \theta(y, 0) &= (\max\{\|g_s^*\|_{\infty, Q_\varepsilon}, \|g_w^*\|_{\infty, Q_\varepsilon}\} + \|g_s^*\|_{\infty, Q_\varepsilon}) e^{-py/\varepsilon} + \|g_w^*\|_{\infty, Q_\varepsilon} \\ &\geq z_{00}(0, y) = g_w^*(y) - E_2(0, y), \end{aligned}$$

and  $E_2(0, y)$  is bounded by  $Ce^{-p_2 y/\varepsilon}$ . Therefore by our maximum principle, Lemma (3.11), the result follows.  $\square$

It is possible to extend the analysis above to bound the first derivatives of  $z_{00}$ , as in ([45]) using the Leibniz integral rule. The complexity of the expression of higher derivatives in terms of modified Bessel functions, however, renders this method extremely complex for obtaining bounds on derivatives

of  $z_{00}$  beyond the first ones. Alternatively we can bound  $z_{00}$  on the entire quarter-plane domain using the maximum principle given in Lemma (3.9) and Remark (3.10), as follows.

**Lemma 3.13.** *For all  $x, y \in Q_1$  we have*

$$|z_{00}(x, y)| \leq \max\{\|g_s^*\|_{\infty, Q_1}, \|g_w^*\|_{\infty, Q_1}\}e^{-pr/\varepsilon} + \|g_w^*\|_{\infty, Q_1}e^{-px/\varepsilon} \\ + \|g_s^*\|_{\infty, Q_1}e^{-py/\varepsilon}$$

**Proof.** Let  $\theta(x, y) = \max\{\|g_s^*\|_{\infty, Q_1}, \|g_w^*\|_{\infty, Q_1}\}e^{-pr/\varepsilon} + \|g_w^*\|_{\infty, Q_1}e^{-px/\varepsilon} + \|g_s^*\|_{\infty, Q_1}e^{-py/\varepsilon}$ , then  $L\theta(x, y) \leq 0$  as before and  $|Lz_{00}(x, y)| \leq |L\theta(x, y)|$ . Also,  $|z_{00}(x, 0)| = |g_s^*(x)| \leq \theta(x, 0)$ . Now,

$$z_{00}(0, y) = g_w^*(y) - E_2(0, y) \text{ and} \\ \theta(0, y) = (\max\{\|g_s^*\|_{\infty, Q_1}, \|g_w^*\|_{\infty, Q_1}\} + \|g_s^*\|_{\infty, Q_1})e^{-py/\varepsilon} + \|g_w^*\|_{\infty, Q_1},$$

therefore, given the bound obtained on  $|E_2(x, y)|$  in (3.43), the desired result follows.  $\square$

**Lemma 3.14.** *For all  $x, y \in Q_1$  we have*

$$|z_{00,y}(x, y)| \leq \max\{\|g_s^*\|_{\infty, Q_1}, \|g_w^*\|_{\infty, Q_1}\}e^{-pr/\varepsilon}\varepsilon^{-1} + \|g_w^*\|_{\infty, Q_1}e^{-px/\varepsilon} \\ + \|g_s^*\|_{\infty, Q_1}e^{-py/\varepsilon}\varepsilon^{-1} \\ |z_{00,x}(x, y)| \leq \max\{\|g_s^*\|_{\infty, Q_1}, \|g_w^*\|_{\infty, Q_1}\}e^{-pr/\varepsilon}\varepsilon^{-1} + \|g_w^*\|_{\infty, Q_1}e^{-px/\varepsilon}\varepsilon^{-1} \\ + \|g_s^*\|_{\infty, Q_1}e^{-py/\varepsilon}$$

**Proof.** Let  $\theta(x, y) = \max\{\|g_s^*\|_{\infty, Q_1}, \|g_w^*\|_{\infty, Q_1}\}e^{-pr/\varepsilon}\varepsilon^{-1} + \|g_w^*\|_{\infty, Q_1}e^{-px/\varepsilon} + \|g_s^*\|_{\infty, Q_1}e^{-py/\varepsilon}\varepsilon^{-1}$ , then  $L\theta(x, y) \leq 0$  as before and  $|Lz_{00,y}(x, y)| \leq |L\theta(x, y)|$ .

Also,  $|z_{00,y}(x, 0)| = 0 \leq \theta(x, 0)$ . Now,

$$z_{00,y}(0, y) = g_w^*(y) - E_2'(0, y) \text{ and}$$

$$\theta(0, y) = (\max\{\|g_s^*\|_{\infty, Q_1}, \|g_w^*\|_{\infty, Q_1}\} + \|g_s^*\|_{\infty, Q_1})e^{-py/\varepsilon}\varepsilon^{-1} + \|g_w^*\|_{\infty, Q_1},$$

therefore, given the bound obtained on  $|E_2'(x, y)|$  in (3.43), the desired result follows. The bound on  $|z_{00,x}|$  is obtained in a similar fashion.  $\square$

**Theorem 3.15.** *For all  $x, y \in Q_1$  we have*

$$\begin{aligned} |D_y^n z_{00}(x, y)| &\leq \max\{\|g_s^*\|_{\infty, Q_1}, \|g_w^*\|_{\infty, Q_1}\}e^{-pr/\varepsilon}\varepsilon^{-n} + \|g_w^*\|_{\infty, Q_1}e^{-px/\varepsilon} \\ &\quad + \|g_s^*\|_{\infty, Q_1}e^{-py/\varepsilon}\varepsilon^{-n} \\ |D_x^m z_{00}(x, y)| &\leq \max\{\|g_s^*\|_{\infty, Q_1}, \|g_w^*\|_{\infty, Q_1}\}e^{-pr/\varepsilon}\varepsilon^{-m} + \|g_w^*\|_{\infty, Q_1}e^{-px/\varepsilon}\varepsilon^{-m} \\ &\quad + \|g_s^*\|_{\infty, Q_1}e^{-py/\varepsilon} \end{aligned}$$

where  $m, n$  are non-negative integers.

**Proof.** The proof is by induction. Note that the cases  $n = 0, 1$  were proven in the previous lemmas. Assume that the result is true for  $n = 0, 1, \dots, k$  where  $k$  is some positive integer. We then use the barrier function,  $\theta(x, y) = \max\{\|g_s^*\|_{\infty, Q_1}, \|g_w^*\|_{\infty, Q_1}\}e^{-pr/\varepsilon}\varepsilon^{-k-1} + \|g_w^*\|_{\infty, Q_1}e^{-px/\varepsilon} + \|g_s^*\|_{\infty, Q_1}e^{-py/\varepsilon}\varepsilon^{-k-1}$ , and Lemma (3.9) to prove the case for  $n = k+1$ , as in Lemma (3.14). Thus by the principle of induction the proof is complete. The proof for  $|D_x^m z_{00}(x, y)|$  is similar.  $\square$

### 3.3.4 Inflow corner component $z_{11}$

#### Growth conditions and Maximum Principle on $Q_2$

Consider the incoming quarter plane problem on  $Q_2 = \{(x, y) \in R^2 : x < 1, y < 1\}$

$$\begin{aligned} Lv \equiv \varepsilon \Delta v + p_1 \frac{\partial v}{\partial x} + p_2 \frac{\partial v}{\partial y} - qv &= f, \quad x < 1, y < 1, \\ v(x, 1) = h_n(x), \quad x < 1, \quad v(1, y) &= h_e(y), \quad y < 1, \end{aligned} \tag{3.52}$$

where  $p_1$ ,  $p_2$  and  $q$  are positive constants as before. We apply the same transformations as in 3.3.1 and using a change of variables we have the solution formula for the transformed problem on  $Q_2$

$$\begin{aligned} v_2(\xi, \eta) &= -\frac{1}{2\pi} \int_{-\infty}^0 \int_{-\infty}^0 f_2(\sigma, \tau) [K_0(\kappa\rho_1) - K_0(\kappa\rho_2) - K_0(\kappa\rho_3) + K_0(\kappa\rho_4)] d\tau d\sigma \\ &+ \frac{\eta\kappa}{\pi} \int_{-\infty}^0 h_{2,n}(\sigma) \left[ \frac{1}{\rho_5} K_1(\kappa\rho_5) - \frac{1}{\rho_6} K_1(\kappa\rho_6) \right] d\sigma \\ &+ \frac{\xi\kappa}{\pi} \int_{-\infty}^0 h_{2,e}(\tau) \left[ \frac{1}{\rho_7} K_1(\kappa\rho_7) - \frac{1}{\rho_8} K_1(\kappa\rho_8) \right] d\tau. \end{aligned} \tag{3.53}$$

As in Section 3.3.3, the solution to (3.52) exists and is given by (3.53) once  $f_2$ ,  $h_{2,n}$  and  $h_{2,e}$  are such that the integrals are convergent. Additionally, it can easily be shown that if  $f_2$  is negative and  $h_{2,n}$  and  $h_{e,2}$  are non-negative then  $v_2$  is non-negative. Using similar arguments to those in Section 3.3.3 we

obtain the following integrability conditions.

$$\begin{aligned}
\int_{|\sigma|>2|\xi|} \int_{|\tau|>2|\eta|} (\sigma^2 + \tau^2)^{-1/4} |f_2(\sigma, \tau)| e^{-\kappa/2(\sigma^2 + \tau^2)^{1/2}} d\tau d\sigma < \infty \\
\int_{|\sigma|>2|\xi|} |\sigma|^{-3/2} |h_{2,n}(\sigma)| e^{-\kappa|\sigma|/2} d\sigma < \infty, \\
\int_{|\tau|>2|\eta|} |\tau|^{-3/2} |h_{2,e}(\tau)| e^{-\kappa|\tau|/2} d\tau < \infty. \tag{3.54}
\end{aligned}$$

In terms of the original variables the conditions are

$$\begin{aligned}
\int_{|x|>2|s|} \int_{|y|>2|t|} r^{-1/2} |f(x, y)| e^{-(\kappa r + p_1|x| + p_2|y|)/2\varepsilon} dy dx < \infty, \\
\int_{|x|>2|s|} |x|^{-3/2} |h_n(x)| e^{-(\kappa + p_1)|x|/2\varepsilon} dx < \infty, \\
\int_{|y|>2|t|} |y|^{-3/2} |h_e(y)| e^{-(\kappa + p_2)|y|/2\varepsilon} dy < \infty. \tag{3.55}
\end{aligned}$$

Our maximum principle for  $Q_2$  then follows:

**Lemma 3.16.** *Let  $\Phi \in C^2(\bar{Q}_2)$  satisfy  $L\Phi \leq 0$  on  $Q_2$ ,  $\Phi(x, 1) \geq 0$  for  $x < 1$ ,  $\Phi(1, y) \geq 0$  for  $y < 1$  and*

$$\begin{aligned}
\left| \int_{x=-\infty}^1 \int_{y=-\infty}^1 (1+r)^{-1/2} L\Phi(x, y) e^{-pr/2\varepsilon} dy dx \right| < \infty, \\
\int_{-\infty}^1 (1+|x|)^{-3/2} \Phi(x, 1) e^{-p|x|/2\varepsilon} dx < \infty, \\
\int_{-\infty}^1 (1+|y|)^{-3/2} \Phi(1, y) e^{-p|y|/2\varepsilon} dy < \infty.
\end{aligned}$$

*Then  $\Phi \geq 0$  in  $Q_2$ . If  $U \in C^2(Q_2)$  satisfies  $|LU(x, y)| \leq |L\Phi(x, y)|$  in  $Q_2$  and  $|U(x, 1)| \leq \Phi(x, 1)$  for  $x < 1$ ,  $|U(1, y)| \leq \Phi(1, y)$  for  $y < 1$ , then  $|U(x, y)| \leq \Phi(x, y)$  in  $Q_2$ .  $\square$*

**Lemma 3.17.** *For all  $x, y \in Q_2$  we have*

$$|z_{11}(x, y)| \leq C$$

**Proof.** Let  $\xi(x, y) = C$ . Then  $L\xi = -qC \leq 0$ ,  $\xi(x, 1) = C \geq |z_{11}(x, 1)|$  and  $\xi(1, y) = C \geq |z_{11}(1, y)|$ , since these boundary conditions are defined in terms of  $z_{00}^*$ ,  $E_1^*$ ,  $E_2^*$  and  $S_2^*$  which are smooth extensions of  $z_{00}$ ,  $E_1$ ,  $E_2$  and  $S_2$  respectively and can be shown to be of  $O(\varepsilon)$  ( $z_{00}$ ,  $E_1$  and  $E_2$ ) and  $O(1)$  ( $S_2$ ) along the boundary of  $Q_2$ . By Lemma 3.16 the result follows.  $\square$

**Lemma 3.18.** *For all  $x, y \in Q_2$  we have*

$$|z_{11,y}(x, y)| \leq C\varepsilon^{-1}$$

$$|z_{11,x}(x, y)| \leq C\varepsilon^{-1}$$

**Proof.** Let  $\theta(x, y) = C\varepsilon^{-1}$ , then  $L\theta(x, y) \leq 0$  and  $|Lz_{11,y}(x, y)| \leq |L\theta(x, y)|$ .

Also,  $|z_{11,y}(x, 1)| = 0 \leq \theta(x, 1)$ . Now for  $y \leq 1$ ,

$$z_{11,y}(1, y) = -E_1^{*'}(1, y) - E_2^{*'}(1, y) - z_{00}^{*'}(1, y) + (\chi(y) - 1)'S_2^*(1, y) + (\chi(y) - 1)S_2^{*'}(1, y),$$

$$\theta(1, y) = C\varepsilon^{-1}.$$

Therefore, given the bounds already obtained on  $|E_1'(x, y)|$ ,  $|E_2'(x, y)|$ ,  $|z_0'(x, y)|$  and  $|S_2'|$ , the desired result follows. The bound on  $|z_{11,x}|$  is obtained in a similar fashion.  $\square$

**Theorem 3.19.** *For all  $x, y \in Q_2$ , with  $n, m$  being non-negative integers we*

have

$$|D_y^n z_{11}(x, y)| \leq C\varepsilon^{-n}$$

$$|D_x^m z_{11}(x, y)| \leq C\varepsilon^{-m}$$

**Proof.** The proof is by induction. Note that the cases  $n = 0, 1$  were proven in the previous lemmas. Assume that the result is true for  $n = 0, 1, \dots, k$  where  $k$  is some positive integer. We then use the barrier function,  $\theta(x, y) = C\varepsilon^{-k}$ , and Lemma (3.16) to prove the case for  $n = k + 1$ , as in Lemma (3.18). Thus by the principle of induction the proof is complete. The proof for  $|D_x^m z_{11}(x, y)|$  is similar.  $\square$

### 3.3.5 Corner components $z_{10}$ and $z_{01}$

#### Maximum Principle on $Q_3$

The open domain  $Q_3$  is defined as  $Q_3 = \{(x, y) \in R^2 : x > 0, y < 1\}$ . Using the approach of 3.3.3 and 3.3.4 we obtain the following maximum principle.

**Lemma 3.20.** *Let  $\Phi \in C^2(\bar{Q}_3)$  satisfy  $L\Phi \leq 0$  on  $Q_3$ ,  $\Phi(x, 1) \geq 0$  for  $x > 0$ ,  $\Phi(0, y) \geq 0$  for  $y < 1$  and*

$$\begin{aligned} \left| \int_{x=0}^{\infty} \int_{y=-\infty}^1 (1+r)^{-1/2} L\Phi(x, y) e^{-(pr/2\varepsilon)} dy dx \right| &< \infty, \\ \int_0^{\infty} (1+x)^{-3/2} \Phi(x, 1) e^{-\kappa x/2\varepsilon} dx &< \infty, \\ \int_{-\infty}^1 (1+|y|)^{-3/2} \Phi(0, y) e^{-\kappa|y|/2\varepsilon} dy &< \infty. \end{aligned}$$

*Then  $\Phi \geq 0$  in  $Q_3$ . If  $U \in C^2(Q_3)$  satisfies  $|LU(x, y)| \leq |L\Phi(x, y)|$  in  $D_3$  and  $|U(x, 1)| \leq \Phi(x, 1)$  for  $x > 0$ ,  $|U(0, y)| \leq \Phi(0, y)$  for  $y < 1$ , then  $|U(x, y)| \leq$*

$\Phi(x, y)$  in  $Q_3$ .  $\square$

### Maximum Principle on $Q_4$

The open domain  $Q_4$  is defined as  $Q_4 = \{(x, y) \in R^2 : x < 1, y > 0\}$  and the corresponding maximum principle is as follows.

**Lemma 3.21.** *Let  $\Phi \in C^2(\bar{Q}_4)$  satisfy  $L\Phi \leq 0$  on  $Q_4$ ,  $\Phi(x, 0) \geq 0$  for  $x < 1$ ,  $\Phi(1, y) \geq 0$  for  $y > 0$  and*

$$\begin{aligned} \left| \int_{x=-\infty}^1 \int_{y=0}^{\infty} (1+r)^{-1/2} L\Phi(x, y) e^{-(\kappa r/2\varepsilon)} dy dx \right| &< \infty, \\ \int_{-\infty}^1 (1+|x|)^{-3/2} \Phi(x, 0) e^{-\kappa|x|/2\varepsilon} dx &< \infty, \\ \int_0^{\infty} (1+y)^{-3/2} \Phi(1, y) e^{-\kappa y/2\varepsilon} dy &< \infty. \end{aligned}$$

Then  $\Phi \geq 0$  in  $Q_4$ . If  $U \in C^2(Q_4)$  satisfies  $|LU(x, y)| \leq |L\Phi(x, y)|$  in  $Q_4$  and  $|U(x, 0)| \leq \Phi(x, 0)$  for  $x < 1$ ,  $|U(1, y)| \leq \Phi(1, y)$  for  $y > 0$ , then  $|U(x, y)| \leq \Phi(x, y)$  in  $Q_4$ .  $\square$

**Lemma 3.22.** *There is a constant  $C$  such that for all  $x, y \in Q_4 = \{(x, y) \in R^2 : x < 1, y > 0\}$*

$$|z_{10}(x, y)| \leq C$$

and for all  $x, y \in Q_3 = \{(x, y) \in R^2 : x > 0, y < 1\}$

$$|z_{01}(x, y)| \leq C$$

**Proof.** Let  $\eta(x, y) = C\varepsilon$ . Then  $L\eta = -qC \leq 0$ , and  $\eta(x, 0) = C \geq |z_{10}(x, 0)|$  by the definition of  $\chi$  and since  $z_{11}$  is itself bounded by  $C$ . Finally  $\eta(1, y) \geq |z_{10}(1, y)| = 0$ , from which the required bound follows using Lemma 3.21. The

proof for the bound on  $z_{01}$  is similar, using Lemma 3.20.  $\square$

**Theorem 3.23.** *Analogous to Theorem 3.19 for all  $x, y \in Q_3$  and  $Q_4$  respectively, with  $n, m$  being non-negative integers we have*

$$|D_y^n z_{10}(x, y)| \leq C\varepsilon^{-n}$$

$$|D_x^m z_{10}(x, y)| \leq C\varepsilon^{-m}$$

$$|D_y^n z_{01}(x, y)| \leq C\varepsilon^{-n}$$

$$|D_x^m z_{01}(x, y)| \leq C\varepsilon^{-m}$$

$\square$

### 3.3.6 Remainder term $\tilde{u}_\varepsilon$

#### Maximum principle on the unit square, $\Omega$

The corresponding maximum principle on  $\Omega$ , the unit square, is set out below.

**Lemma 3.24.** *Let  $\Phi \in C^2(\bar{\Omega})$  satisfy  $L\Phi \leq 0$  on  $\Omega$ ,  $\Phi(x, 0) \geq 0$  and  $\Phi(x, 1) \geq 0$  for  $0 < x < 1$ , and  $\Phi(0, y) \geq 0$  and  $\Phi(1, y) \geq 0$  for  $0 < y < 1$ . Then  $\Phi \geq 0$  in  $\Omega$ . If  $U \in C^2(\Omega)$  satisfies  $|LU(x, y)| \leq |L\Phi(x, y)|$  in  $\Omega$ ,  $|U(x, 0)| \leq \Phi(x, 0)$  and  $|U(x, 1)| \leq \Phi(x, 1)$  for  $0 < x < 1$ , and  $|U(0, y)| \leq \Phi(0, y)$  and  $|U(1, y)| \leq \Phi(1, y)$  for  $0 < y < 1$ , then  $|U(x, y)| \leq \Phi(x, y)$  in  $\Omega$ .  $\square$*

**Theorem 3.25.** *There is a constant  $C$  such that for all  $x, y \in \Omega$ , using the maximum principle stated above and analysis as per Section 3.3.4, we have*

$$|D_y^n \tilde{u}_\varepsilon(x, y)| \leq C\varepsilon^{-n}$$

$$|D_x^m \tilde{u}_\varepsilon(x, y)| \leq C\varepsilon^{-m}$$

with  $n, m$  being non-negative integers.  $\square$

### 3.3.7 Solution of the original problem $u_\varepsilon$

**Theorem 3.26.** *There is a constant  $C$  such that for all  $x, y \in \Omega$*

$$\begin{aligned} |u_\varepsilon(x, y)| &\leq C \\ |D_y^n u_\varepsilon(x, y)| &\leq C(1 + \varepsilon^{-n}) \\ |D_x^m u_\varepsilon(x, y)| &\leq C(1 + \varepsilon^{-m}) \end{aligned}$$

with  $n, m$  being non-negative integers.

**Proof.** Combining the bounds achieved on each of the components on the half and quarter planes, as well as the bound on the remainder term in  $\Omega$ , we obtain the above bound on  $u_\varepsilon$ , the solution to the original problem (3.1), and its derivatives on  $\Omega$ .  $\square$

## 3.4 Summary

The result obtained in Theorem 3.15 and Theorem 3.26 indicate that the effect of the discontinuity in the boundary conditions at the southwest corner of the domain  $\Omega$  is greatest close to  $(0, 0)$ . The smaller  $\varepsilon$ , the more the effect of the discontinuity is localised: the case in which the effect of the discontinuity is most evident is when we have large  $\varepsilon$  and small  $r$  and its influence decays exponentially. This effect carries through to the other corner components of the solution, including the remainder term. While the overall bounds in Theorem 3.26 are somewhat disappointing the insight into this behaviour motivates the domain decomposition numerical method described the next

chapter, in which we seek to develop a parameter-uniform numerical method to solve this type of problem. While error bounds are not obtained, numerical results are presented supporting this approach.

## Chapter 4

# On A Schwarz method for a singularly perturbed convection-diffusion problem with discontinuous boundary conditions

### 4.1 Introduction

We are concerned with a two dimensional steady state convection-diffusion problem with discontinuous outflow boundary conditions, similar to that under consideration in the previous chapter. It is well known that, where the boundary conditions are sufficiently smooth and compatible, such a problem can be solved with uniform accuracy with respect to the small parameter  $\varepsilon$  using a standard finite difference operator on special piecewise uniform meshes [72], [21] and [91]. Where the outflow boundary data are only weakly regular

and compatible, parameter-uniform solutions may also be obtained by this method [21]. However, for large values of  $\varepsilon$  (and by extension for small  $\varepsilon$  with a sufficiently large number of mesh intervals), orders of convergence are small and pointwise errors are large.

Numerical methods for singularly perturbed problems comprising domain decomposition and Schwarz iterative techniques have been examined by a number of authors, for example, in [72], [91], [73], [66] and [67]. In [72], Miller et al. examine a continuous overlapping Schwarz method for a singularly perturbed convection-diffusion equation with arbitrary fixed interface positions and find it to be uniformly convergent with respect to the perturbation parameter. In [67] MacMullen et al. consider the corresponding discrete overlapping Schwarz method for the same problem and find that, in the discrete case the numerical solution obtained converges to the solution of upwinding on a quasi-uniform mesh. Furthermore, they show that if the interface positions for the overlapping discretised domains are based on layer-resolving piecewise uniform fitted meshes then the numerical solutions obtained fail to converge to the analytical solution. As an alternative they construct a discrete non-overlapping Schwarz method on uniform meshes with artificial Dirichlet interface conditions for singularly perturbed linear convection-diffusion problems in two dimensions with sufficiently smooth and compatible boundary data and show it to be first order convergent for  $\varepsilon \leq N^{-1}$ .

In the previous chapter we analysed the solution of a problem similar to that described below and obtained bounds on its components which revealed a localisation of the effect of the singularity which arises from the discontinuity at the outflow corner. This behaviour suggests a domain decomposition approach to the numerical solution of the problem under consideration. While we do not give error bounds for the methods shown in this chapter we ex-

amine experimentally the performance of a number of domain decomposition methods which, unlike those outlined in the previous paragraph, are extended to the class of singularly perturbed convection-diffusion problems with more general boundary conditions and set out numerical results for those methods.

We consider the following model problem in a domain  $\Omega$ , the unit square.

$$\begin{aligned}
 Lu &\equiv \varepsilon \Delta u_\varepsilon + \frac{\partial u_\varepsilon}{\partial x} + \frac{\partial u_\varepsilon}{\partial y} = 0 \text{ in } \Omega, & (4.1) \\
 u_\varepsilon(x, 0) &= 5 - 4x^{1/6} = g_B(x), \quad u_\varepsilon(x, 1) = 1, \quad x \in (0, 1) \\
 u_\varepsilon(0, y) &= y^{1/2} = g_L(y), \quad u_\varepsilon(1, y) = 1, \quad y \in (0, 1)
 \end{aligned}$$

where  $0 < \varepsilon \leq 1$ . While it is of a similar nature to the problem examined in the previous chapter, in this chapter we do not enforce the requirement that the coefficient of  $u$  be less than zero. The problem exhibits regular layers along the outflow boundaries, a corner boundary layer at the outflow boundary corner as well as a discontinuity similar to that treated in Chapter 3, see Figure 4.1. We implement domain decomposition methods to isolate the neighbourhood of the singularity, along with a discrete Schwarz iterative technique with the aim of producing parameter-uniformly accurate solutions for all values of  $\varepsilon$  on the whole domain in the presence of such a singularity.

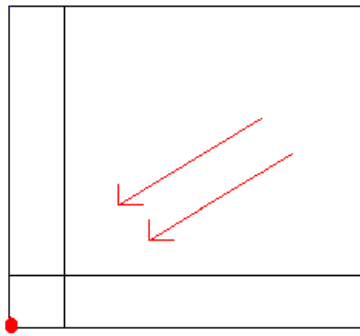


Figure 4.1: Picture of our domain,  $\Omega$ , with the location of the boundary layers and the discontinuity at the outflow corner

## 4.2 Direct Method: non-iterative discrete method on piecewise uniform fitted meshes

A tensor product of two piecewise-uniform fitted meshes  $\Omega^N$  is used on  $\Omega$ , where the transition parameter  $\sigma$  is chosen as

$$\sigma = \min\{1/2, \varepsilon \ln N\} \quad (4.2)$$

along with the upwind finite difference operator

$$L_\varepsilon^N Z_i^j = [\varepsilon(\delta_x^2 + \delta_y^2) + D_x^+ + D_y^+] Z_i^j. \quad (4.3)$$

and two mesh widths  $2\sigma/N$  and  $2(1 - \sigma)/N$ .

The differences between the numerical solutions for various values of  $N$  and the numerical solution for  $N = 256$ , which are indicative of nodal errors are shown in Table 4.1, where

$$E_\varepsilon^N = \max_{x_i, y_j \in \Omega_\varepsilon^N} |U_\varepsilon^N - \bar{U}_\varepsilon^{256}|, \quad E^N = \max_\varepsilon E_\varepsilon^N.$$

The computed orders of convergence for various values of  $N$  and  $\varepsilon$ , defined by

$$D_\varepsilon^N = \max_{x_i, y_j \in \Omega_\varepsilon^N} |U_\varepsilon^N - \bar{U}_\varepsilon^{2N}|,$$

$$p_\varepsilon^N = \log_2 D_\varepsilon^N / D_\varepsilon^{2N}.$$

are shown in Table 4.2. It is clear from Tables 4.1 and 4.2 that the method fails for problem (4.1) for large values of  $\varepsilon$ . While at first glance these results appear to be satisfactory for small  $\varepsilon$ , since outside the corner region when a

standard Shishkin mesh is applied the error is not significant and the error does not propagate outside the corner region, see Fig. 4.2. However, as  $N$  increases the results worsen for smaller values of  $\varepsilon$ , see Table 4.1. It can therefore be inferred that the bad behaviour for large  $\varepsilon$  will be replicated for small  $\varepsilon$  where  $N$  is large enough and we conclude that the direct method fails when applied to problem (4.1).

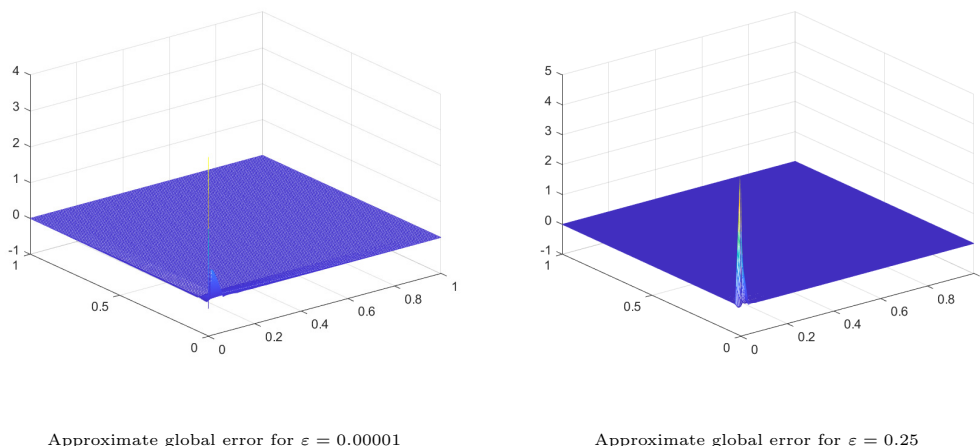


Figure 4.2: Approximate global error for problem (2.38) with  $\varepsilon = 0.0001$  and  $N = 64$ .

Table 4.1: Maximum pointwise errors  $E_\varepsilon^N$  and  $E^N$  for the Direct Method applied to problem (4.1).

$\varepsilon$	Number of intervals $N$			
	16	32	64	128
1	0.0218	0.0243	0.0244	0.0191
$2^{-1}$	0.0184	0.0227	0.0237	0.0188
$2^{-2}$	0.0122	0.0190	0.0223	0.0183
$2^{-3}$	0.0242	0.0150	0.0186	0.0172
$2^{-4}$	0.0390	0.0223	0.0176	0.0140
$2^{-6}$	0.0835	0.0471	0.0227	0.0145
$2^{-8}$	0.1202	0.0739	0.0376	0.0149
$2^{-10}$	0.1412	0.0907	0.0489	0.0192
$2^{-12}$	0.1535	0.0992	0.0543	0.0220
$2^{-14}$	0.1620	0.1045	0.0569	0.0230
$2^{-16}$	0.1687	0.1084	0.0587	0.0234
$2^{-18}$	0.1740	0.1116	0.0601	0.0238
$2^{-20}$	0.1782	0.1141	0.0612	0.0240
$2^{-22}$	0.1816	0.1161	0.0621	0.0243
$2^{-24}$	0.1843	0.1177	0.0628	0.0245
$2^{-26}$	0.1865	0.1189	0.0634	0.0246
$2^{-28}$	0.1882	0.1199	0.0638	0.0248
$E^N$	0.1882	0.1199	0.0638	0.0248

Table 4.2: Computed orders of convergence  $p^N$  for the Direct Method applied to problem (4.1).

$\varepsilon$	Number of intervals $N$		
	16	32	64
1	-0.18	-0.11	-0.08
$2^{-1}$	-0.30	-0.16	-0.10
$2^{-2}$	-0.70	-0.30	-0.15
$2^{-3}$	0.50	-0.17	-0.30
$2^{-4}$	0.40	0.00	0.00
$2^{-6}$	0.63	0.74	0.00
$2^{-8}$	0.43	0.66	0.69
$2^{-10}$	0.36	0.55	0.68
$2^{-12}$	0.35	0.53	0.62
$2^{-14}$	0.35	0.53	0.62
$2^{-16}$	0.34	0.54	0.63
$2^{-18}$	0.34	0.55	0.64
$2^{-20}$	0.34	0.56	0.65
$2^{-22}$	0.34	0.56	0.65
$2^{-24}$	0.34	0.57	0.66
$2^{-26}$	0.34	0.57	0.66
$2^{-28}$	0.34	0.57	0.66

### 4.3 Schwarz Method 1: domain decomposition with restricted overlap region

In all of Schwarz methods in this chapter we use the BiCGStab solver. Given the location of the incompatibility it is natural to consider partitioning the solution domain  $\Omega$  into the following two overlapping subregions

$$\Omega_S = (0, 1)^2 \setminus (0, \frac{\sigma}{a}) \times (0, \frac{\sigma}{b}), \quad a, b > 1$$

$$\Omega_P = \{(x, y) \in (0, R)^2 : x^2 + y^2 < R^2\}, \quad R = C_R \sigma, \quad C_R < 1$$

where  $C_R$  is a constant, as pictured in Figure 4.3. On  $\Omega_P$  we use the following translation

$$v = e^{(x+y)/2\varepsilon} u_\varepsilon,$$

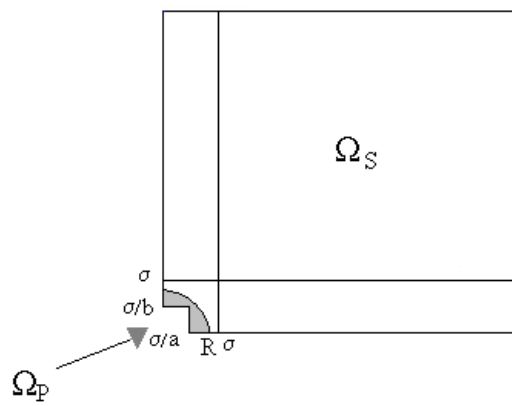


Figure 4.3: Domain decomposition with restricted overlap region,  $\Omega_S$  is pictured with the overlapping subdomain,  $\Omega_P$ , depicted in grey

yielding the translated equation

$$2\varepsilon^2 \Delta v - v = 0.$$

In polar coordinates, required due to the shape of the subdomain and the nature of the discontinuity in the boundary conditions (see Figure 4.4), the equation becomes

$$2\varepsilon^2 \left( v_{rr} + \frac{1}{r} v_r + \frac{1}{r^2} v_{\theta\theta} \right) - v = 0.$$

We use a tensor product of uniform meshes with  $N$  intervals on this domain in all remaining sections of this chapter.

For each  $k \geq 1$ ,

$$\begin{aligned} U_\varepsilon^{[k]}(x_i, y_j) &= U_S^{[k]}(x_i, y_j), \quad (x_i, y_j) \in \Omega_S^N \\ U_\varepsilon^{[k]}(x_i, y_j) &= \bar{U}_P^{[k]}(x_i, y_j), \quad (x_i, y_j) \in \Omega_P \cap \Omega_S^N \end{aligned}$$

where

$$\begin{aligned} i &= 0, 1, \dots, N, \quad j = 0, 1, \dots, N, \\ x_{N/2} &= y_{N/2} = \sigma, \\ \Omega_S^N &= \Omega^N \setminus \{(x_i, y_j) \mid x_i < \sigma/a, y_j < \sigma/b\}, \end{aligned}$$

We use the same grid as in the Direct Method in Section 4.3 here also and in all further sections of this chapter.  $\bar{U}_i^{[k]}$  is the bilinear interpolant of  $U_i^{[k]}$ .

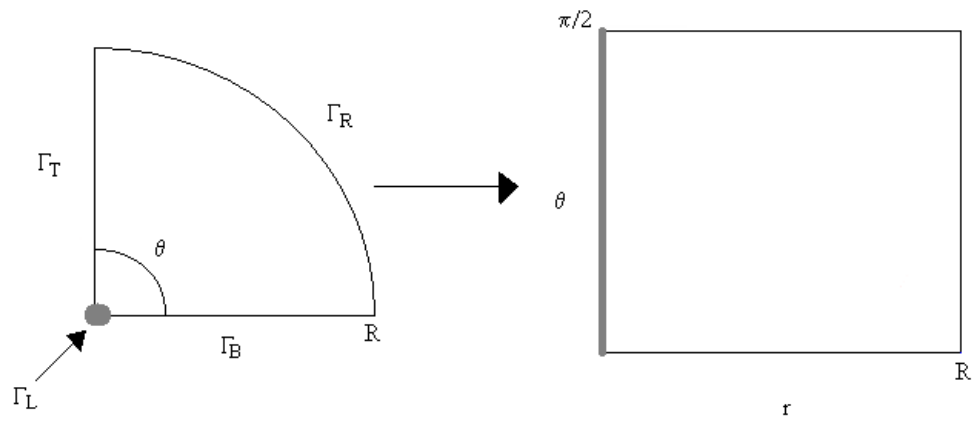


Figure 4.4: The advantage of the shape of subregion  $\Omega_P$  is that translating to polar coordinates here enables us to smooth out the discontinuity when solving on this subdomain. The point of discontinuity becomes our left hand boundary in polar coordinates and we use linear interpolation to give us smooth boundary conditions in polar coordinates.

Then for  $k = 1$ ,

$$\begin{aligned}
L_\varepsilon^N U_S^{[1]} &= 0, \quad (x_i, y_j) \in \Omega_S^N, \\
U_S^{[1]}(x_i, y_j) &= u_\varepsilon(x_i, y_j), \quad \forall \{(x_i, 0) | \sigma/a \leq x_i \leq 1\}, \\
&\quad \{(x_i, 1) | 0 \leq x_i \leq 1\}, \{(0, y_j) | \sigma/b \leq y_j \leq 1\}, \{(1, y_j) | 0 \leq y_j \leq 1\} \\
U_S^{[1]}(x_i, \sigma/b) &= G(x_i), \quad 0 \leq x_i \leq \sigma/a, \\
U_S^{[1]}(\sigma/a, y_j) &= H(y_j), \quad 0 \leq y_j \leq \sigma/b,
\end{aligned}$$

where  $G$  and  $H$  are arbitrary functions such that

$$\begin{aligned}
G(0) &= u_\varepsilon(0, \sigma/b), \quad H(0) = u_\varepsilon(\sigma/a, 0), \\
G(\sigma/a, \sigma/b) &= H(\sigma/a, \sigma/b).
\end{aligned}$$

And

$$L_P^N U_P^{[1]} = 0, \quad (r_i, \theta_j) \in \Omega_P^N, \quad U_P^{[1]}(R, \theta_j) = \bar{U}_S^{[1]}(R, \theta_j),$$

where  $U_P^{[1]}(0, \theta_j)$  is a linear interpolant of  $g_B(0)$  and  $g_L(0)$ .

For  $k > 1$ ,

$$\begin{aligned}
L_\varepsilon^N U_S^{[k]} &= 0, \quad (x_i, y_j) \in \Omega_S^N, \\
U_S^{[k]}(x_i, y_j) &= \bar{U}_P^{[k-1]}(x_i, y_j), \\
&\quad (x_i, y_j) \in \Omega_S \cap \Omega_P
\end{aligned}$$

and

$$L_P^N U_P^{[k]} = 0, \quad (r_i, \theta_j) \in \Omega_P^N, \quad U_P^{[k]}(R, \theta_j) = \bar{U}_S^{[k-1]}(R, \theta_j).$$

We define the finite difference operators as

$$\begin{aligned} L_\varepsilon^N Z_i^j &= [\varepsilon(\delta_x^2 + \delta_y^2) + D_x^+ + D_y^+] Z_i^j \\ L_P^N Z_i^j &= 2\varepsilon^2 \left[ \delta_r^2 + \frac{1}{r_i} D_r^0 + \frac{1}{r_i^2} \delta_\theta^2 \right] Z_i^j - Z_i^j \end{aligned} \quad (4.4)$$

where

$$\delta_x^2 Z(x_i, y_i) = \frac{2}{x_{i+1} - x_{i-1}} (D_x^+ - D_x^-) Z(x_i, y_j)$$

with

$$\begin{aligned} D_x^+ Z(x_i, y_j) &= \frac{Z(x_{i+1}, y_j) - Z(x_i, y_j)}{x_{i+1} - x_i}, \\ D_x^- Z(x_i, y_j) &= \frac{Z(x_i, y_j) - Z(x_{i-1}, y_j)}{x_i - x_{i-1}}, \\ D_x^0 Z(x_i, y_j) &= \frac{Z(x_{i+1}, y_j) - Z(x_{i-1}, y_j)}{x_{i+1} - x_{i-1}}. \end{aligned}$$

The iterative process starts with solving on  $\Omega_S$  with arbitrary boundary values along the boundary of the notch. We then solve on  $\Omega_P$ , taking the boundary values of the curved boundary of this domain from the interpolated solution previously obtained on  $\Omega_S$ . In the second iteration the boundary values along the boundary of the notch come from the interpolated solution obtained on  $\Omega_P$  in the first iteration. We solve on  $\Omega_P$  as per the first iteration. We continue to iterate until the difference between the solutions on  $\Omega_S$  for successive iterations is less than  $10^{-4}$ . The final solution then comprises the solution on  $\Omega_S$  with the solution on  $\Omega_P$  interpolated over the notch region.

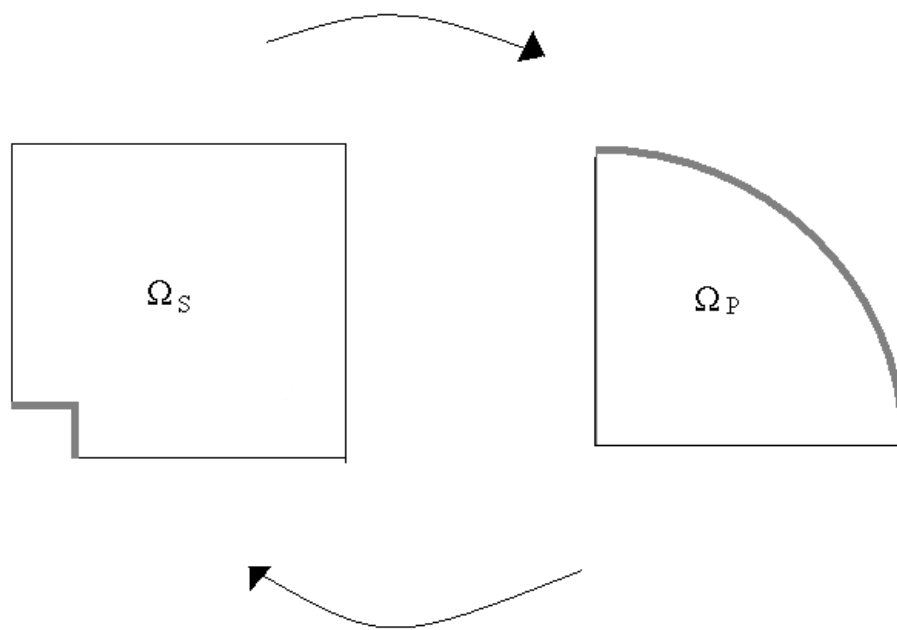


Figure 4.5: The iterative process

It is important to note that, in order for the discrete overlapping Schwarz method to converge to the correct solution, the overlap region between subdomains must be sufficiently large. This can be seen in Table 4.3, which shows the number of iterations for Schwarz Method 1 to converge for a range of values of  $R$  for a tolerance level of

$$\max_{x_i, y_j \in \Omega_\varepsilon^N} |U_S^{[k]}(x_i, y_j) - U_S^{[k-1]}(x_i, y_j)| \leq 10^{-4}.$$

From the definition of  $\Omega_S$  and  $\Omega_P$  it follows that the width of the overlap region at its minimum point is

$$\left( C_R - \sqrt{\frac{1}{a^2} + \frac{1}{b^2}} \right) \sigma,$$

thus placing the restriction on our choice of  $C_R$  that

$$C_R > \sqrt{\frac{1}{a^2} + \frac{1}{b^2}}.$$

However, in addition to considering the necessary overlap width required by Schwarz Method 1 for convergence, we must also bear in mind the choice of  $R$ , the radius of the quarter-disk subregion. In the presence of the incompatibility we require  $R$  to be small in order to cluster more grid points in the neighbourhood of the singularity, since it was shown the previous chapter that the influence of the discontinuity is greatest in the region where  $r \leq \varepsilon$ . We can see from Table 4.4 below that the computed orders of convergence are not satisfactory for larger  $N$  as the radius chosen,  $0.4\sigma$ , was too large. Since the width of the overlap is proportional to  $\sigma$ , for large values of  $\varepsilon$  the above restriction imposed by this decomposition prevents us from choosing  $R$  sufficiently small to resolve the singularity. This can clearly be seen the graphs

included here in Figures 4.6 and 4.7 showing the pointwise errors for various values of  $\varepsilon$  and  $R$ .

Table 4.3: Iteration counts for Schwarz Method 1 (restricted overlap) applied to problem (4.1) for tolerance  $10^{-4}$ , variable  $R$

$\varepsilon$	$C_R$								
	0.36	0.37	0.38	0.39	0.40	0.80	1.20	1.60	2.00
1	24	15	12	10	9	4	4	3	3
$2^{-1}$	25	15	12	11	10	4	4	3	3
$2^{-2}$	26	16	13	11	10	4	4	3	3
$2^{-3}$	27	16	13	11	10	4	4	3	3
$2^{-4}$	28	17	13	11	10	4	4	3	3
$2^{-6}$	30	18	14	12	10	4	4	3	3
$2^{-8}$	31	18	14	12	11	4	4	3	3
$2^{-10}$	31	18	14	12	11	4	3	3	3
$2^{-12}$	32	19	14	12	11	4	3	3	3
$2^{-14}$	32	19	15	12	11	4	3	3	3
$2^{-16}$	32	19	15	12	11	4	3	3	3
$2^{-18}$	32	19	15	13	11	4	3	3	3
$2^{-20}$	33	19	15	13	11	4	3	3	3
$2^{-22}$	33	19	15	13	11	4	3	3	3
$2^{-24}$	33	19	15	13	11	4	3	3	3
$2^{-26}$	33	19	15	13	11	4	3	3	3
$2^{-28}$	33	19	15	13	11	4	3	3	3

Table 4.4: Computed orders of convergence for Schwarz Method 1 (restricted overlap) applied to problem (4.1) with  $R = 0.4\sigma$ .

$\varepsilon$	Number of intervals $N$		
	16	32	64
1	1.50	0.14	0.15
$2^{-1}$	1.33	0.15	0.14
$2^{-2}$	0.76	0.88	0.35
$2^{-3}$	0.50	1.27	0.92
$2^{-4}$	0.30	0.28	0.28
$2^{-6}$	0.63	0.74	0.82
$2^{-8}$	0.44	0.66	0.81
$2^{-10}$	0.36	0.55	0.68
$2^{-12}$	0.35	0.53	0.62
$2^{-14}$	0.35	0.53	0.62
$2^{-16}$	0.34	0.54	0.63
$2^{-18}$	0.34	0.55	0.64
$2^{-20}$	0.34	0.56	0.65
$2^{-22}$	0.34	0.56	0.65
$2^{-24}$	0.34	0.57	0.66
$2^{-26}$	0.34	0.57	0.66
$2^{-28}$	0.34	0.57	0.66

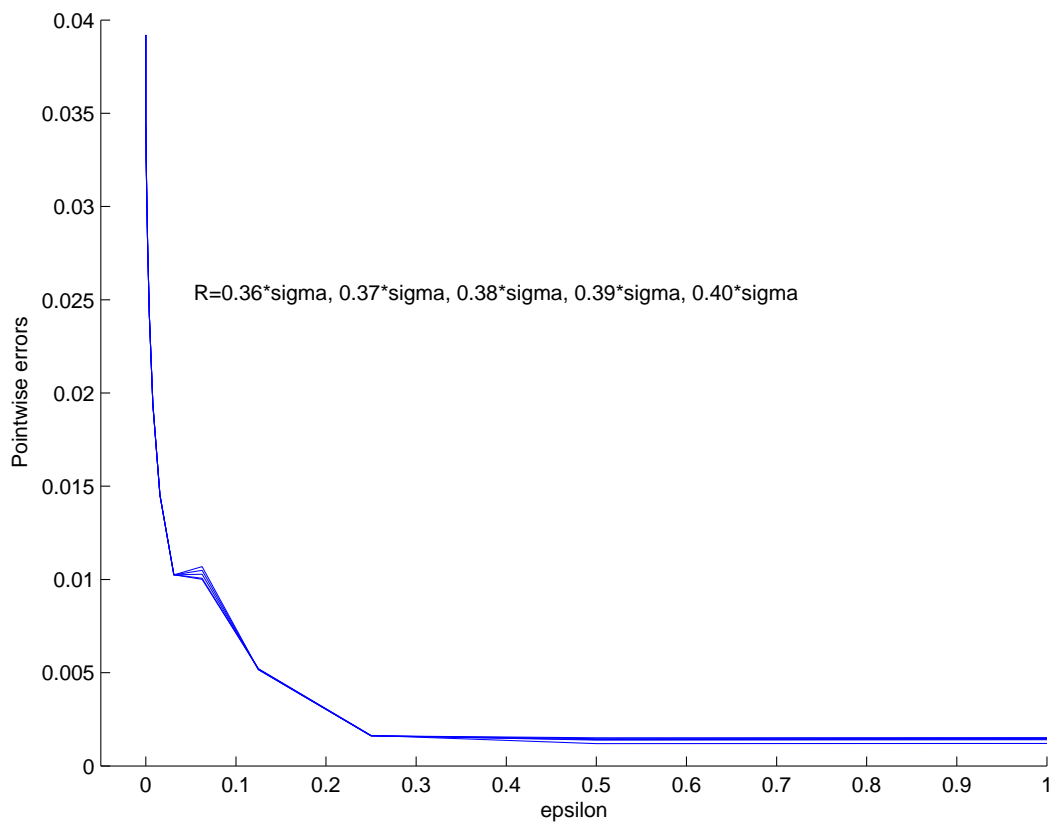


Figure 4.6:  $N = 64$ . When  $R$  is small we get satisfactory results for the pointwise errors using Schwarz Method 1. However, the method requires many iterations to converge when  $R$  is small.

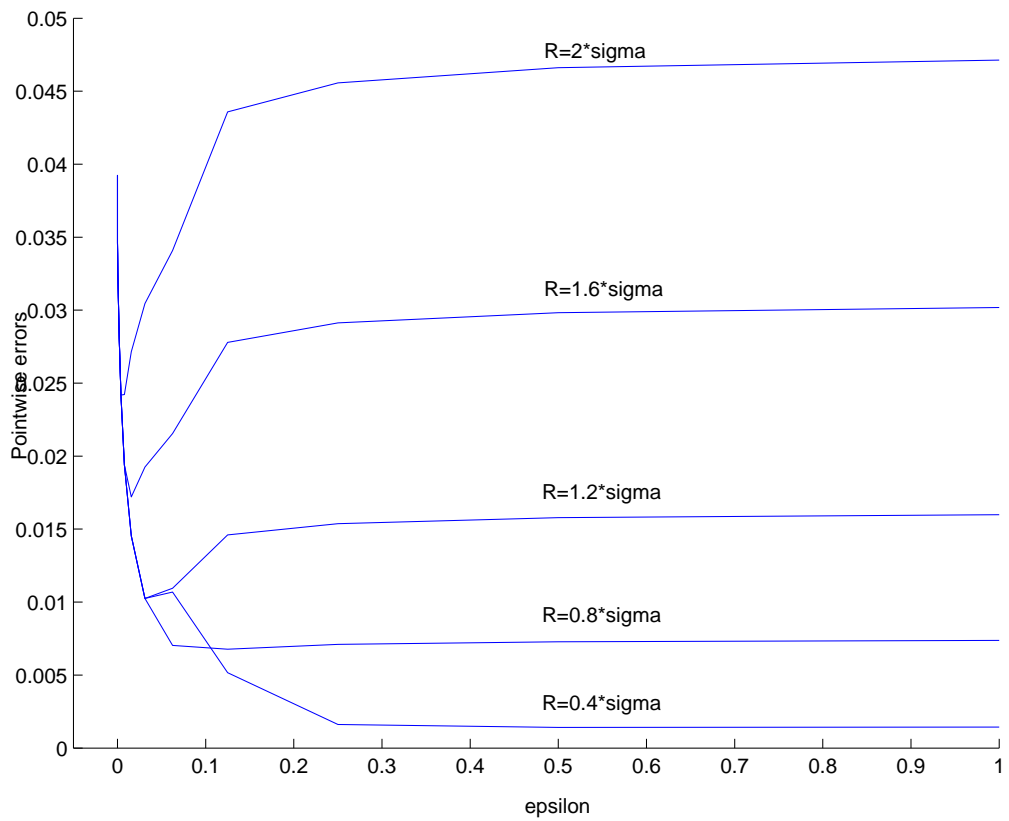


Figure 4.7:  $N = 64$ . With large  $R$  we see the pointwise errors for Schwarz Method 1 blow up.

## 4.4 Schwarz Method 2: domain decomposition with maximal overlap region

In order to choose  $R$  large enough to resolve the singularity we let

$$\Omega_S = \Omega$$

thereby removing the restriction on the choice of  $R$ , which we define as

$$R = \sqrt{2}\sigma/8,$$

thus ensuring that the overlap region is sufficiently large for the convergence of the Schwarz method, pictured in Figure 4.8.

A tensor product of two piecewise-uniform fitted meshes  $\Omega_S^N$  is used on  $\Omega$ , with  $\sigma$  defined as in (4.2). Uniform meshes  $\Omega_P^N$  are used on  $\Omega_P$ .

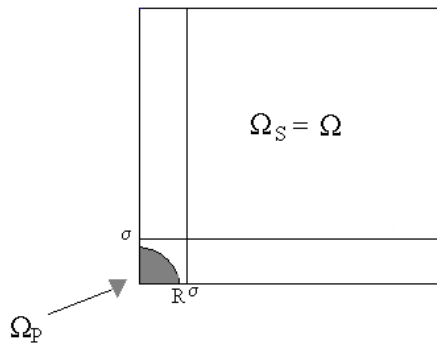


Figure 4.8: Domain decomposition with maximal overlap.

We use the identical translation in the polar region as in Schwarz Method

1. Our discrete iterative method is then as follows:

For each  $k \geq 1$ ,

$$U_\varepsilon^{[k]}(x, y) = \begin{cases} U_S^{[k]}(x, y), & (x, y) \in \Omega_S^N \\ \bar{U}_P^{[k]}(x, y), & (x, y) \in \Omega_P \cap \Omega_S^N \end{cases}$$

where  $\bar{U}_i^{[k]}$  is the bilinear interpolant of  $U_i^{[k]}$ . Then for  $k = 1$ ,

$$\begin{aligned} L_\varepsilon^N U_S^{[1]} &= 0, \quad (x_i, y_j) \in \Omega_S^N, \\ U_S^{[1]}(x_i, 0) &= 5 - 4x_i^{1/6}, \quad U_S^{[1]}(x_i, 1) = 1, \quad x_i \in (0, 1) \\ U_S^{[1]}(0, y_j) &= y_j^{1/2}, \quad U_S^{[1]}(1, y_j) = 1, \quad y_j \in (0, 1) \end{aligned}$$

and

$$L_P^N U_P^{[1]} = 0, \quad (r_i, \theta_j) \in \Omega_P^N, \quad U_P^{[1]}(R, \theta_j) = \bar{U}_S^{[1]}(R, \theta_j),$$

where  $U_P^{[1]}(0, \theta_j)$  is a linear interpolant of  $g_B(0)$  and  $g_L(0)$ .

For  $k > 1$ ,

$$\begin{aligned} L_\varepsilon^N U_S^{[k]} &= 0, \quad (x_i, y_j) \in \Omega_S^N, \\ U_S^{[k]}(x_i, y_j) &= \bar{U}_P^{[k-1]}(x_i, y_j), \quad x_i \in (0, R), \quad y_j \in (0, R), \end{aligned}$$

and

$$L_P^N U_P^{[k]} = 0, \quad (r_i, \theta_j) \in \Omega_P^N, \quad U_P^{[k]}(R, \theta_j) = \bar{U}_S^{[k-1]}(R, \theta_j).$$

We define the finite difference operators as in Schwarz Method 1.

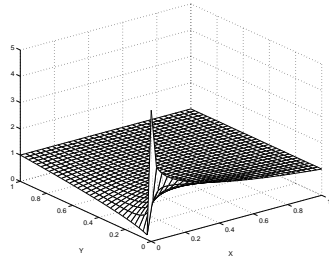
The numerical solutions are depicted in Figures 4.9 and 4.10 for  $N = 32$  and  $\varepsilon = 2^{-1}$  and  $2^{-6}$  respectively, alongside plots of the numerical solutions obtained by the Direct Method for the same parameters for the purpose of comparison. In Table 4.5 the required iteration counts are given for a tolerance level of

$$\max_{x_i, y_j \in \bar{\Omega}_\varepsilon^N} |U_S^{[k]}(x_i, y_j) - U_S^{[k-1]}(x_i, y_j)| \leq 10^{-4}$$

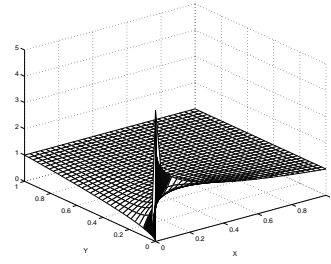
The differences between the numerical solutions for various values of  $N$  and the numerical solution for  $N = 256$ , which are indicative of nodal errors are shown in Table 4.6 and the computed orders of convergence for various values of  $N$  and  $\varepsilon$  are shown in Table 4.7. Both tables show a notable improvement in the magnitude of the error and the orders of convergence for large values of  $\varepsilon$  on the results obtained by the Direct Method, seen in Tables 4.1 and 4.2. However, there is a noticeable drop in the convergence rates for intermediate values of  $\varepsilon$  which requires further consideration.

Table 4.5: Iteration counts for Schwarz Method 2 applied to problem (4.1) with domain decomposition allowing maximal overlap.

$\varepsilon$	Number of intervals $N$				
	16	32	64	128	256
1	3	6	5	4	3
$2^{-1}$	3	6	5	4	3
$2^{-2}$	3	6	5	4	3
$2^{-3}$	3	6	5	3	3
$2^{-4}$	3	6	5	3	4
$2^{-6}$	3	6	5	4	4
$2^{-8}$	3	6	5	4	4
$2^{-10}$	3	6	5	4	4
$2^{-12}$	2	6	5	4	4
$2^{-14}$	2	6	5	4	4
$2^{-16}$	2	6	5	4	4
$2^{-18}$	2	6	5	4	4
$2^{-20}$	2	6	5	4	4
$2^{-22}$	2	6	5	4	4
$2^{-24}$	2	6	5	4	4
$2^{-26}$	2	6	5	4	4
$2^{-28}$	2	6	5	4	4

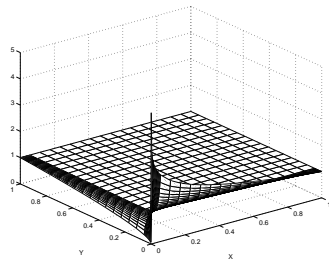


Direct Method

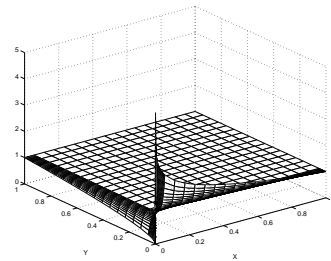


Schwarz Method 2

Figure 4.9: Numerical solutions of problem (4.1) for  $\varepsilon = 2^{-1}$ ,  $N = 32$



Direct Method



Schwarz Method 2

Figure 4.10: Numerical solutions of problem (4.1) for  $\varepsilon = 2^{-6}$ ,  $N = 32$

Table 4.6: Maximum pointwise errors  $E_\varepsilon^N$  and  $E^N$  for Schwarz Method 2 applied to problem (4.1) with domain decomposition allowing maximal overlap.

$\varepsilon$	Number of intervals $N$			
	16	32	64	128
1	0.0218	0.0076	0.0019	0.0004
$2^{-1}$	0.0184	0.0065	0.0015	0.0003
$2^{-2}$	0.0122	0.0054	0.0025	0.0008
$2^{-3}$	0.0242	0.0150	0.0080	0.0028
$2^{-4}$	0.0390	0.0223	0.0114	0.0087
$2^{-6}$	0.0835	0.0471	0.0227	0.0082
$2^{-8}$	0.1202	0.0739	0.0376	0.0138
$2^{-10}$	0.1412	0.0907	0.0489	0.0192
$2^{-12}$	0.1535	0.0992	0.0543	0.0220
$2^{-14}$	0.1620	0.1045	0.0569	0.0230
$2^{-16}$	0.1687	0.1084	0.0587	0.0234
$2^{-18}$	0.1740	0.1116	0.0601	0.0238
$2^{-20}$	0.1783	0.1141	0.0612	0.0240
$2^{-22}$	0.1816	0.1161	0.0621	0.0243
$2^{-24}$	0.1843	0.1177	0.0628	0.0245
$2^{-26}$	0.1865	0.1189	0.0634	0.0246
$2^{-28}$	0.1882	0.1199	0.0638	0.0248
$E^N$	0.1882	0.1199	0.0638	0.0248

Table 4.7: Computed orders of convergence  $p_\varepsilon^N$  for Schwarz Method 2 applied to problem (4.1) with domain decomposition allowing maximal overlap.

$\varepsilon$	Number of intervals $N$		
	16	32	64
1	1.49	1.91	1.92
$2^{-1}$	1.48	2.02	2.05
$2^{-2}$	1.13	1.34	0.93
$2^{-3}$	0.50	1.23	0.91
$2^{-4}$	0.65	0.28	0.28
$2^{-6}$	0.63	0.74	0.82
$2^{-8}$	0.43	0.66	0.81
$2^{-10}$	0.36	0.55	0.68
$2^{-12}$	0.35	0.53	0.62
$2^{-14}$	0.35	0.53	0.62
$2^{-16}$	0.34	0.54	0.63
$2^{-18}$	0.34	0.55	0.64
$2^{-20}$	0.34	0.56	0.65
$2^{-22}$	0.34	0.56	0.65
$2^{-24}$	0.34	0.57	0.66
$2^{-26}$	0.34	0.57	0.66
$2^{-28}$	0.34	0.57	0.66

#### 4.4.1 Alternative translation in polar region

On  $\Omega_P$  we use the alternative translation

$$w = e^{(x+y)/2\varepsilon} u_\varepsilon - \phi(x, y)$$

where  $\phi$  is defined as follows

$$\phi(x, y) = 10/\pi(\pi/2 - \arctan(y/x))$$

yielding the translated equation

$$2\varepsilon^2 \Delta w - w = \phi.$$

This has the effect of directly resolving the discontinuity at the outflow corner. Solving the translated equation using the domain decomposition, finite difference operators (4.4) and iterative method as before, the numerical results obtained do not differ visibly from those for Schwarz Method 2 and for this

reason I have not included them in this chapter.

#### 4.4.2 Use of upwinding in the polar region

When Schwarz Method 2 is modified to use upwinding rather than central differencing in the polar region we obtain slightly worse results for pointwise errors and convergence rates in the case of large  $\varepsilon$ , as seen below. Iteration counts are not affected.

Table 4.8: Iteration counts for modified Schwarz Method 2 applied to problem (4.1) with domain decomposition allowing maximal overlap and upwinding in the polar region.

$\varepsilon$	Number of intervals $N$				
	16	32	64	128	256
1	3	6	5	4	3
$2^{-1}$	3	6	5	4	3
$2^{-2}$	3	6	5	4	3
$2^{-3}$	3	6	5	4	3
$2^{-4}$	3	6	5	3	3
$2^{-5}$	3	6	5	3	3
$2^{-6}$	3	6	5	3	4
$2^{-7}$	3	6	5	3	4
$2^{-8}$	3	6	5	3	4
$2^{-9}$	3	6	5	3	4
$2^{-10}$	3	6	5	3	4
$2^{-11}$	3	6	5	3	4
$2^{-12}$	2	6	5	4	4
$2^{-13}$	2	6	5	4	4
$2^{-14}$	2	6	5	4	4
$2^{-15}$	2	6	5	4	4
$2^{-16}$	2	6	5	4	4
$2^{-17}$	2	6	5	4	4
$2^{-18}$	2	6	5	4	4
$2^{-19}$	2	6	5	4	4
$2^{-20}$	2	6	5	4	4
$2^{-21}$	2	6	5	4	4
$2^{-22}$	2	6	5	4	4
$2^{-23}$	2	6	5	4	4
$2^{-24}$	2	6	5	4	4
$2^{-25}$	2	6	5	4	4
$2^{-26}$	2	6	5	4	4
$2^{-27}$	2	6	5	4	4
$2^{-28}$	2	6	5	4	4

Table 4.9: Computed orders of convergence  $p_\varepsilon^N$  for modified Schwarz Method 2 applied to problem (4.1) with domain decomposition allowing maximal overlap and upwinding in the polar region.

$\varepsilon$	Number of intervals $N$		
	16	32	64
1	1.52	1.92	0.25
$2^{-1}$	1.52	1.90	0.09
$2^{-2}$	1.10	1.37	0.40
$2^{-3}$	0.50	1.23	0.91
$2^{-4}$	0.64	0.28	0.28
$2^{-5}$	0.70	0.68	0.40
$2^{-6}$	0.63	0.74	0.82
$2^{-7}$	0.52	0.72	0.84
$2^{-8}$	0.43	0.66	0.81
$2^{-9}$	0.39	0.59	0.74
$2^{-10}$	0.36	0.55	0.68
$2^{-11}$	0.35	0.53	0.64
$2^{-12}$	0.35	0.53	0.62
$2^{-13}$	0.35	0.53	0.61
$2^{-14}$	0.35	0.53	0.62
$2^{-15}$	0.34	0.54	0.62
$2^{-16}$	0.34	0.54	0.63
$2^{-17}$	0.34	0.55	0.63
$2^{-18}$	0.34	0.55	0.64
$2^{-19}$	0.34	0.56	0.64
$2^{-20}$	0.34	0.56	0.65
$2^{-21}$	0.34	0.56	0.65
$2^{-22}$	0.34	0.56	0.65
$2^{-23}$	0.34	0.57	0.65
$2^{-24}$	0.34	0.57	0.66
$2^{-25}$	0.34	0.57	0.66
$2^{-26}$	0.34	0.57	0.66
$2^{-27}$	0.34	0.57	0.66
$2^{-28}$	0.34	0.57	0.66

Table 4.10: Maximum pointwise errors  $E_\epsilon^N$  and  $E^N$  for modified Schwarz Method 2 applied to problem (4.1) with upwinding in the polar region

$\epsilon$	Number of intervals $N$			
	16	32	64	128
1	0.0218	0.0074	0.0018	0.0013
$2^{-1}$	0.0184	0.0063	0.0018	0.0012
$2^{-2}$	0.0122	0.0054	0.0025	0.0012
$2^{-3}$	0.0242	0.0150	0.0080	0.0028
$2^{-4}$	0.0390	0.0223	0.0114	0.0087
$2^{-5}$	0.0605	0.0336	0.0164	0.0078
$2^{-6}$	0.0835	0.0471	0.0227	0.0082
$2^{-7}$	0.1039	0.0613	0.0301	0.0109
$2^{-8}$	0.1202	0.0739	0.0376	0.0138
$2^{-9}$	0.1323	0.0836	0.0441	0.0168
$2^{-10}$	0.1412	0.0907	0.0489	0.0192
$2^{-11}$	0.1480	0.0956	0.0522	0.0210
$2^{-12}$	0.1535	0.0992	0.0543	0.0220
$2^{-13}$	0.1580	0.1021	0.0558	0.0226
$2^{-14}$	0.1620	0.1045	0.0569	0.0230
$2^{-15}$	0.1655	0.1066	0.0579	0.0232
$2^{-16}$	0.1687	0.1084	0.0587	0.0234
$2^{-17}$	0.1715	0.1101	0.0594	0.0236
$2^{-18}$	0.1740	0.1116	0.0601	0.0238
$2^{-19}$	0.1762	0.1129	0.0607	0.0239
$2^{-20}$	0.1783	0.1141	0.0612	0.0240
$2^{-21}$	0.1800	0.1151	0.0617	0.0242
$2^{-22}$	0.1816	0.1161	0.0621	0.0243
$2^{-23}$	0.1831	0.1169	0.0625	0.0244
$2^{-24}$	0.1843	0.1177	0.0628	0.0245
$2^{-25}$	0.1855	0.1183	0.0631	0.0246
$2^{-26}$	0.1865	0.1189	0.0634	0.0246
$2^{-27}$	0.1874	0.1195	0.0636	0.0247
$2^{-28}$	0.1882	0.1199	0.0638	0.0248
$E^N$	0.1882	0.1199	0.0638	0.0248

## 4.5 Schwarz Method 3: alternative domain decomposition with square sub-region

It is interesting to consider an alternative Schwarz method with a square subregion,  $\Omega_C = (0, R)^2$ ,  $R = \sigma/8$  at the outflow corner replacing the quarter-disk region used in the two Schwarz methods above, see Figure 4.11. The finite difference operator in this region is then the same as that used on the entire domain, (4.3). The iterative method is essentially similar to that used in the previous two Schwarz methods, with upwinding used in each subdomain and a uniform mesh in the small square subdomain.

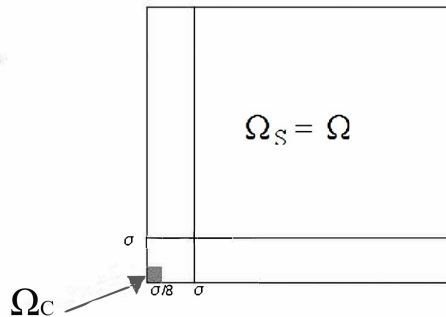


Figure 4.11: Domain decomposition with square overlap region of side  $\sigma/8$ , i.e., the overlap region is comparable magnitude to that of the quarter disk subdomain for the domain decomposition with maximal overlap.

Our discrete iterative method is then as follows:

For each  $k \geq 1$ ,

$$U_\varepsilon^{[k]}(x, y) = \begin{cases} U_S^{[k]}(x, y), & (x, y) \in \Omega_S^N \\ \bar{U}_C^{[k]}(x, y), & (x, y) \in \Omega_C \cap \Omega_S^N \end{cases}$$

where  $\bar{U}_i^{[k]}$  is the bilinear interpolant of  $U_i^{[k]}$ . Then for  $k = 1$ ,

$$\begin{aligned} L_\varepsilon^N U_S^{[1]} &= 0, \quad (x_i, y_j) \in \Omega_S^N, \\ U_S^{[1]}(x_i, 0) &= 5 - 4x_i^{1/6}, \quad U_S^{[1]}(x_i, 1) = 1, \quad x_i \in (0, 1) \\ U_S^{[1]}(0, y_j) &= y_j^{1/2}, \quad U_S^{[1]}(1, y_j) = 1, \quad y_j \in (0, 1). \end{aligned}$$

and

$$\begin{aligned} L_C^N U_C^{[1]} &= 0, \quad (x_i, y_j) \in \Omega_C^N, \\ U_C^{[1]}(x_i, 0) &= 5 - 4x_i^{1/6}, \quad U_C^{[1]}(x_i, \sigma/8) = \bar{U}_S^{[1]}(x_i, \sigma/8), \quad x_i \in (0, \sigma/8) \\ U_C^{[1]}(0, y_j) &= y_j^{1/2}, \quad U_C^{[1]}(\sigma/8, y_j) \\ &= \bar{U}_S^{[1]}(\sigma/8, y_j), \quad y_j \in (0, \sigma/8) \end{aligned}$$

For  $k > 1$ ,

$$\begin{aligned} L_\varepsilon^N U_S^{[k]} &= 0, \quad (x_i, y_j) \in \Omega_S^N, \\ U_S^{[k]}(x_i, y_j) &= \bar{U}_C^{[k-1]}(x_i, y_j), \quad x_i \in (0, \sigma/8), \quad y_j \in (0, \sigma/8), \end{aligned}$$

and

$$L_C^N U_C^{[k]} = 0, \quad (x_i, y_j) \in \Omega_C^N, \quad U_C^{[k]}(x_i, y_j) = \bar{U}_S^{[k-1]}(x_i, y_j), \quad x_i \in (0, \sigma/8), \quad y_j \in (0, \sigma/8).$$

We define the finite difference operators as in Schwarz Method 1.

Tables 4.12 and 4.13 show that the performance of this method is no better than that of the Direct Method for large values of  $\varepsilon$  when applied to problem (4.1). This is perhaps to be expected as, unlike Schwarz Methods 1 and 2 which use a quarter-disk subregion around the area of the discontinuity, with a square subregion there is no translation to polar coordinates. Translating to polar coordinates has the advantage of spreading the point of discontinuity smoothly over the lefthand boundary of the translated subdomain. In this method there is merely a greater concentration of meshpoints in the region of the discontinuity; the method therefore fails in similar manner to the Direct Method.

Table 4.11: Iteration counts for Schwarz Method 3 applied to problem (4.1).

$\varepsilon$	Number of intervals $N$				
	16	32	64	128	256
1	0	0	0	0	3
$2^{-1}$	0	0	0	0	3
$2^{-2}$	0	0	0	0	3
$2^{-3}$	0	0	0	0	3
$2^{-4}$	0	0	0	0	3
$2^{-5}$	0	0	0	0	3
$2^{-6}$	0	0	0	0	3
$2^{-7}$	0	0	0	0	3
$2^{-8}$	0	0	0	0	3
$2^{-9}$	0	0	0	0	3
$2^{-10}$	0	0	0	0	3
$2^{-11}$	0	0	0	0	2
$2^{-12}$	0	0	0	0	2
$2^{-13}$	0	0	0	0	2
$2^{-14}$	0	0	0	0	2
$2^{-15}$	0	0	0	0	2
$2^{-16}$	0	0	0	0	2
$2^{-17}$	0	0	0	0	2
$2^{-18}$	0	0	0	0	2
$2^{-19}$	0	0	0	0	2
$2^{-20}$	0	0	0	0	2
$2^{-21}$	0	0	0	0	2
$2^{-22}$	0	0	0	0	2
$2^{-23}$	0	0	0	0	2
$2^{-24}$	0	0	0	0	2
$2^{-25}$	0	0	0	0	2
$2^{-26}$	0	0	0	0	2
$2^{-27}$	0	0	0	0	2
$2^{-28}$	0	0	0	0	2

Table 4.12: Maximum pointwise errors  $E_\varepsilon^N$  and  $E^N$  for Schwarz Method 3 applied to problem (4.1).

$\varepsilon$	Number of intervals $N$			
	16	32	64	128
1	0.0221	0.0246	0.0244	0.0191
$2^{-1}$	0.0190	0.0235	0.0238	0.0188
$2^{-2}$	0.0110	0.0204	0.0223	0.0183
$2^{-3}$	0.0242	0.0150	0.0187	0.0172
$2^{-4}$	0.0390	0.0223	0.0171	0.0139
$2^{-6}$	0.0835	0.0471	0.0227	0.0145
$2^{-8}$	0.1202	0.0739	0.0376	0.0149
$2^{-10}$	0.1412	0.0907	0.0489	0.0192
$2^{-12}$	0.1535	0.0992	0.0543	0.0220
$2^{-14}$	0.1620	0.1045	0.0569	0.0230
$2^{-16}$	0.1687	0.1084	0.0587	0.0234
$2^{-18}$	0.1740	0.1116	0.0601	0.0238
$2^{-20}$	0.1782	0.1141	0.0612	0.0240
$2^{-22}$	0.1816	0.1161	0.0621	0.0243
$2^{-24}$	0.1843	0.1177	0.0628	0.0245
$2^{-26}$	0.1865	0.1189	0.0634	0.0246
$2^{-28}$	0.1882	0.1199	0.0638	0.0248
$E^N$	0.1882	0.1199	0.0638	0.0248

Table 4.13: Computed orders of convergence  $p_\varepsilon^N$  for Schwarz Method 3 applied to problem (4.1).

$\varepsilon$	Number of intervals $N$		
	16	32	64
1	-0.17	-0.10	-0.07
$2^{-1}$	-0.30	-0.13	-0.09
$2^{-2}$	-0.74	-0.23	-0.14
$2^{-3}$	0.50	-0.18	-0.29
$2^{-4}$	0.42	0.01	-0.01
$2^{-6}$	0.63	0.74	0.00
$2^{-8}$	0.43	0.66	0.70
$2^{-10}$	0.36	0.55	0.68
$2^{-12}$	0.35	0.53	0.62
$2^{-14}$	0.35	0.53	0.62
$2^{-16}$	0.34	0.54	0.63
$2^{-18}$	0.34	0.55	0.64
$2^{-20}$	0.34	0.56	0.65
$2^{-22}$	0.34	0.56	0.65
$2^{-24}$	0.34	0.57	0.66
$2^{-26}$	0.34	0.57	0.66
$2^{-28}$	0.34	0.57	0.66

## 4.6 Conclusion

The analysis in Chapter 3 revealed the localised nature of the effect of the singularity arising from the discontinuity in the outflow boundary data, as well as its interaction with the characteristic layers present. A number of numerical methods motivated by the analysis in Chapter 3, are outlined above. Numerical results for the methods discussed here in this chapter are consistent with the behaviour indicated in Chapter 3's analysis. The numerical method which is best adapted to that behaviour is Schwarz Method 2. The results obtained by this method applied to problem (4.1) with domain decomposition allowing maximal overlap are an improvement on those obtained by the Direct Method for this problem. However, further development of the method is required in order to solve problem (4.1)  $\varepsilon$ -uniformly as the results are not entirely satisfactory for intermediate values of  $\varepsilon$ .

# Bibliography

- [1] M. Abramovitz and Stegun I. *Handbook of mathematical functions*. National Bureau of Standards, 1965.
- [2] V. B. Andreev. Uniform mesh approximation to nonsmooth solutions of a singularly perturbed convection-diffusion equation in a rectangle. *Diff. Eq.*, 45:973–982, 2009.
- [3] V. B. Andreev. Pointwise approximation of corner singularities for singularly perturbed elliptic problems with characteristic layers. *Int. J. Numer. Anal. Model.*, 7 (3):416–427, 2010.
- [4] Ali R Ansari. Shishkin meshes and their applications. In *Department of Mathematics, Gulf University for Science and Technology, Winter Conference in Mathematics, Hawally*, volume 32093, 2004.
- [5] Ali R Ansari and Alan F Hegarty. A note on iterative methods for solving singularly perturbed problems using non-monotone methods on Shishkin meshes. *Computer methods in applied mechanics and engineering*, 192(33-34):3673–3687, 2003.
- [6] Ali R Ansari and Alan F Hegarty. Numerical solution of a convection diffusion problem with robin boundary conditions. *Journal of computational and applied mathematics*, 156(1):221–238, 2003.

- [7] Ali R Ansari, Alan F Hegarty, and Grigori I Shishkin. Parameter-uniform numerical methods for a laminar jet problem. *International Journal for Numerical Methods in Fluids*, 43(8):937–951, 2003.
- [8] Ali R Ansari, Alan F Hegarty, and Grigori I Shishkin. A parameter robust method for a problem with a symmetry boundary layer. In *Numerical Analysis and Its Applications: Second International Conference, NAA 2000 Rouse, Bulgaria, June 11–15, 2000 Revised Papers 2*, pages 18–26. Springer, 2001.
- [9] Ali R Ansari, John JH Miller, and Grigori I Shishkin. A robust numerical method for flow through a pipe driven by an oscillating pressure gradient. *International journal for numerical methods in fluids*, 53(3):471–484, 2007.
- [10] Ali R Ansari and Grigori I Shishkin. On the singularly perturbed character of the turbulent free jet and its robust numerical solution. *International journal for numerical methods in fluids*, 70(8):977–984, 2012.
- [11] AR Ansari, SA Bakr, and GI Shishkin. A parameter-robust finite difference method for singularly perturbed delay parabolic partial differential equations. *Journal of computational and applied mathematics*, 205(1):552–566, 2007.
- [12] Komal Bansal and Kapil K Sharma. Parameter-robust numerical scheme for time-dependent singularly perturbed reaction–diffusion problem with large delay. *Numerical Functional Analysis and Optimization*, 39(2):127–154, 2018.

- [13] Paul Binding. Singularly perturbed optimal control problems. I: Convergence. *SIAM Journal on Control and Optimization*, 14(4):591–612, 1976.
- [14] Igor Boglaev. Monotone iterative algorithms for a nonlinear singularly perturbed parabolic problem. *Journal of computational and applied mathematics*, 172(2):313–335, 2004.
- [15] AE Caola and RA Brown. Robust iterative methods for solution of transport problems with flow: a block two-level preconditioned Schwarz-domain decomposition method for solution of nonlinear viscous flow problems. *Chemical engineering science*, 57(21):4583–4594, 2002.
- [16] Dmitrii Chaikovskii and Ye Zhang. Convergence analysis for forward and inverse problems in singularly perturbed time-dependent reaction-advection-diffusion equations. *Journal of Computational Physics*, 470:111609, 2022.
- [17] Pratibhamoy Das and Jesus Vigo-Aguiar. Parameter uniform optimal order numerical approximation of a class of singularly perturbed system of reaction diffusion problems involving a small perturbation parameter. *Journal of Computational and Applied Mathematics*, 354:533–544, 2019.
- [18] Willy Dörfler. Uniform a priori estimates for singularly perturbed elliptic equations in multidimensions. *SIAM journal on numerical analysis*, 36(6):1878–1900, 1999.
- [19] R.K. Dunne. *Finite difference methods for singularly perturbed problems on non-rectangular domains*. PhD thesis, Dublin City University, 2005.

- [20] RK Dunne, E O’Riordan, and GI Shishkin. Fitted mesh numerical methods for singularly perturbed elliptic problems with mixed derivatives. *IMA journal of numerical analysis*, 29(3):712–730, 2009.
- [21] P.A. Farrell, A.F. Hegarty, J.J.H. Miller, E. O’Riordan, and G.I. Shishkin. *Robust Computational Techniques for Boundary Layers*. CRC, Boca Raton, FL, 2000.
- [22] P.A. Farrell, A.F. Hegarty, J.J.H. Miller, E. O’Riordan, and G.I. Shishkin. Global maximum norm parameter-uniform numerical method for a singularly perturbed convection-diffusion problem with a discontinuous convection coefficient. *Math. Comput. Modelling*, 40:1375–1392, 2004.
- [23] P.A. Farrell, A.F. Hegarty, J.J.H. Miller, E. O’Riordan, and G.I. Shishkin. Singularly perturbed convection-diffusion problems with boundary and weak interior layers. *J. Comput. & Appl. Math.*, 166:133–151, 2004.
- [24] PA Farrell, PW Hemker, and GI Shishkin. Discrete approximations for singularly perturbed boundary value problems with parabolic layers. *Journal of Computational Mathematics*, pages 71–97, 1996.
- [25] Paul A Farrell and Grigorii I Shishkin. Schwarz methods for singularly perturbed convection-diffusion problems. *Nova Science Publishers, Huntington, NY*, pages 33–42, 2000.
- [26] G. M. Fichtenholz. *Differential and integral calculus, Vol. I*. Fizmatgiz, Moscow, 1962.
- [27] M Gonzalez, AF Hegarty, and SR Thomas. Glycolysis as a source of “external osmoles”: The vasa recta transient model. In *BAIL 2008-*

*Boundary and Interior Layers: Proceedings of the International Conference on Boundary and Interior Layers-Computational and Asymptotic Methods, Limerick, July 2008*, pages 153–161. Springer, 2009.

- [28] MT Gonzalez, AF Hegarty, and SR Thomas. A shunt model of the inner medullary nephron with pre-bend transitions. In *AIP Conference Proceedings*, volume 1168, pages 1469–1471. American Institute of Physics, 2009.
- [29] JL Gracia, E O’Riordan, and ML Pickett. A parameter robust second order numerical method for a singularly perturbed two-parameter problem. *Applied Numerical Mathematics*, 56(7):962–980, 2006.
- [30] Jose Luis Gracia and Eugene O’Riordan. Parameter-uniform numerical methods for singularly perturbed parabolic problems with incompatible boundary-initial data. *Applied Numerical Mathematics*, 146:436–451, 2019.
- [31] Jose Luis Gracia and Eugene O’Riordan. Parameter-uniform approximations for a singularly perturbed convection-diffusion problem with a discontinuous initial condition. *Applied Numerical Mathematics*, 162:106–123, 2021.
- [32] Jose Luis Gracia and Eugene O’Riordan. Singularly perturbed reaction–diffusion problems with discontinuities in the initial and/or the boundary data. *Journal of Computational and Applied Mathematics*, 370:112638, 2020.
- [33] José Luis Gracia and Eugene O’Riordan. Singularly perturbed reaction-diffusion problems with non-smooth initial and/or boundary data. *XVII CMA/XXVII CEDYA*, page 63, 2022.

- [34] C. Grossmann, H-G Roos, and M. Stynes. *Numerical Treatment of Partial Differential Equations*. Springer, Berlin Heidelberg, 2007.
- [35] W. Guo and M. Stynes. Pointwise error estimates for a streamline diffusion scheme on a Shishkin mesh for a convection-diffusion problem. *IMA J. Num. Anal.*, 17:29–59, 1997.
- [36] A.F. Hegarty and E. O’Riordan. Fitted finite element methods for singularly perturbed elliptic problems of convection-diffusion type. *Applied Numerical Mathematics*, 196:183–198, 2024.
- [37] A.F. Hegarty and E. O’Riordan. A numerical method for singularly perturbed convection-diffusion problems posed on smooth domains. *Journal of Scientific Computing*, 92(3):84, 2022.
- [38] Alan F Hegarty, Stephen BG O’Brien, and Stephen Sikwila. Numerical solution of a rimming flow problem using a moving mesh method. *Computational Methods in Applied Mathematics*, 3(3):373–386, 2003.
- [39] H.Han and R.B. Kellogg. Differentiability properties of solutions of the equation  $-\varepsilon^2 \Delta u + ru = f(x, y)$  in a square. *SIAM J. Math. Anal.*, 21, 1990.
- [40] Robin Stanley Johnson. *Singular perturbation theory: mathematical and analytical techniques with applications to engineering*. Springer Science & Business Media, 2005.
- [41] B. Kellogg and A. Tsan. Analysis of some difference approximations for a singular perturbation problem without turning points. *Mathematics of Computation*, 32:1025–1039, 1978.

- [42] R. Bruce Kellogg. Boundary value problems and integral equations in nonsmooth domains. In M. Costabel, M. Dauge, and S. Nicaise, editors, *Lecture Notes in Pure and Appl. Math.*, volume 167, pages 121–149, New York, 1994. Marcel Dekker Inc.
- [43] R. Bruce Kellogg. Corner singularities and singular perturbations. *Ann. Univ. Ferrara Sez. VII (N.S.)*, 47:177–206, 2001.
- [44] R. Bruce Kellogg. Some simple boundary value problems with corner singularities and boundary layers. *Comput. and Math. with Appl.*, 51:783–792, 2006.
- [45] R. Bruce Kellogg and Martin Stynes. Corner singularities and boundary layers in a simple convection-diffusion problem. *J. Comput. Diff. Eq.*, 213:81–120, 2005.
- [46] R. Bruce Kellogg and Martin Stynes. A singularly perturbed convection-diffusion problem in a half-plane. *Appl. Analysis*, 85 (12):1471–1485, 2006.
- [47] R. Bruce Kellogg and Martin Stynes. Sharpened bounds for corner singularities and boundary layers in a simple convection-diffusion problem. *Appl. Math. Letters*, 20:539–544, 2007.
- [48] R. Bruce Kellogg and Martin Stynes. Layers and corner singularities in singularly perturbed elliptic problems. *BIT Num. Math.*, 48:309–314, 2008.
- [49] Jirair K Kevorkian and Julian D Cole. *Multiple scale and singular perturbation methods*, volume 114. Springer Science & Business Media, 2012.

- [50] N. Kopteva. Uniform pointwise convergence of difference schemes for convection-diffusion problems on layer-adapted meshes. *Computing*, 66:179–197, 2001.
- [51] N. Kopteva and E. O’Riordan. Shishkin meshes in the numerical solution of singularly perturbed differential equations. 2010.
- [52] N. Kopteva and M. Pickett. A robust overlapping Schwarz method for a singularly perturbed semilinear reaction-diffusion problem with multiple solutions. *International Journal of Numerical Analysis & Modeling*, 6(4), 2009.
- [53] N. Kopteva and M. Pickett. A second-order overlapping Schwarz method for a 2d singularly perturbed semilinear reaction-diffusion problem. *Mathematics of Computation*, 81(277):81–105, 2012.
- [54] Sunil Kumar and BV Rathish Kumar. A domain decomposition Taylor-Galerkin finite element approximation of a parabolic singularly perturbed differential equation. *Applied Mathematics and Computation*, 293:508–522, 2017.
- [55] Sunil Kumar and Mukesh Kumar. An analysis of overlapping domain decomposition methods for singularly perturbed reaction–diffusion problems. *Journal of computational and applied mathematics*, 281:250–262, 2015.
- [56] Sunil Kumar and S Chandra Sekhara Rao. A robust overlapping Schwarz domain decomposition algorithm for time-dependent singularly perturbed reaction–diffusion problems. *Journal of computational and applied mathematics*, 261:127–138, 2014.

- [57] Sunil Kumar and S Chandra Sekhara Rao. A robust domain decomposition algorithm for singularly perturbed semilinear systems. *International Journal of Computer Mathematics*, 94(6):1108–1122, 2017.
- [58] Runchang Lin and Martin Stynes. A balanced finite element method for singularly perturbed reaction-diffusion problems. *SIAM Journal on Numerical Analysis*, 50(5):2729–2743, 2012.
- [59] T. Linss. Layer-adapted meshes for convection diffusion problems. *Comput. Methods Appl. Mech. Engrg.*, 192:1061–1105, 2003.
- [60] T. Linss and M. Stynes. A hybrid difference scheme on a Shishkin mesh for linear convection-diffusion problems. *Applied Numerical Mathematics*, 31:255–270, 1999.
- [61] T. Linss and M. Stynes. Asymptotic analysis and Shishkin-type decomposition for an elliptic convection-diffusion problem. *J. Math. Anal. Appl.*, 261, 2001.
- [62] T. Linss and M. Stynes. Numerical methods on Shishkin meshes for linear convection-diffusion problems. *Comput. Methods Appl. Mech. Engrg.*, 190:3527–3542, 2001.
- [63] Torsten Linß. *Layer-adapted meshes for reaction-convection-diffusion problems*. Springer, 2009.
- [64] Vladimir D Liseikin. *Layer resolving grids and transformations for singular perturbation problems*. Walter de Gruyter GmbH & Co KG, 2018.
- [65] Scott MacLachlan and Niall Madden. Robust solution of singularly perturbed problems using multigrid methods. *SIAM Journal on Scientific Computing*, 35(5):A2225–A2254, 2013.

- [66] H. MacMullen, J.J.H. Miller, E. O’Riordan, and G.I. Shishkin. A second-order parameter uniform overlapping Schwarz method for reaction-diffusion problems with boundary layers. *J. Comput. & Appl. Math.*, 130:231–244, 2001.
- [67] H. MacMullen, E. O’Riordan, and G.I. Shishkin. The convergence of classical Schwarz methods applied to convection-diffusion problems with regular boundary layers. *Appl. Num. Math.*, 43:297–313, 2002.
- [68] Peter A Markowich and CA Ringhofer. A singularly perturbed boundary value problem modelling a semiconductor device. *SIAM Journal on Applied Mathematics*, 44(2):231–256, 1984.
- [69] Tarek PA Mathew. *Domain decomposition methods for the numerical solution of partial differential equations*. Springer, 2008.
- [70] Giovanni Migliorati and Alfio Quarteroni. Multilevel Schwarz methods for elliptic partial differential equations. *Computer methods in applied mechanics and engineering*, 200(25-28):2282–2296, 2011.
- [71] J.J.H. Miller and E. O’Riordan. A parameter-uniform Schwarz method for a singularly perturbed reaction–diffusion problem with an interior layer. *Applied Numerical Mathematics*, 35(4):323–337, 2000.
- [72] J.J.H. Miller, E. O’Riordan, and G. Shishkin. *Fitted numerical methods for singular perturbation problems: Error estimates in the maximum norm for linear problems in one and two dimensions, revised edition*. World Scientific, 2012.
- [73] J.J.H. Miller, E. O’Riordan, G.I. Shishkin, and S. Wang. A parameter-uniform Schwarz method for a singularly-perturbed reaction-diffusion problem with an interior layer. *Appl. Num. Math.*, 35:323–337, 2000.

- [74] K.W. Morton. *Numerical Solution of Convection Diffusion Problems*. Chapman and Hall, London, 1996.
- [75] A. Naughton, R. Bruce Kellogg, and Martin Stynes. Regularity and derivative bounds for a convection-diffusion problem with a Neumann outflow condition. *J. Diff. Equations*, 247:2495–2516, 2009.
- [76] A. Naughton and Martin Stynes. Regularity and derivative bounds for a convection-diffusion problem with Neumann boundary conditions on characteristic boundaries. *Z. Anal. Anwend.*, 29:163–181, 2010.
- [77] Robert E O’Malley et al. *Historical developments in singular perturbations*. Springer, 2014.
- [78] E. O’Riordan. Opposing flows in a one dimensional convection-diffusion problem. *Centr. Eur. J. Math.*, 10:85–100, 2012.
- [79] E O’Riordan, ML Pickett, and GI Shishkin. Numerical methods for singularly perturbed elliptic problems containing two perturbation parameters. *Mathematical Modelling and Analysis*, 11(2):199–212, 2006.
- [80] Eugene O’Riordan, Maria L Pickett, and Georgii I Shishkin. Singularly perturbed problems modeling reaction-convection-diffusion processes. *Computational Methods in Applied Mathematics*, 3(3):424–442, 2003.
- [81] E. O’Riordan. Interior layers in singularly perturbed problems.
- [82] E O’RIORDAN and ML Pickett. Localized parameter-explicit bounds on the derivatives of the solution to a singularly perturbed two parameter elliptic problem. 2010.
- [83] Eugene O’Riordan. Parameter-uniform numerical methods for singularly perturbed problems. In *Fourteenth International Conference Zaragoza–*

*Pau on Mathematics and its Applications: Jaca (Spain), September 12,*  
volume 41, pages 159–169. Prensas de la Universidad de Zaragoza, 2018.

- [84] Eugene O’Riordan, M Pickett, and G Shishkin. Parameter-uniform finite difference schemes for singularly perturbed parabolic diffusion-convection-reaction problems. *Mathematics of Computation*, 75(255):1135–1154, 2006.
- [85] Eugene O’Riordan and ML Pickett. A parameter-uniform numerical method for a singularly perturbed two parameter elliptic problem. *Advances in Computational Mathematics*, 35:57–82, 2011.
- [86] Eugene O’Riordan and ML Pickett. Numerical approximations to the scaled first derivatives of the solution to a two parameter singularly perturbed problem. *Journal of Computational and Applied Mathematics*, 347:128–149, 2019.
- [87] Andrei D. Polyanin. *Handbook of Linear Partial Differential Equations for Engineers and Scientists*. Chapman and Hall, Boca Raton, FL, 2002.
- [88] H.-G. Roos. Layer-adapted grids for singular perturbation problems. *ZAMM, Z. Angew. Math. Mech.*, 78, 1998.
- [89] H-G Roos, M. Stynes, and L. Tobiska. *Robust Numerical Methods for Singularly Perturbed Differential Equations*. Springer, Berlin Heidelberg, 2008.
- [90] Shaw-Ching Sheen and Jeun-Len Wu. Preconditioning techniques for the BiCGstab algorithm used in convection-diffusion problems. *Numerical Heat Transfer*, 34(2):241–256, 1998.

- [91] G.I. Shishkin. *Grid Approximations of Singularly Perturbed Elliptic and Parabolic Equations*. Ural Branch of Russian Acad. Sci., Ekaterinburg, 1992. in Russian.
- [92] G.I. Shishkin. Robust novel high-order accurate numerical methods for singularly perturbed convection-diffusion problems. *Mathematical Modelling and Analysis*, 10(4):393–412, 2005.
- [93] G.I. Shishkin. Grid approximation of a singularly perturbed elliptic convection–diffusion equation in an unbounded domain. *Russian Journal of Numerical Analysis & Mathematical Modelling*, 21(1), 2006.
- [94] G.I. Shishkin. Difference scheme for a singularly perturbed parabolic convection–diffusion equation in the presence of perturbations. *Computational Mathematics and Mathematical Physics*, 55:1842–1856, 2015.
- [95] G.I. Shishkin and L. Shishkina. *Difference methods for singular perturbation problems*. Chapman and Hall/CRC, 2008.
- [96] G.I. Shishkin and L.P. Shishkina. *Difference Methods for Singular Perturbation Problems*. Chapman and Hall/CRC, Boca Raton, FL, 2009.
- [97] Grigorii Ivanovich Shishkin. Grid approximations of singularly perturbed systems for parabolic convection-diffusion equations with counterflow. , 1(3):281–297, 1998.
- [98] S Sikwila, AF Hegarty, and GI Shishkin. Novel robust adaptive techniques for the numerical solution of convection diffusion problem. In *Proceedings of BAIL 2004 Conference, Toulouse*, 2004.
- [99] S Sikwila, AF Hegarty, and GI Shishkin. An adaptive method for the numerical solution of an elliptic convection diffusion problem. In *Proc.*

*Int'l Conf. Boundary and Interior Layers-Computational and Asymptotic Methods, Georg-August University Göttingen*, pages 1–7, 2006.

- [100] Gerard LG Sleijpen, Henk A Van der Vorst, and Diederik R Fokkema. BiCGstab (l) and other hybrid Bi-CG methods. *Numerical Algorithms*, 7:75–109, 1994.
- [101] M. Stephens and N. Madden. A parameter-uniform Schwarz method for a coupled system of reaction-diffusion equations. *J. Comp. Appl. Math.*, 230:360–370, 2009.
- [102] G. Sun and M. Stynes. Finite element methods for singularly perturbed high-order elliptic two-point boundary value problems. ii: convection-diffusion-type problems. *IMA J. Num. Anal.*, 15:197–219, 1995.
- [103] Peter Szmolyan. A singular perturbation analysis of the transient semiconductor device equations. *SIAM Journal on Applied Mathematics*, 49(4):1122–1135, 1989.
- [104] IV Tselishcheva, Pieter W Hemker, and Grigory I Shishkin. Parameter-robust domain decomposition methods for semilinear singularly perturbed parabolic reaction-diffusion equations in a composed domain. In *An International Conference on Boundary and Interior Layers—Computational and Asymptotic Methods BAIL*, pages 465–470, 2004.
- [105] IV Tselishcheva and GI Shishkin. Sequential and parallel domain decomposition methods for a singularly perturbed parabolic convection-diffusion equation. *Proceedings of the Steklov Institute of Mathematics*, 261:206–227, 2008.

- [106] Ferdinand Verhulst. *Methods and applications of singular perturbations: boundary layers and multiple timescale dynamics*, volume 50. Springer Science & Business Media, 2006.
- [107] Jin Zhang, Xiaoqi Ma, and Yanhui Lv. Finite element method on Shishkin mesh for a singularly perturbed problem with an interior layer. *Applied Mathematics Letters*, 121:107509, 2021.